THE ANTI-CANCER EFFECT OF THE EXTRACT FROM DIFFERENT PARTS

OF *MOMORDICA COCHINCHINENSIS* (LOUR.) SPRENG. AGAINST PROSTATE

CANCER CELLS.

SEKSOM CHAINUMNIM

Graduate School Srinakharinwirot University

2021

การออกฤทธิ์ของสารสกัดจากส่วนต่างๆ ของฟักข้าวในการต้านมะเร็งต่อมลูกหมาก

เสกสม ใจนุ่มนิ่ม

THE ANTI-CANCER EFFECT OF THE EXTRACT FROM DIFFERENT PARTS
OF *MOMORDICA COCHINCHINENSIS* (LOUR.) SPRENG. AGAINST PROSTATE
CANCER CELLS.

SEKSOM CHAINUMNIM

A Dissertation Submitted in Partial Fulfillment of the Requirements

for the Degree of DOCTOR OF PHILOSOPHY

(Biomedical Sciences)

Faculty of Medicine, Srinakharinwirot University

2021

THE DISSERTATION TITLED

THE ANTI-CANCER EFFECT OF THE EXTRACT FROM DIFFERENT PARTS

OF *MOMORDICA COCHINCHINENSIS* (LOUR.) SPRENG. AGAINST PROSTATE CANCER CELLS.

BY

SEKSOM CHAINUMNIM

HAS BEEN APPROVED BY THE GRADUATE SCHOOL IN PARTIAL FULFILLMENT

OF THE REQUIREMENTS FOR THE DOCTOR OF PHILOSOPHY

IN BIOMEDICAL SCIENCES AT SRINAKHARINWIROT UNIVERSITY

....

(Assoc. Prof. Dr. Chatchai Ekpanyaskul, MD.)

Dean of Graduate School

....

ORAL DEFENSE COMMITTEE

.... Major-advisor

(Asst. Prof. Dr.Wanlaya Tanechpongtamb)

.... Co-advisor

(Prof. Dr.Sunit Suksamrarn)

.... Chair

(Assoc. Prof. Dr.Klaokwan Srisook)

.... Committee

(Asst. Prof. Dr.Yamaratee Jaisin)

.... Committee

(Asst. Prof. Dr.Srisombat Puttikamonkul)

Title	THE ANTI-CANCER EFFECT OF THE EXTRACT FROM DIFFERENT PARTS OF *MOMORDICA COCHINCHINENSIS* (LOUR.) SPRENG. AGAINST PROSTATE CANCER CELLS.
Author	SEKSOM CHAINUMNIM
Degree	DOCTOR OF PHILOSOPHY
Academic Year	2021
Thesis Advisor	Assistant Professor Dr. Wanlaya Tanechpongtamb
Co Advisor	Professor Dr. Sunit Suksamrarn

Prostate cancer is one of the most common cancers among men, which is marked by the abnormal control of cell division in the prostate gland. Although the incidence of prostate cancer is presently declining, the number of patients in the metastatic stage has increased over the last decade. Hence, new ways of treatment especially the uses of natural products is worth studying. In the present study, *Momordica cochinchinensis* (MC) or Gac fruit has various biological activities and was therefore be selected for cytotoxic screening and evaluation for the ability of metastasis inhibition against prostate cancer cells. Methanol extracts from different parts of MC were firstly prepared (stems, roots, seeds, leaves, and arils) and a cytotoxic screening with MTT assay comparing between prostate cancer cells (PC-3) and representative of normal cells (Vero). The results showed that stem extract at 24 h from MC has the highest cytotoxicity and selectivity which IC_{50} for PC-3 cells was 0.62 mg/ml, while for Vero cells it was 2 mg/mL. The mechanism for apoptotic death induced by the stem extract was further evaluated in PC-3 cells. As a result, all characteristics were clearly observed, including nuclear cell condensation, fragmentation, accumulation of Sub-G1 population, and dissipation of mitochondrial membrane potential. In addition, stem extract could increase the amount of pro-apoptotic Noxa and caspase-3, while the anti-apoptotic both BcL-xL and McL-1 were significantly decreased. To determine the chemical composition of the stem extract, chromatographic techniques were used, in which the main constituents of the stem extract were characterized as α-spinasterol and ligballinol, as well as some fatty acids. However, to further investigate the effect of aril extract on metastasis process, especially, cell migration was performed. The IC_{50} of PC-3 cells were 2.01 mg/mL, 0.59 mg/mL for 48, and 72 h, differ from LNCaP cells were 0.56 mg/mL for 24 h, but at 48, and 72 h of treatment extracts, tended to induce cell proliferation. In addition, a cell damage with sonicated water extract was clearly observed by using LDH assay. The property of metastasis inhibition was examined by wound healing, transwell insert migration assay, and MMPs expression. The results demonstrated that sonicated water extract could inhibit PC-3 cell migration, and reduced MMPs, together. These results demonstrated that the stem extract of *M. cochinchinensis* has cytotoxic and apoptotic effects in PC-3 cells. In addition, sonicated water extract could inhibit cell proliferation, migration in PC-3 cells. These data provided basic knowledge for developing anticancer agents for prostate cancer in the future.

Keyword : Momordica cochinchinensis, stem extracts, apoptosis, metastasis, prostate cancer, sonicated water extract

ACKNOWLEDGEMENTS

TABLE OF CONTENTS

List of Tables

List of Figures

CHAPTER 1

INTRODUCTION

1.1 Background

      Prostate cancer is the second leading causes of death in men worldwide. In 2020, prostate cancer has been reported as the most common cancer found in American men which new cases were at 191,930 (20%) cases and deaths were at 33,330 cases (1). For Thailand, prostate cancer ranked as number four of cancer found in male in 2020 and has the possibility to increase high within the group of elderly. And as Thailand is presently facing of ageing society, so it means that the number of prostate cancer will probably increase in the near future and also the number of deaths may rise as well. Treatment for prostate cancer depends on the stage and grading of cancer that influence the doctor to make decision. At the moment there are several ways of treatment either surgery, chemotherapy, radiation, androgen deprivation therapy (ADT) or immunotherapy. All these methods have pros and cons, so the doctor needs to be carefully making decision for each patient. Importantly, if cancer staging is in the late stage or metastasis, it is really untreatable. So, it is interesting if we could reduce the number of cancer cells before further growing to the late stage or blocking the ability to transform into metastatic phase, the number of deaths may reduce.

      From this hypothesis, this research is interested to find an agent that having this ability. Natural crude extract and bioactive compound is considered as it would have less in cytotoxicity to the normal cells and received much attention worldwide. *Momordica cochinchinensis* or Gac fruit is selected for this work as it is a local plant in Thailand, easily planting, and crucially it has been shown the property of anticancer. Seed extract could inhibit proliferation, metastasis of lung cancer [2, 3] and induce apoptosis via multiple signaling [4, 5]. Water extract from Gac fruit suppressed the proliferation of colon cancer (colon 26-20) and hepatocarcinoma (HepG2) [6]. In addition, cochinin B protein extracted from seed of Gac has the ability to inhibit protein synthesis and cytotoxic to cervical cancer cell (Hela), human embryonic kidney (HEK 293) and

human small cell lung cancer (NCI-H187) [7]. This data supports that Gac is an interesting material and worth studying as an anticancer agent for prostate cancer.

Therefore, several parts of Gac (stems, leaves, roots, seeds, and arils) are selected to evaluate the anticancer activity against prostate cancer cells. The crude extracts from these parts were prepared and screened for cancer cytotoxicity in prostate cancer cell lines compared to other cancer cell types and the representative of normal cells. The potential crude extracts with high toxicity to cancer cells (but less for normal cells) were further selected and purified for a bioactive compound. After that, the mode of cell death induced by potential crude extract and the pure compound was determined.

The apoptosis mechanism was chosen as a drug target in this study as it is a pathway that could reduce the number of cancer cells by not initiating the inflammation. The characteristics of apoptotic cell death were evaluated, including nuclear condensation and fragmentation and the dissipation of mitochondrial membrane potential. The molecular signaling involving apoptotic induction, both pro-apoptotic and anti-apoptotic mediators, are also investigated. In addition, the blockage of metastasis is determined by observing the effect on key regulators of the migration process, including MMP-2, MMP-9, and TIMP-1.

Therefore, from this work it is postulated that the bioactive compound and crude extract from Gac would have a benefit acting as anticancer agent by inducing apoptosis signaling and inhibiting the metastasis process.

1.2 Objectives

According to the preliminary screening (the results are described in chapter III), it is demonstrated that crude extracts from different parts of *M. cochinchinensis* have different potential biological activity against prostate cancer cells. Therefore, the purposes of this study are divided into two parts.

Part I: Study the effect of crude extracts from stems, leaves, roots and seeds of *M. cochinchinensis* on prostate cancer cells proliferation and apoptosis mechanism. The sub-objectives of this part are as follows:

- To prepare crude extracts from stems, leaves, roots, and seeds of *M. cochinchinensis.*

- To study the cytotoxic effect of crude extracts in prostate cancer cells compared to other cancer cell types and the representation of normal cells.

- To investigate the apoptosis mechanism of the potential crude extract in prostate cancer cells.

- To isolate bioactive compounds from the potential crude extract of *M. cochinchinensis* and characterize the chemical structure.

- To determine the cytotoxic effect of purified compound against prostate cancer cells.

Part II: Study the effect of crude extracts from aril part of *M. cochinchinensis* on prostate cancer cell metastasis. The sub-objectives of this part are as follows:

- To prepare crude extracts from the aril part of *M. cochinchinensis.*

- To investigate the cytotoxicity of crude extracts from aril in prostate cancer cells and the representation of normal cells.

- To determine the mode of cell death induced by potential aril extract.

- To evaluate the effect of potential aril extract on the prostate cancer cell migration

- To investigate the effect of potential aril extract on the expression of protein mediators of migration process

1.3 Hypothesis

The crude extracts and bioactive compound from *M. cochinchinensis* may acts as anticancer agent by trigger apoptosis via extrinsic or intrinsic pathway and inhibiting metastatic process.

CHAPTER 2

LITERATURE REVIEWS

2.1 Prostate gland

2.1.1 Prostate gland characteristic

The prostate gland is one part of the reproductive system in male. It is a walnut-like shaped gland that located between the bladder and the distal colon. The size of prostate gland varies with age. At puberty, it has the size of a walnut and starts to enlarge when reaching 40 years of age which called benign prostatic hyperplasia (BPH). Prostate gland functions as the fertility organ by secreting seminal fluid; alkaline, milky or white in appearance for nourishing and transport the sperm [8]. The prostate gland itself surrounds the urethra, so it can press the urethra when becoming larger. This result leading to inflammation or malignancy. The epidemiology statistic indicated that prostate cancer is diagnosed as the second most common cancer in men worldwide (Figure 1).
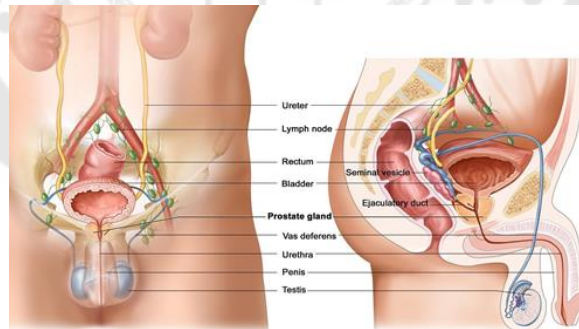
Figure 1 The morphological characteristics of prostate gland.

Source: Brandywine Urology Consultants [Internet]. New Castle: Helen F. Graham Cancer Center; 2014 [cited 2014 April 19]. Available from: https://www.brandywineuc.com/about-us/.

2.2 Prostate cancer

2.2.1 Definition of prostate cancer

Prostate cancer is the most common cancers affecting older men in developing countries and developed countries. In most cases, prostate cancer symptoms are not clearly seen in the early stage of the disease. Then, routine screenings of digital rectal exams (DRE) and prostate-specific androgen (PSA) tests are important. Also, men at the age of 50 and above with one or more risk factors for prostate cancer should consult the physician

Estimated New Cases (Males)		
Prostate	191,930	21%
Lung	116,300	13%
Colon	78,300	9%
Urinary	62,100	7%
Estimated Deaths		
Lung	72,500	23%
Prostate	33,330	10%
Colon	28,630	9%
Pancreas	24,640	8%

Figure 2 The incidence and mortality of cancer in 2020. The four Leading Cancer Types for the New Cancer Cases and Deaths by Sex, United States, 2020 which modified from Siegel RL, et al. (2020).

Source: Siegel RL, Miller KD, Jemal A. Cancer statistics, 2020. CA Cancer J Clin. 2020;70(1):7-30.

The epidemiology of prostate cancer in the U.S. in 2020 showing that new cases of prostate cancer and deaths would be at 191,930 and 33,330 cases, respectively. Prostate cancer alone accounting for almost 1 in 5 of new diagnoses in

men (Figure 2). For Thailand, the statistics from Hospital-based cancer registry in 2020 reported that prostate cancer ranking as number 4 of new cancer patient [9]. The age of patients were in the range of 60-75 years old.

2.2.2 Stage of prostate cancer

Stage I: The cancerous prostate closely resembles normal prostate tissues. A stage I cancer cells that look like normal cells.

Stage IIA and IIB: This stage describes a tissue still has well-formed glands that is too small to be felt.

Stage III: The tissue still has recognizable glands, but the cancer has spread beyond the outer layer and invade surrounding tissue.

Stage IV: This stage describes many tumor cells are invading the surrounding tissue that has spread to other sites of the body.

2.2.3 Symptoms of prostate cancer

Prostate cancer may cause no signs and symptoms in both early and mid-stage [10]. In the late stage, signs and symptoms are including trouble urinating, decreased force in the stream of urine, discomfort in the pelvic area, blood in semen, bone pain and erectile dysfunction.

2.2.4 Risk factors of prostate cancer

Prostate cancer has several risk factors. It is clearly shown that the incidence of prostate cancer increasing with the age. The race is also an important risk factor. The black men have a high possibility of prostate cancer than men of other races. In addition, prostate cancer in black men is more likely to be more aggressive and/or advanced. Family history of prostate cancer are also have high risk. Importantly, if having a family history of breast cancer genes (BRCA1 or BRCA2) the risk of prostate cancer may be higher. The level of androgen hormone is another risk factor that influences the incidence and type of prostate cancer. Prostate cancers that relatively need high levels of androgens to grow are referred to as androgen dependent or androgen sensitive which could be treated by decreasing androgen levels. However, most prostate cancers eventually become "castration resistant," which means that it can continue to grow even the level of androgen is depleted.

2.2.5 Diagnosis of prostate cancer

There is no single definite diagnostic test for prostate cancer. It depends on the pros and cons of each method [11].

- Physical exam and history
- Digital rectal exam (DRE)
- Prostate-specific antigen (PSA) test
- Transrectal ultrasound:
- Transrectal magnetic resonance imaging (MRI)
- Biopsy

2.2.6 Treatment of prostate cancer

Treatment is different between early and advanced prostate cancers and several factors such as rate of growth and spreading of cancer cells [11].

2.2.6.1 Early-stage prostate cancer

• Radical prostatectomy

• Brachytherapy; replaced by radioactive seeds into the prostate gland to deliver targeted radiation treatment.

2.2.6.2 Advanced prostate cancer

The advanced stage is a spreading of cancer cells throughout the body. Treatments are as following methods.

• Chemotherapy

• Androgen deprivation therapy (ADT) is a hormone treatment that reducing the effect of androgen. Reducing androgen levels can slow down cancer growth/ stop cancer proliferation.

Anti-androgen are anti-hormone drug that used for non-metastasis prostate cancer by suppress male hormone synthesis. For example, Eulexin (Flutamide), Casodex (Bicalutamide), Nilandron (Nilutamide), Cyproterone acetate, Ketoconazole.

2.2.6.3 Drug for non-metastatic castration-resistant prostate cancer

Apalutamide (Erleada) is a non-steroidal anti-androgen (NSAA) [12]. This drug is prevents binding transcription of AR-responsive genes, resulting in inhibits the expression of genes correlated with regulate prostate cancer cell proliferation.

2.2.6.4 Chemotherapy

Docetaxel is a chemotherapy medication used to treat a number of types of cancer including prostate cancer. It may be used by itself or along with other chemotherapy medication. The machanism of Docetaxel is binds to microtubules and inhibit the cell division in S-phase. However, it is use castrate resistant or metastasis treatment by coupling with Prednisolone.

2.2.6.5 New drug for metastatic prostate cancer treatment before chemotherapy

Enzalutamide (Xtandi) is a non steroidal anti-androgen (NSAA) that used for the treatment of metastatic in prostate cancer, castration-resistant prostate cancer (CRPC) by prevents binding of AR to DNA and AR to co-activator proteins [13].

2.2.6.6 Monoclonal antibody therapy

Denosumab (Xgeva) is a monoclonal antibody that would help when prostate cancer spreads to bone [14]. This drug blocks the function of osteoclast, so prevent or delay of bone fracture. It is evaluated for bone metastases treatment.

2.2.6.7 Radiopharmaceuticals

Ra-223 (Xofigo) has been approved for use in prostate cancer petients with metastases to the bone but not to other internal organs [15]. Radium is like calcium and it migates to bone where it acts locally. As an alpha emitter, radiation from redium dose not travel far enough in the body to damage other healthy tissues. It is administered by an injection into vein. It can cause nausea, diarrhea, and low blood counts.

2.2.6.8 Bisphosphonates

The bisphosphonates are a drugs group that used to treat various conditions such as osteopenia and osteoporosis. It can also lower elevated blood levels of calcium. It works by affecting cells in bone called osteoclasts, thus preventing bone fractures and bone resorption. Zometa is the most common bisphosphonates for prostate cancer [16].

2.2.6.9 Immunotherapy/vaccine therapy

Provenge (Sipuleucel-T) is a vaccine therapy used to treat prostate cancer that has metastasized. Provenge therapy involves taking some of your own blood cells and growing them outside the body in the presence of a substance that is specific for prostate cancer. The cells are then given back to the patient by infusing them into the bloodstream. These cells can attack prostate cancer cells and can help program other blood cells to do the same such treatment cause few side effects and can prolong survival by several months [17]. **2.3 Definition of apoptosis**

Apoptosis is a process of cell death, which was programmed in multi-organisms. It plays important role as well as cell division, cell proliferation and cell differentiation. In normal cells, apoptosis regulates embryogenesis, development, homeostasis and immunity in order to maintain cell populations in tissues.

They are including cellular shrinkage, membrane blebbing, highly condensed of chromatin and fragmentation of nuclear, formation of apoptotic bodies and the exposure of phosphatidylserine at the membrane (Figure 3) [18]. The process of apoptosis is very complicated and needs many groups of proteins to mediate the initiation and progression [19].

Apoptosis is an essential target for many anticancer drugs [20, 21].
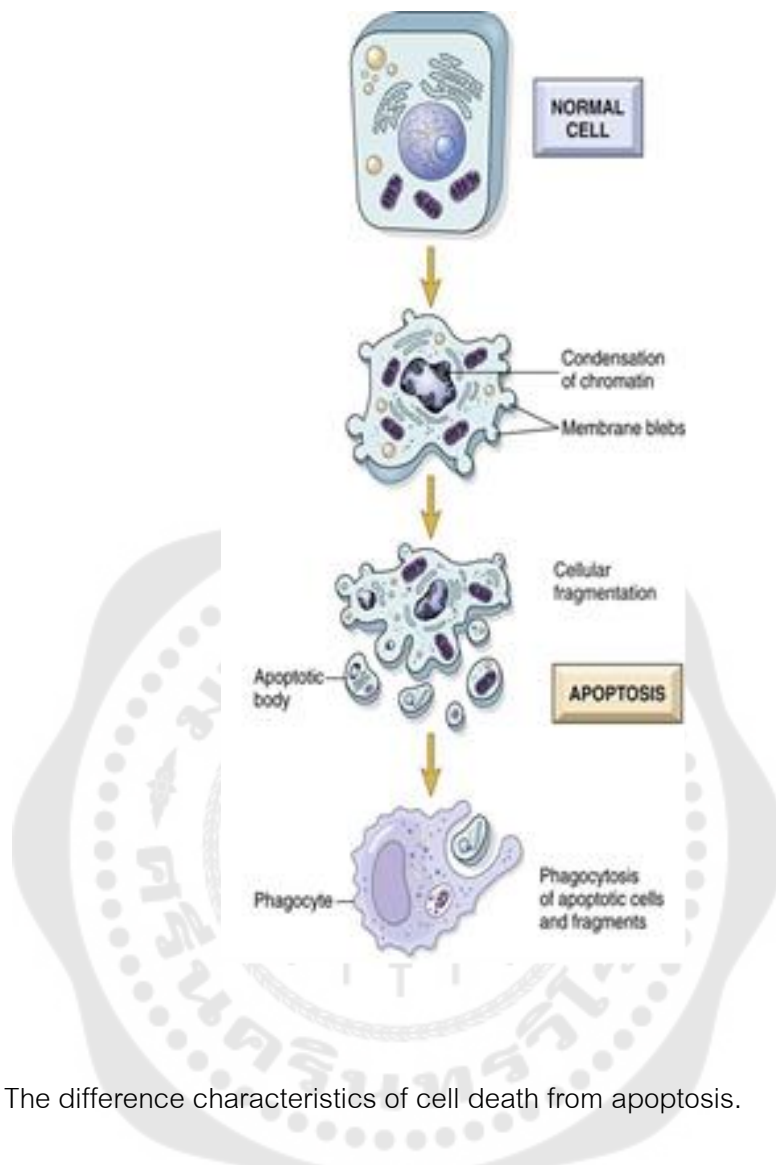
Figure 3 The difference characteristics of cell death from apoptosis.

Source: Vinay K, et al. 2010. Robbins & Cotran Pathologic Basis of Disease. United States: Philadelphia; 2010 [cited 2018 January 31]. Available from: https://basicmedicalkey.com/cell-injury-aging-and-death/.

2.3.1 Mediator of apoptosis

2.3.1.1 Caspases

Caspases (cysteine-aspartic proteases) are play critical roles in regulating inflammation and apoptosis. Caspases are synthesized as pro-caspases (or zymogen) which having N-terminal at pro-domain and C-terminal as the catalytic domain. Caspases need activation before function as protease. The activation is processed by proteolytic cleavage at specific aspartate residues of the pro-domain to become active and releasing of the large subunit (p20) and small subunit (p10). Then, the large and small subunit associate together to form the heterodimer caspase. This heterodimer caspase or activated form of caspase uses a cysteine side chain for catalysis peptide bond cleavage at aspartyl residues of their substrates [22]. Caspases are classified as three groups; group I or inflammatory caspases (caspase 1, 4, 5, 11,12, and 14), group II or initiator caspases (caspase 2, 8, 9 and 10), and group III or effector caspases (caspase 3, 6 and 7). (Figure 4) All three groups have common core structure of homologous domains of CARD (caspase recruitment domain), DED (death effects domain), large subunit and small subunit [23].
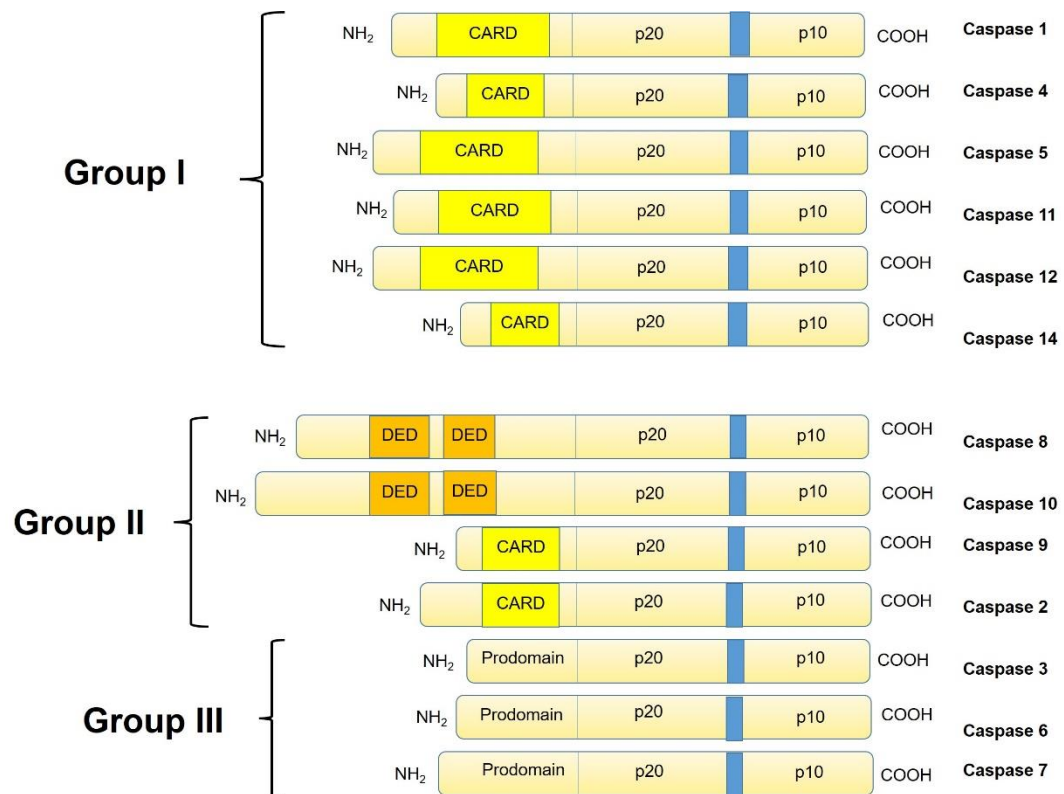
Figure 4 The classification of caspases. Homologous domains structure of caspase group I, II and III, the CARD, the DED, and the large (p20) and small (p10) catalytic subunits are indicated which modifiled from Lavrik IN, et al. (2005).

Caspase-3 is the most critical effector caspase found in most cells. This protein is an interacts with caspase-8 and caspase-9. Caspase-3 has been shown to prefer the peptide sequence of DEVDG (Asp-Glu-Val-Asp-Gly), where cleavage occurs between the aspartic acid (D) and the glycine (G). As an effecter caspase, the procaspase-3 became active-caspasse-3, which was cleaved by an initiator caspase when apoptotic signaling events have occurred [24]. The activated caspase-3 could induce cell death by cleavage of several critical proteins—for example, the endonuclease CAD (caspase-activated DNase). CAD is usually associated with its

inhibitor ICAD (inhibitor of caspase-activated DNase), so it cannot function in nuclear degradation. However, in apoptotic cells condition, activated caspase-3 cleaves ICAD to release CAD. This protein degrades chromosomal DNA into oligomeric fragments within the nuclei and causes nuclear fragmentation. Other important substrates cleaved by caspase-3 include nuclear enzyme poly (ADP-ribose) polymerase (PARP), protein kinase C, sterol-regulatory element binding protein (SREBPs), MEKK and the DNA fragmentation (DFF) [25].

Caspase-8 is the primary initiator caspases of the extrinsic apoptosis pathway. The activation of caspase-8 involves the interaction of the death ligand and death receptor. The signaling upon ligand interaction triggers the trimerization of death receptors and, consequently the aggregation of intracellular death domains (DD). This triggers homotypic interaction of adaptor proteins, Fas-associated death domain (FADD) and pro-caspase-8 to form a protein complex called death-inducing signaling complex (DISC). The autoactivation of pro-caspase-8 occurs in DISC but the precise mechanism is still unclear. However, after activation, the activated caspase-8 would further cleave downstream effector pro-caspase-3 and trigger apoptosis. In addition, activated caspase-8 could mediate BID cleavage to the truncated form (tBID) and trigger apoptosis via the mitochondrial pathway.

Caspase-9 is a key initiator caspase of intrinsic apoptosis pathway [26] that composite of three domains include N-terminal pro-domain, large subunit and a small subunit. The activation into active form undergoes autoproteolytic processing and activation in the apoptosome complex. This complex comprises cytochrome c, apoptosis protease activating factor 1 (Apaf1), pro-caspase-9, and dATP. Once activated, caspase-9 would further activate a downstream enzyme, caspase-3. However, apoptosis can be triggered by various factors such as DNA damage or oxidative stress [27, 28].

2.3.1.2 Inhibitor of apoptosis proteins (IAPs)

IAPs are a family of functionally and structurally related proteins that regulates multiple pathways such as cytokinesis, proliferation, differentiation, apoptosis,

and signal transduction [29, 30]. The structure of IAP consists of BIR1-BIR3 domain, ubiquitin-associated domain (UBA), conserved caspase recruitment domain (CARD), really interesting new gene (RING) domain.

The human IAP family contains eight members as shown in Figure 5. The characterized of IAP is XIAP, which binds caspase-9, effector caspases as caspase-3, and caspase-7, thereby inhibiting their activation and preventing apoptosis [31].
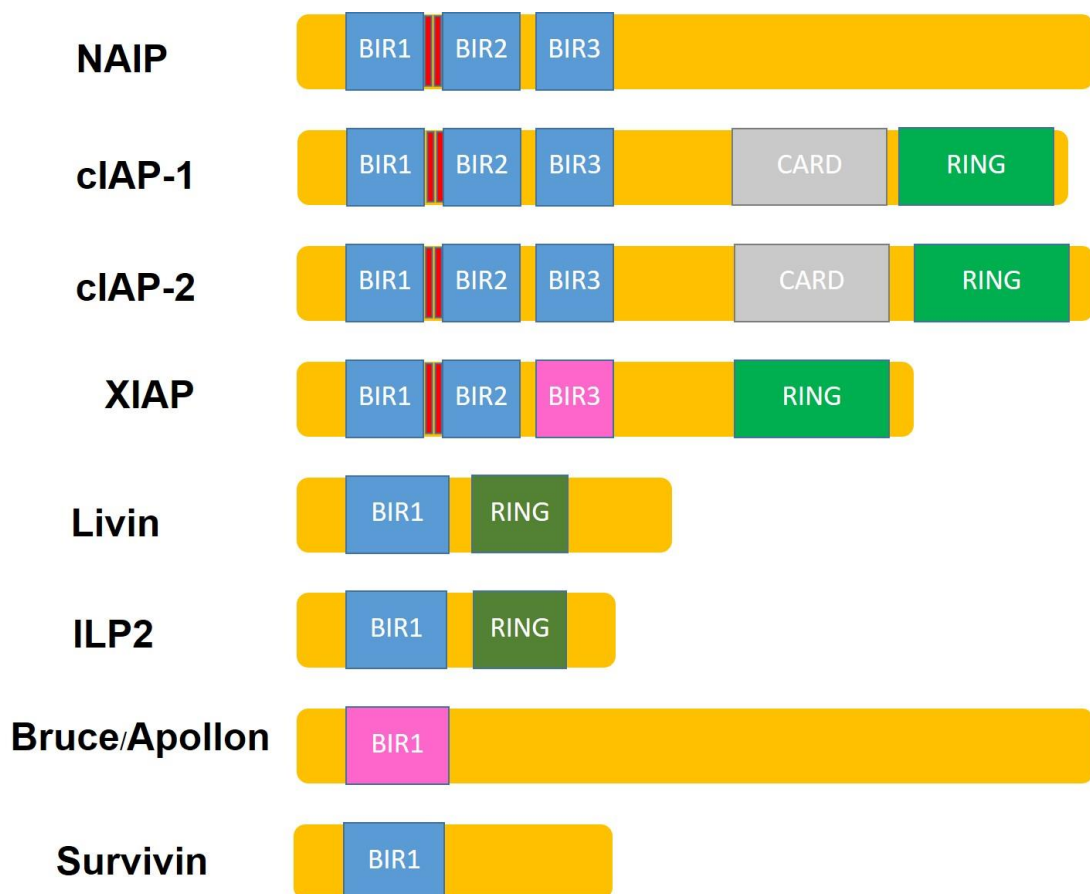
Figure 5 Mammalian Inhibitor of apoptosis proteins (IAPs) family which modified from Ribe EM, et al. (2008).

Source: Ribe EM, Serrano-Saiz E, Akpan N, Troy CM. Mechanisms of neuronal death in disease: defining the models and the players. Biochem J. 2008;415(2):165-82.

2.3.1.3 BCl-2 family protein

Bcl-2 and/ or B-cell lymphoma 2 proteins are gene encodes of Bcl-2 gene in human. They play crucial role in promoting cellular survival and block the apoptotic death by controlling the mitochondrial membrane permeability [32, 33]. The Bcl-2 family consists of both anti-apoptotic and pro-apoptotic members. To date, a total of 28 genes have been identified in the Bcl-2 family [34]. All members of homology entitled the Bcl-2 homology (BH) domains including BH1, BH2, BH3 and BH4.

• Anti-apoptotic proteins

The Bcl-2 family proteins in this group are BCL-2, BCL-xL, BCL-w, MCL-1, and A1/BFL-1. They have conserved domains of BH1, BH2, BH3 and BH4 [35]. Their function is promoting cell survival from UV, gramma-irradiation, cytokine deprivation and chemotherapeutic drugs [36].

• Pro-apoptotic and BH-3 only proteins

Pro-apoptotic Bcl-2 family proteins are subdivided into two groups as the Bax family that containing BH1, BH2 and BH3 and the BH3 only family that have only BH3 in their structure. The members of Bax family are Bax, Bak and Bok/MTD, while the BH3 only family are Bim, Bid, and Bad [37].

2.3.1.4 Cytochrome C

Cytochrome C is a 12 kDa protein located in the mitochondrial intermembrane space. Cytochrome C is important for the electron transport chain process and plays a crucial role in cellular oxidations in both plants and animals [38].

In addition, the damage of mitochondria from intracellular stresses activates Bax family to form channel at outer mitochondrial membrane. This triggers the release of cytochrome c into the cytosol [39] and further forming apoptosome complex with Apaf-1, inactive/ pro-caspase-9 and dATP. The apoptosome complex induces caspase-9 activation and further caspase-3 activation. Then, the release of cytochrome c is known to be one crucial marker of apoptosis process.

2.3.1.5 Smac/DIABLO

Smac/DIABLO is a mitochondrial protein. It is also known as second mitochondria-derived activator of caspases (SMAC). This protein promotes apoptosis by

directly binding to the inhibitor of apoptosis proteins (IAPs), localized in the mitochondrial intermembrane space [40, 41].

2.3.1.6 Apoptosis inducing factor (AIF)

Apoptosis inducing factor (AIF) is an ancient conserved flavoprotein that has both NADH oxidizing and apoptosis-inducing activity. It resides in the mitochondrial intermembrane space and oligomerizes in response to cytochrome c release to form a large complex known as the apoptosome.

2.3.1.7 Endonuclease G

The endonuclease G is one of the most abundant nuclease enzyme in eukaryotic cells. It is encoded in nucleus and imported to the mitochondrial membrane space. It involves apoptosis by translocating from mitochondria to nucleus and degrade the chromatin [42]. Endonuclease G cleaves DNA at GC tracts into large (50 to 300 kb) fragments different from the action of CAD. In normal condition, endonuclease G is bound to Hsp70 and will dissociate when oxidative stress is activated [43, 44].

2.4 Mechanism of apoptosis

Apoptosis can be processed as two pathways: extrinsic and intrinsic signaling. The extrinsic pathway is induced via the specific binding of death ligand and death receptor such as TNF/TNF receptor, Fas / Fas receptor etc. The binding triggers the association of adaptor protein (cytoplasmic death domain with Fas-associated death domain adaptor protein, FADD) and inactive/pro-caspase-8 at the cytosolic part of the receptor. This formation is a death-inducing signaling complex (DISC), which activates procaspase-8 into the active form, resulting in effector caspases actives such as caspase-3 or caspase-7, causing cell death or apoptosis [45-47].

In contrast, the intrinsic pathway (mitochondrial pathway), can be triggered in response to various nonreceptor-mediated stimuli such as hypoxia, radiation, chemical insults, reactive oxygen species, DNA damage, some chemotherapeutic agents and toxins [48]. In addition, other stimuli such as growth factors, hormones, and cytokines can cause the failure to suppress death programs [49].These factors trigger the changes in the inner mitochondrial membrane that resulting in the formation of pore at

the outer mitochondrial membrane [50]. Bcl-2 proteins that influence this mitochondrial membrane permeability include pro-apoptotic members. The changes in membrane permeability cause the free release of pro-apoptotic proteins such as Smac/DIABLO, and cytochrome c from the intermembrane space into the cytosol. In the cytosol, cytochrome c binds and activates apoptotic peptidase activating factor 1(Apaf-1) and pro-caspase-9, forming an "apoptosome." The active form of caspase-9 further activates caspase-3/caspase-7, leading to cell death (Figure 6) [51]. In addition, it has cross-talk between extrinsic and intrinsic pathway, which can be activated through Bid protein. Bid is activated by caspase 8 activities, contributing to cleavage Bid protein into 2 fragment include p17 and p15 to became active form as truncated Bid (tBid). This protein translocated to outer membrene of mitochondria to form pore and enhance the recruitment of cytosolic Bax into mitochondrial membrane, resulting to cytohrome c release and caspase 3/7 activation undergoing apoptosis.
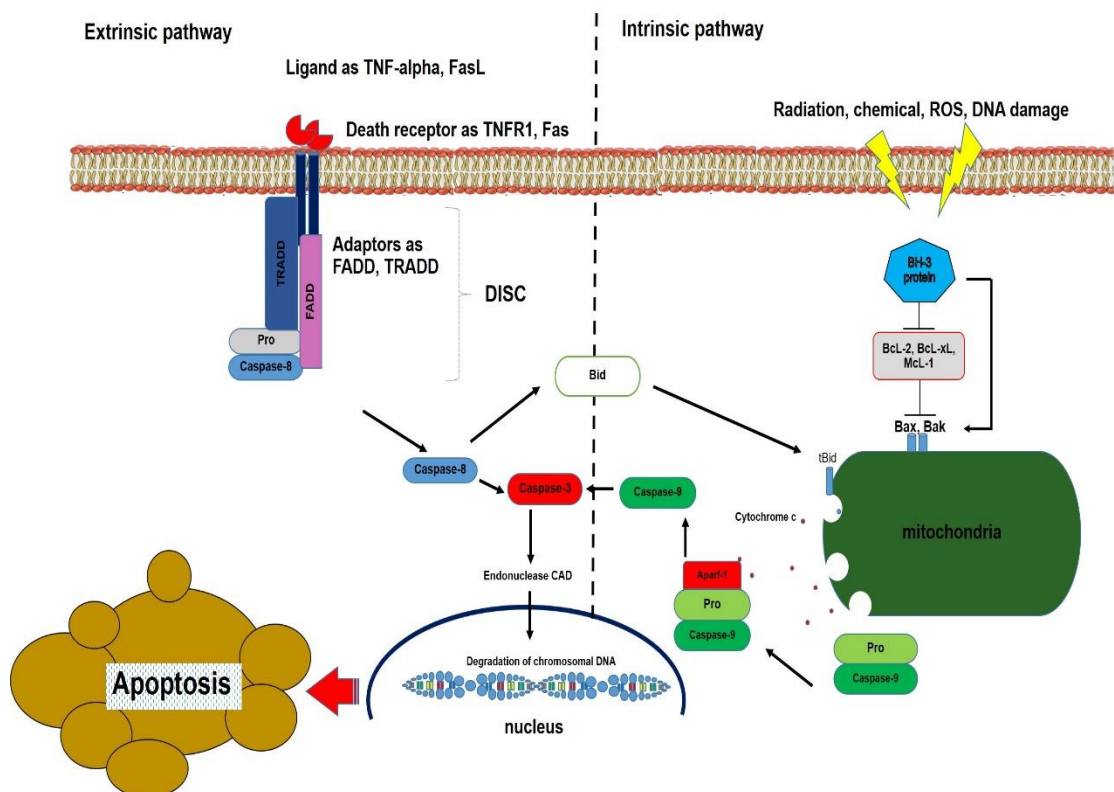
Figure 6 The extrinsic and intrinsic pathways of apoptosis which modified from Cuda CM, et al. (2016).

Source: Cuda CM, Pope RM, Perlman H. The inflammatory role of phagocyte apoptotic pathways in rheumatic diseases. Nat Rev Rheumatol. 2016;12(9):543-58.

2.5 Metastasis

Cancer cells have the property of spreading locally by moving to normal tissue. They can also apply to nearly tissues, or organs, lymph nodes. In addition, they can spread to distant sites of the body as known called metastatic cancer. This process comprises of several steps for moving cells out of the tumor. The common sites of metastasis are shown in Table 1.

Table 1 Common sites of metastasis.

Cancer Type	Main Sites of Metastasis
Bladder	Bone, liver, lung
Breast	Bone, brain, liver, lung
Colon	Liver, lung, peritoneum
Kidney	Adrenal gland, bone, brain, liver, lung
Lung	Adrenal gland, bone, brain, liver, other lung
Melanoma	Bone, brain, liver, lung, skin, muscle
Ovary	Liver, lung, peritoneum
Pancreas	Liver, lung, peritoneum
Prostate	bone, liver, lung, Adrenal gland
Rectal	Liver, lung, peritoneum
Stomach	Liver, lung, peritoneum
Thyroid	Bone, liver, lung
Uterus	Bone, liver, lung, peritoneum, vagina

Source: Metastatic Cancer: When Cancer Spreads [Internet]. MD: National Cancer Institute; 2014 [cited 2014 May 20]. Available from https://www.cancer.gov/types/metastatic-cancer.

2.5.1 Steps of Metastasis

Metastasis is a complex process that involves several steps. Firstly, the primary tumor starts the vascularization around the cancer itself. After that, cancer cells are detached from the primary site/tumor and start invading through the extracellular matrix (ECM) into the vascular system. To do this step, cancer cells need to secrete special enzymes called matrix metalloproteinase (MMP) to degrade ECM and basement membrane. Once the cancer cells move into the blood circulation or called intravasation, cancer cells have to associate with other cells in the circulation and travel along the blood vessels until they find a suitable place to settle; the cancer cells then enter and grow in new tissue. This step is called extravasation, and again it needs MMP to invade through the basement membrane to start the secondary tumor (Figure 7) [52].
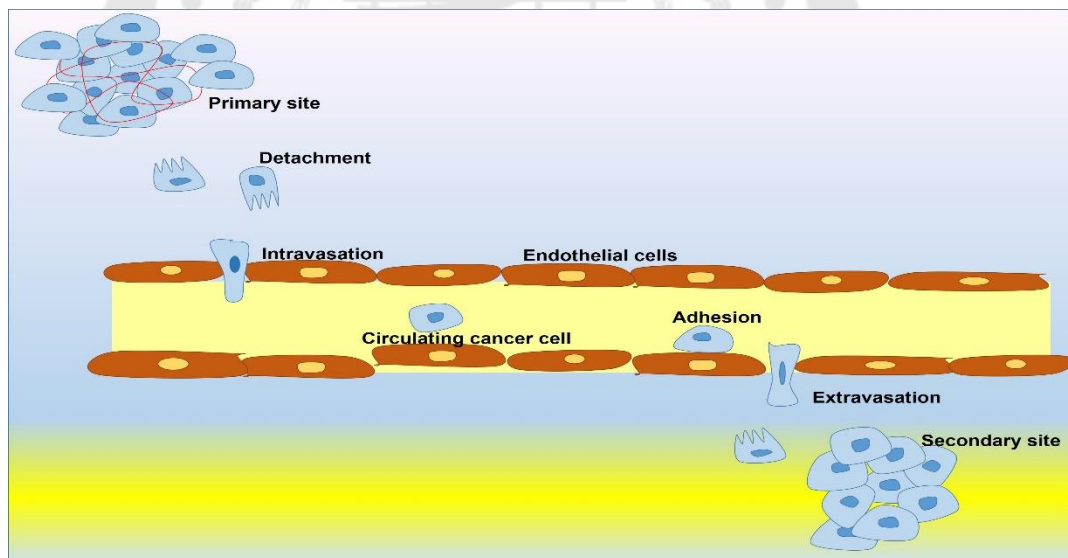
Figure 7 The steps for metastasis to site in the body with cancers interactions and mechanical forces in metastasis, which modified from Wirt D, et al. (2011).

Source: Wirtz D, Konstantopoulos K, Searson PC. The physics of cancer: the role of physical interactions and mechanical forces in metastasis. Nat Rev Cancer. 2011;11(7):512-522. Published 2011 Jun 24. doi:10.1038/nrc3080

2.5.2 Metrix metalloproteinases

Matrix metalloproteinases (MMPs) family are calcium-dependent zinc-containing endopeptidases. MMPs are thought to play a significant role in physiological ECM tissue remodeling such as cell proliferation, cell movement (adhesion/dispersion), differentiation, angiogenesis, inflammation, apoptosis, uterine cycling, postpartum involution, and tissue repair [53, 54]. Most MMPs are synthesized in the latent form (Zymogen/inactive form). They are secreted as pro-enzyme/inactive proproteins and require extracellular activation.

Recent studies have classified MMPs as 23 types and subdivided them into groups including collagenases, stromelysins, matrilysins, gelatinases, and others membrane-type [55]. They have common three domains (Figure 8), which is linked to the catalytic domain by a flexible hinge region [56]. MMPs that have important role in tumor invasion and metastasis are gelatinases-A (MMP-2: 72 kDa) and gelatinases-B (MMP-9: 92 kDa). In mice that did not have MMP-2 gene, demonstrated a decrease in the angiogenesis and tumor progression process as well as MMP-9 gene that not found metastasis and cancer progression [57]. Thus, it is considered that MMP is important for the spread of cancer and would be a target for new anticancer agent [58].
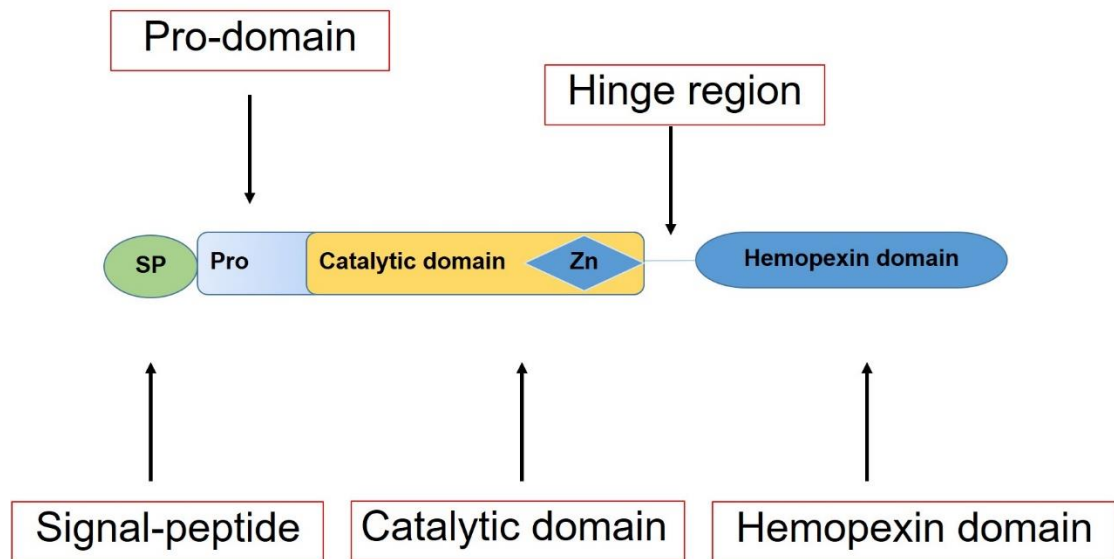
Figure 8The general protein structure domain of MMPs. The structure consist of pro-domain has the cysteine residue ligates the zinc ion in the catalytic domain for prevention the enzyme-active and hemopexin-like module of MMPs contains four repeat units connected by a disulfide bond which modified from Yong VW, et al. (2001).

Source: Yong VW, Power C, Forsyth P, Edwards DR. Metalloproteinases in biology and pathology of the nervous system. Nat Rev Neurosci. 2001;2(7):502-11.
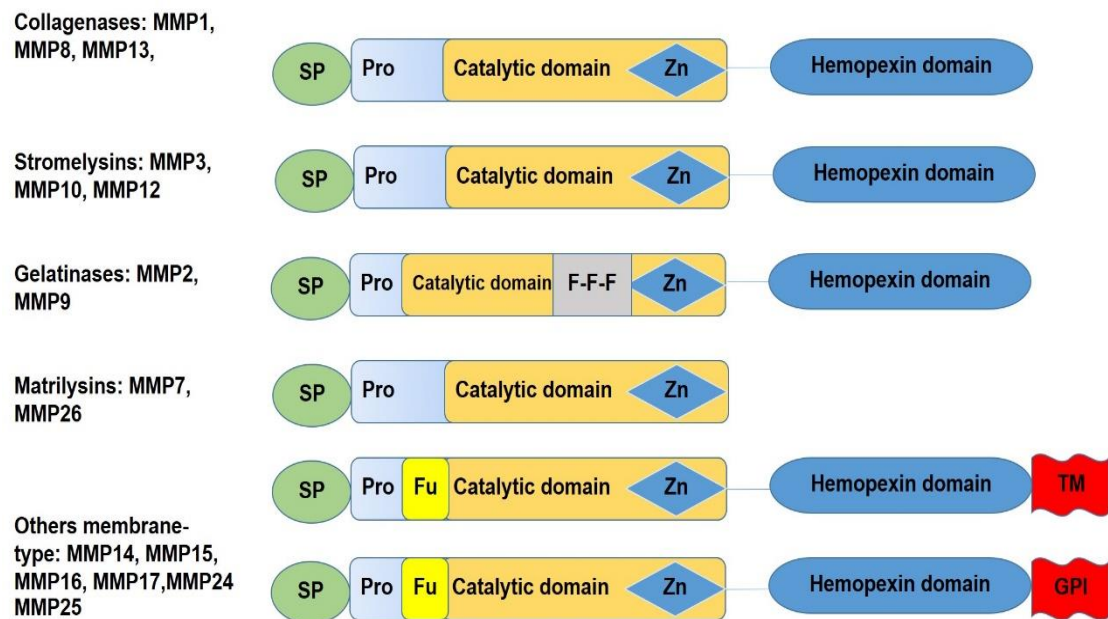
Figure 9 Protein structure classification of Mammalian MMPs as 5 Groups include, collagenases, stromelysins, gelatinases, matrilysins, and others membrane type which modified from Gong Y, et al. (2014).

Source: Gong Y, Chippada-Venkata UD, Oh WK. Roles of matrix metalloproteinases and their natural inhibitors in prostate cancer progression. Cancers (Basel). 2014;6(3):1298-327.

2.5.4 Inhibitor of MMPs

The tissue inhibitor of metalloproteinases (TIMPs) are specific inhibitors which composed of four families as TIMP-1, TIMP-2, TIMP-3, and TIMP-4 [59]. These inhibitors participate in controlling the MMPs activities in tissues. TIMP-1 is a 28.5 kDa glycoprotein containing 184 amino acid. Generally, TIMP-1 can inhibit both active matrix metalloproteinases-9 (MMPs) and pro-MMP-9 by forming non-covalent complexes with high affinity and regulate remodeling process during degradation of extracellular matrix [60]. Previous studies demonstrated that overexpress of TIMP-1 could inhibit apoptosis in breast epithelial cell lines by activation of focal adhesion kinase (FAK) signaling for the cell survival pathway [61, 62]. TIMP-2 is a 21.5 kDa non-glycosylated protein that has 194 amino acids. There is a 41% sequence homology with TIMP-1. In addition, It plays an important role in ECM degradation associated with cancer metastasis. However, TIMP-2 is an inhibitor that can bind to the either latent or active form of MMP-2 [63]. TIMP-3 is a 21 kDa unglycosylated protein with 188 amino acids. It's a peptidases group involved in degradation of the ECM and inhibits all MMPs, especially MMP-2 and MMP-9 [64]. TIMP-4 is a family of extracellular matrix (ECM) metalloproteinase inhibitors that are overexpressed in several cancers [65]. TIMP-4 has a molecular weight 22.4 kDa and does not have any N-glycosylation site. TIMP-4 also affects the cell death that consistent with the increase of apoptosis-signaling protein such as control of apoptosis from Inhibitors of Apoptosis Proteins (IAP), FLICE-like inhibitor proteins (FLIP) and decreasing of Bcl-2 family members in cervical cancer cells [66, 67]. In the same way, TIMP-4 can inhibit the tumor growth and metastasis of human breast cancers transfected with a full-length TIMP-4 cDNA [68].

2.6 Gac fruit

Momordica cochinchinensis (Lour.) Spreng. or ฟักข้าว is a climber plant in the family Cucurbitaceae the same as cucumber and balsam pear. *M cochinchinensis* also known as Gac, Spiny Bitter Gourd and Sweet Gourd. Gac is found throughout the Southeast Asian region, South China and Northeastern Australia. In Vietnam, Gac is commonly used for cooking or festive occasions in most rural areas (Figure 10).

Figure 10 The morphology of *M. cochinchinensis* or Gac friut.

Source: Chainumnim.S (2016).

2.6.1 Characteristic of *M. cochinchinensis*

Gac is a tropical vine plant. It climbs along the home fence or another plants. Leave is heart-like shape, alternate with three to five deeply separated lobes. Tendrils are simple and stout. Flowers are white to ivory yellow. Flowering occurs during June to September and fruiting during December and January. The Fruit has mild taste just like avocado. (Figure 11)

A1

A2

A3

A4

A5

A6
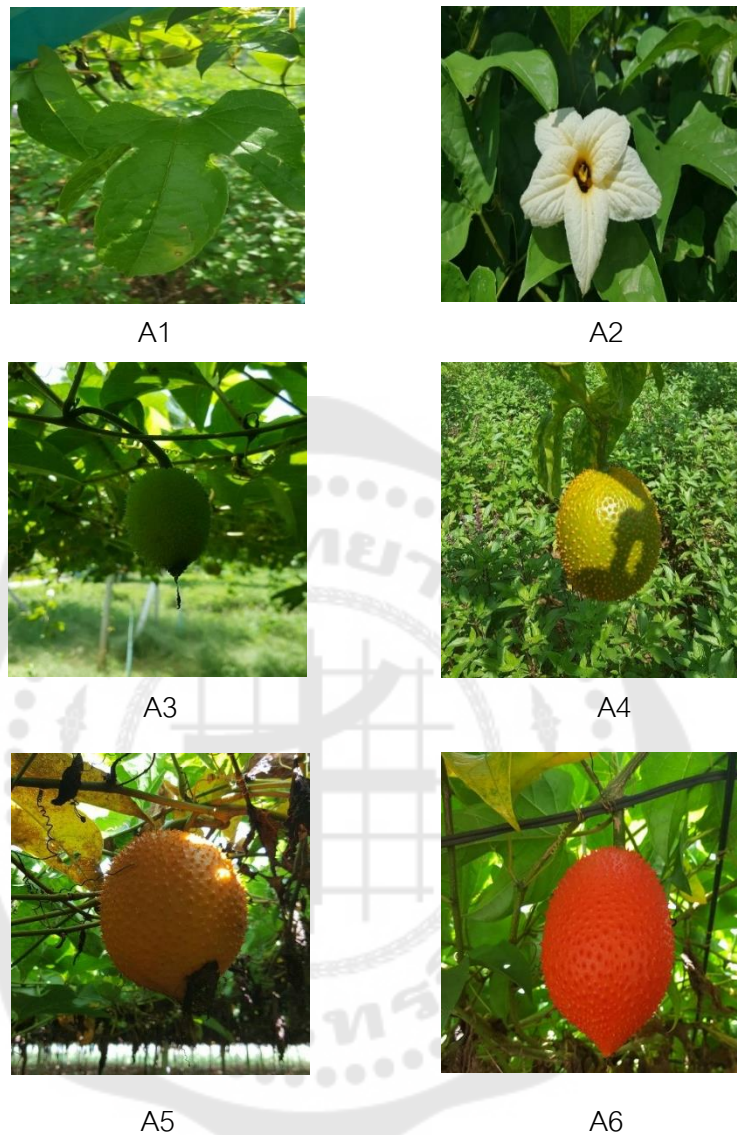
Figure 11 The characteristic of *M. cochinchinensis* as leaves (A1), flower (A2), young fruit to mature fruit (A3-6).

Source: Chainumnim.S (2016).

Gac is a good source of nutrients, vitamins, minerals and a high carotenoid content, especially lycopene and Beta-carotene. It contains high amount of lycopene at about 10-12 times of other plants, while the amount of beta carotene is higher than that of carrot 10 times. Gac aril is the major part that containing lycopene and beta carotene

which have been reported of having the anti-oxidant activity [69-71]. In addition, the crude ethanolic extract of aril has been found to reduce blood pressure, decreasing oxidative stress and enhancing antioxidant glutathione in rat receiving oxidative stress inducer, L-Name [72]. Moreover, the component of Gac aril extract demonstrated non-toxic property as it was not damaged the male reproduction system of mice [73]. Fatty acids composition in Gac has also been proposed to reduce coronary heart disease [74]. Particularly, Gac aril that 22 percentage quantity of fatty acid is composed of oleic acid (32%), palmitic acid (29%) and linoleic acid (28%). While, Gac seeds consisted of most stearic acids (60.5%) and other acids such as linoleic acid (20%), oleic acid (9%) and palmitic acid and trace amount of arachidic, cis-vaccenic, linoleic, palmitoleic, eicosa-11-enoic acids, eicosa-13-enoic acids [75, 76]. Apart from this, Gac fruit is recognized as healthy food whilst 100 gram is composed of 10.5 g of carbohydrate, 1.8 g of dietary Fiber, 2.1 g of protein, 56 mg of calcium, 6.4 mg of phosphorus, 7.9 g of total fat, 0.7 g of ash and 77 g of water [77, 78]. Furthermore, seeds part consist of momordins I-III, momordins Ia-c, and momordins IIa-d, saponins, and peptides as anticancer [4], antioxidant [79], anti-inflammation [80], and reno-protective activities [81].

Additionally, it has been demonstrated that Gac is a remarkable fruit with variety of biological activities. For example, peel extract of Gac showed antibacterial activity, scavenging activity and anti-genotoxicity [82]. Besides, it is reported that Gac has ability of anticancer. Seed extract could inhibit proliferation, metastasis of lung cancer [3] and induce apoptosis via multiple signaling [4]. In addition, Zheng, et al (2015) reported that *M. cochinchinensis* seed extract suppressed MDA-MB-231 cell growth, G2 phase arrest and apoptosis induction [83]. Aril part, Water extract from Gac fruit suppressed the proliferation of colon cancer (colon 26-20) and hepatocarcinoma (HepG2) [6]. Petchsak, et al (2015) reported that *M. cochinchinensis* aril extract induced apoptosis via both intrinsic and extrinsic pathways of signaling [84].

CHAPTER 3

MATERAILS AND METHODS

3.1 Research Framework

Aim: Study the effect of MC on the viability and migration ability

of prostate cancer cells

Part I

Part II

MC extract preparation from stems, roots, seeds, and leaves

Preparation of aril extracts from different methods

Cytotoxicity screening comparing between

prostate cancer, other cancer cell types and normal cells

Cell viability assay

The most effective extract was selected

Most effective extract

Biological activity

Chemical characterization

Apoptotic detections

Pure compound

1.Nuclear staining

2.Sub-G1 detection

3.Mitochondria membrane potential

4.Protein expressions

1. Cell damage assay

2. Cell cycle assay

3. Wound healing assay

4. Transwell insert migration assay

5. Signaling proteins determination

3.2 Materials

In this study can divided material into; (1) antibodies, (2) chemicals and reagents, (3) equipments.

3.2.1 Antibodies

1. Anti-mouse IgG, HRP-link Antibody (Cell Signaling Technology)

2. Anti-rabbit IgG, HRP-link Antibody (Cell Signaling Technology)

3. Bcl-xl, Product no. 2764T, (Cell Signaling Technology)

4. Caspase-3, Product no. 9662, (Cell Signaling Technology)

5. GAPDH, Product no. 2118S, (Cell Signaling Technology)

6. Mcl-1, Product no. 5453T, (Cell Signaling Technology)

7. MMP-9, Product no. 13667, (Cell Signaling Technology)

8. Noxa, Product no. 14766S, (Cell Signaling Technology)

9. TIMP-1, Product no. 8946, (Cell Signaling Technology)

3.2.2 Chemicals and reagents

1. 0.25% trypsin-EDTA, (Gibco)

2. 40% Acrylamind-Bis ready-to use, (Merck)

3. Ammonium persulfate (APS), (Sigma-Aldrich)

4. Bovine serum albumin (BSA), (Sigma-Aldrich)

5. Crystal violet, (Sigma-Aldrich)

6. Dimethyl sulfoxide (DMSO), (Sigma-Aldrich)

7. Dulbecco's Modified Eagle Medium (DMEM), (Gibco)

8. Eagle's minimum essential medium (EMEM), (Gibco)

9. Fetal bovine serum (FBS), (Gibco)

10. Hydrogen peroxide (H_2O_2), (Merck)

11. Hoechst 33342, (Invitrogen)

12. LDH assay (G-Bioscience, St. Louis, MO)

13. JC-1 kit, (Biotium)

14. MTT, (Sigma-Aldrich)

15. Propidium iodide (PI), (Merck)

16. Penicillin-Streptomycin, (Gibco)

17. Roswell park memorial institute medium (RPMI-1640), (Gibco)

18. Sodium carbonate ($NaCO_3$), (Merck)

19. Sodium dodecyl sulfate (Fisher chemical)

20. Trypan blue dye, (Sigma-Aldrich)

21. TEMED, (Omnipur)

3.2.3 Equipments

1. Bruker Avance 300 FT-NMR spectrometer

2. Column chromatography

3. CO_2 incubator

4. Evaporator

5. Fluorescence microscope (Olympus IX73, Tokyo, Japan)

6. Gel documentation (UVITEC)

7. Hemacytometer (Boeco)

8. Jasco-1020 polarimeter.

9. Inverted microscope (OLYMPUS CKX41)

10. Multi-Mode Microplate reader (Synergy HT, BioTek)

11. TLC silica gel 60 (>230 mesh), (Merck)
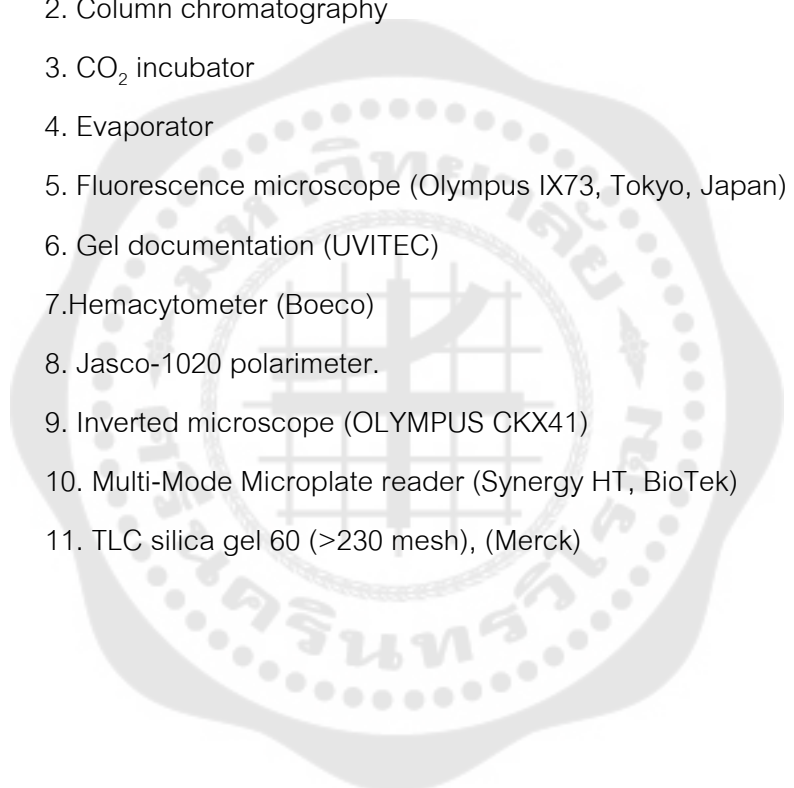
3.3 Part I: Study the effect of crude extracts from leaves, seeds, stems, and roots of *M. cochinchinensis* on prostate cancer cells proliferation and apoptosis mechanism

3.3.1Preparation of MC extracts

3.3.1.1 Plant material

MC plants were locally cultivated in a community in Nakhon Pathom, Province, Thailand. Leaves, seeds, stems and roots of the adult plant were collected in September 2016. A voucher has been deposited under number SC001 at the Laboratory of Natural Product Research Unit, Department of Chemistry, Faculty of Science, Srinakharinwirot University, Thailand.

3.3.1.2 Methanol extract

Each plant part was thoroughly washed with tap water, cut into small pieces, and sun-dried. The MC's leaves, seeds, stems, and roots (each 100 g) were individually macerated in MeOH (500 mL) 3 times every two weeks at room temperature. After that, the methanol extract was filtered (Whatman no. 1 paper), combined, and evaporated to dry using a rotary evaporator at 40 °C. The dried MeOH extracts (leaves 3.15 g, seeds 6.25 g, stems 0.77 g, and roots 0.8 g) were stored at -20 °C before cytotoxic screening. All parts were dissolved in dimethyl sulfoxide (DMSO) by a water-bath sonicator until completely dissolved.

3.3.2 Cell lines and cell culture

PC-3 (human androgen-independent prostate adenocarcinoma; grade IV cell line (ATCC[®] CRL-1435™)), A549 (human non-small cell lung cancer (NSCLC) cell line (ATCC[®] CCL-185™)), HeLa (human cervical cancer cell line (ATCC[®] CCL-2™)), and MDA-MB-231 (human breast adenocarcinoma cancer cell line (ATCC[®] HTB-26™)) were purchased from ATCC (American Type Culture Collection). All the cells were maintained as a monolayer in Dulbecco's modified Eagle's medium (DMEM) supplemented with 10% fetal bovine serum (FBS), 100 units/mL penicillin and 0.1 mg/mL streptomycin and incubated at 37 °C in an atmosphere of 5% CO_2.

3.3.2.1 Cell viability determination

The viability of cells were firstly investigated by using an MTT assay. This method is a colorimetric assay that measures the ability of mitochondrial succinate

dehydrogenase enzymes to convert the yellow tetrazolium MTT solution into an insoluble purple formazan product. Then, the color formation is correlated to the number of living cells. To quantitate the color intensity, the optical density (OD) was used at a wavelength of 570 nm.

The cell viability was performed using an MTT assay. Briefly, the cells were harvested with 0.25% trypsin containing 1 mM EDTA, plated in 96-well plates at densities of 1×10^4 cells per well, and allowed to adhere for 24 h. Next, the cells were treated with various concentrations of the compound tested, including MC extracts (0–5 mg/mL), while the concentrations of dimethyl sulfoxide (DMSO; 0.5%) were used as the vehicle control. Then, all the plates were incubated for 24 h at 5% CO_2, 37 °C. After incubation, the MTT solution (5 mg/mL) was added to each well, and further incubated for 4 h. Subsequently, the medium was carefully removed, and DMSO was added to each well to dissolve the formazan precipitate. The cell viability was evaluated by measuring the OD at wavelength 570 nm with a multimode microplate reader (Synergy; BioTek Instruments, Inc.). The inhibitory concentration at 50% (IC_{50}) was calculated with GraphPad Prism 5.03 software (GraphPad Software, Inc., San Diego, CA, USA).

3.3.2.2 Determination of nuclei morphology

The nuclear condensation and fragmentation, markers of apoptosis were determined using Hoechst 33342 (A DNA-specific fluorescence dye) staining. This dye is a bis-benzimidazole compound that can also pass into the cell and binds explicitly to AT-rich sequences in the minor groove of double-stranded DNA. When Hoechst 33342 binds to DNA in apoptotic cells would result in the blue-fluorescent nucleic, which are simply identified under a fluorescence microscope.

The effect of stem extract on chromatin condensation and fragmentation of PC-3 cells, characteristic of the apoptotic nuclei, was investigated using Hoechst 33342 staining. Briefly, the cells were harvested with 0.25% trypsin containing 1 mM EDTA, plated in 6-well plates at a density of 5×10^5 cells/well containing 10% FBS medium, and allowed to adhere for 24 h. After that, the medium in each well was removed and the fresh medium containing drug concentrations; at 0, 0.3, 0.6, 0.9 and

1.2 mg/mL, respectively, were replaced. The plate was incubated until completely times. Then, Hoechst 33342 was added to each well at a final concentration of 10 µM and further incubated in the dark for 30 minutes at 37°C in 5% CO_2. The characteristics of cells with fragmented and condensed nuclei were recorded under a fluorescence microscope (IX73; Olympus, Tokyo, Japan) using a magnification of 20×.

3.3.2.3 Determination of sub-G1 induction

The cell cycle consists of two major phases: the interphase; G0, G1, S, G2, and the mitotic (M) phase. During interphase, radiation, drugs, chemicals and stress can interfere DNA synthesis process leading to the loss of nuclear DNA content in each phase. This event of each phase can be observed by using a red-fluorescent dye and analyzed by using flow cytometry. The propidium iodide is commonly a red-fluorescent dye used to evaluate cell viability or DNA content, which interacts with DNA. The fluorescent intensity of the flow cytometer correlated with amounts of DNA in each phase and represented DNA content as a histogram.

The sub-G1 content effect of stem extract on PC-3 cells was detected using PI staining followed by flow cytometry to detect the sub-G1 peak. Cells were harvested with 0.25% trypsin containing 1 mM EDTA, plated in 6-well plates at 5×10^5 cells per well, and allowed to adhere overnight. Then, the cells were treated with or without DMEM containing drug concentrations at 0, 0.6, 0.9, and 1.2 mg/ mL, respectively. After incubation for 24 h, the cells were washed with cold 1X PBS 2 times, harvested and centrifuged at 1,800 rpm for 5 min. Subsequently, the cells were fixed in ice-cold 70% ethanol overnight at 4 ^{o}C. After fixation, the cells were removed EtOH out and washed two times with ice-cold PBS. The fixed cells were incubated in 0.5% Triton-x, 50 µg/mL PI, and 100 µg/mL RNase A for 30 min at 37 ^{o}C. Propidium iodide (PI)-DNA complexes were quantified using FAC Scan cytometry (Merk Millipore Crop., Merck KGaA).

3.3.2.4 Measurement of Mitochondrial Membrane Potential (MMP)

JC-1 is internalized and concentrated by respiring mitochondria and can reflect changes in MMP in living cells. During apoptosis process, the protein related-apoptosis contribute to mitochondrial loss membrane potential as pore and release

cytochrome c to the cytoplasm [85]. This event is associated with protein signaling cascades, resulting to activate caspase-9/ -3 activities and leading to cell death as apoptosis. Therefore, the mitochondrial membrane potential is considered as a key intrinsic apoptosis marker [86]. Mitochondrial membrane potential is commonly detected by using a JC-1 as cationic fluorescent dye, which can accumulation in mitochondria. In general, High-potential mitochondria represent in healthy cells, the dye forms complex as a J-aggregates, red-fluorescent signal, whereas low potential mitochondria represent in apoptotic cells, the dye remains monomer as green fluorescence signal.

The mitochondrial membrane potential was monitored by using JC-1 staining. To examine the effect of stem extract induced apoptosis in PC-3 cells, the cells were treated with various concentrations (0, 0.6, 0.9, and 1.2 mg/mL) of stem extract, and 0.5% DMSO was used for the control group. Next, the cells were collected by trypsinization and centrifuged at 500× g for 5 min at 4 °C, followed by PBS washing. After that, the cells were incubated with JC-1 dye for 15 min, centrifuged at 500× g for 5 min, re-suspended in PBS, and analyzed by using a flow cytometry (Guava EasyCyte and Guava Mitopoteintial software version 3.3 (Merck KGaA)).

3.3.2.5 Determination of Noxa, caspase-3, Bcl-xL, Mcl-1, by using Western blot assay.

Western blotting is a technique that used worldwide for detection and analysis of protein expression. To perform the experiment, PC-3 cells were seeded in 6-well plate at a density of 5×10^5 cell per well in DMEM containing 10% FBS and cultured for 24 h. Then, the cells were treated with various concentrations: (0-1.2 mg/mL) stem extract, for 24 h. After incubation, the medium and cells were collected and centrifuged at 3,500 rpm for 5 min. The cells were washed for 2 times with cold-PBS and the pellet cells were lysed with RIPA buffer (1 M Tris-HCl pH 7.4, 5 M NaCl, 20% NP-40, 10% sodium deoxycholate, 20% SDS and protease inhibitor cocktail) on ice for 30 min, centrifuged at 14,000 g at 4°C for 20 min. The protein concentration was measured using a Bradford protein assay. Equal amounts (20-30 µg) of the total protein extracts were separated by 8%-15% SDS-polyacrylamide gel electrophoresis (SDS-PAGE) and transferred to PVDF membranes. The membranes were blocked with 5% skim milk in

TBS-T buffer (5% w/v skim milk, 1X Tris-buffered saline solution and 0.1% Tween-20) at room temperature for 1 h and then incubated with primary antibodies against caspase-3 (1:1,000; product no. 9662), Bcl-xl (1:1,000; product no. 2764T), Mcl-1 (1:1,000; product no. 5453T), Noxa (1:1,000; product no. 14766S), and GAPDH (1:1,000; product no. 2118S; all from Cell Signaling Technology, Inc.) at 4°C overnight. After washing 3 times, the membranes were incubated with horseradish peroxidase-conjugated anti-mouse (1:5,000; product no. 7076P2) or anti-rabbit IgG antibodies (1:5,000; product no. 7074P2; both from Cell Signaling Technology, Inc.) for 1 h. The membranes were visualized by enhanced chemiluminescence using ECL plus™ western blotting detection reagents (Bio-Rad Laboratories). The intensities of the protein bands were quantified by ImageJ software [Java 1.8.0_112 (64_bit)].

3.3.2.6 Phytochemical isolation of the stem extract

For further phytochemical isolation of the stem extract that exhibited the highest cytotoxicity screening, dried stems (16 kg) were collected and then extracted with MeOH at room temperature to yield a brownish residue (320 g). Then, the dried MeOH stem extract was suspended in water and successively partitioned with ethyl acetate (EtOAc) and *n*-butanol (*n*-BuOH), and the combined solution of each extract was evaporated under reduced pressure to yield the EtOAc (greenish sticky mass, 61 g) and *n*-BuOH (brownish sticky mass, 17 g) extracts. Based on the yield of the two fractions, the EtOAc soluble fraction was considered the main fraction and was subjected to further isolation. The EtOAc fraction (56 g) was subjected to column chromatography (CC) using a gradient system of hexane–EtOAc (98:2 to 0:100) as the eluent to produce 6 main fractions (E1─E6) based on the thin-layer chromatography (TLC) investigations. An oily fraction E1 (26.4 g, 0.16% w/w based on the dry plant weight) was then evaluated for its fatty acid content. Subfractions E2─E5 displayed similar TLC results, and a colorless solid of α-spinasterol (C1, 979 mg) was precipitated from fraction E2 (4.3 g). Fraction E6 (12.5 g) was subjected to repeated CC eluting with a gradient of EtOAc–CH$_2$Cl$_2$ (98:2 to 0:100) to obtain 10 subfractions (E.6.1─E.6.10). Subfraction E.6.5 (4.5 g) was further purified by CC using the same eluent to provide 8

subfractions (E6.5.1─E6.5.8). Ligballinol (C**2**, colorless needle, 27 mg) was successfully obtained from subfraction E.6.5.4 (2.8 g).

Flow charts of the extract step
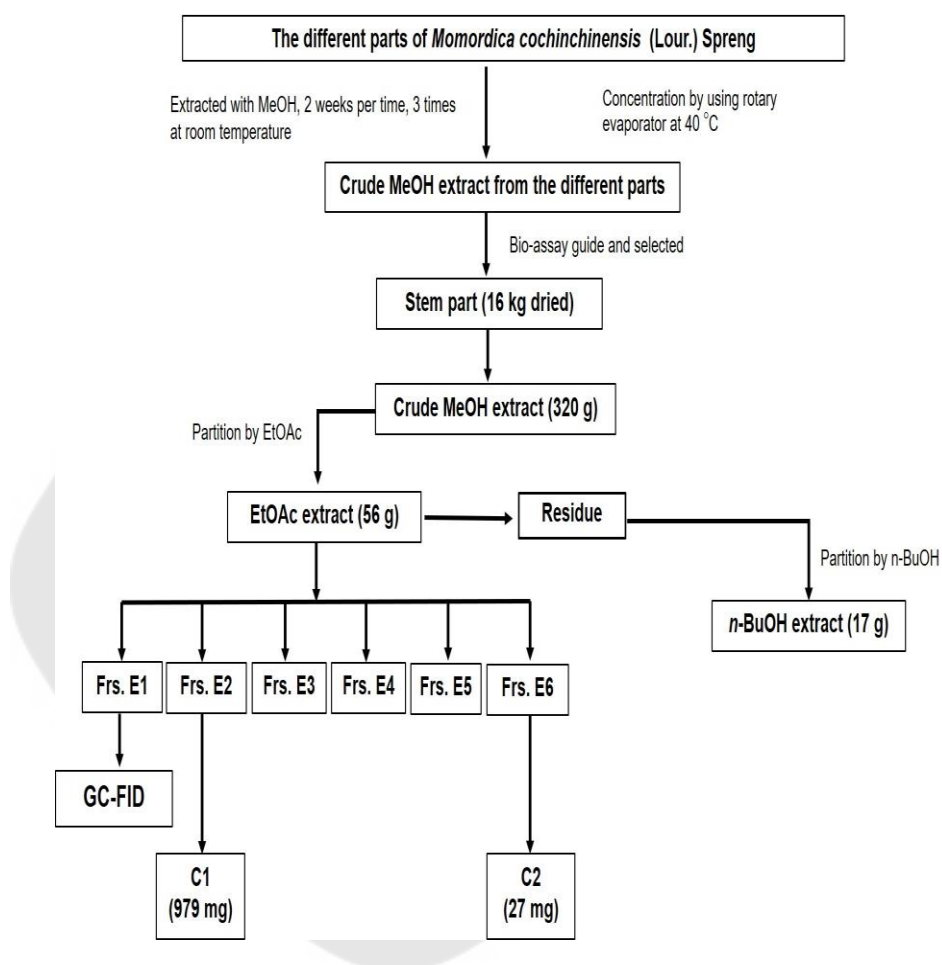
Figure 12 Preparation of organic fractions of *Momordica cochinchinensis* methanolic extract. Flow chart representing the steps used to prepare the various organic fractions of *M. cochinchinensis* starting from its methanolic extract from different parts and selected the stem extract as excellent active ingredient to continue extraction to find the main active ingredient.

3.3.2.7 Analysis of fatty acid composition

Preparation of fatty acid methyl esters. A solution of methanolic sodium hydroxide (9:1, 5 mL) was added to an oil sample (30 mg), and the mixture was heated under reflux for 90 min. After cooling, deionized water (10 mL) was added, and the mixture was shaken for a few seconds. Un-saponified fatty acids were discarded by extraction with hexane (3 × 5 mL). The layer below was collected and adjusted to pH 3 (by 6 N HCl), followed by extraction with hexane (3 × 5 mL). The organic layer was removed under reduced pressure. The obtained fatty acid was further mixed with a solution of 2% H_2SO_4 in methanol, and the mixture was heated under reflux at 80 °C for 90 min. After cooling to ambient temperature, water (0.5 mL) was added, followed by extraction with hexane (3 × 5 mL). The methyl ester was evaporated to dryness, weighed and solubilized in hexane (1 mL) before injection into the gas chromatograph.

GC FID-analysis. Gas chromatography was performed with a Shimadzu version 3, model GC-17A, equipped with a flame ionization detector (FID). FAME analyses were achieved on a Phenomenex BPX70 capillary column (30 m, 0.25 mm i.d.). The initial oven temperature for the analysis of the injection port and FID detector was programmed at 60 °C for 0.5 seconds and heated to 200 °C for 4 min. The injector and detector temperatures were 250 °C. Helium was used as the carrier gas at a flow rate of 1.25 mL/min, and the split-less time was 1 min for both instruments. The experiment was analyzed by Shimadzu GC solution software V. 2.10, and the results were compared with known standards of fatty acids.

3.3.2.8 Cell viability determination of active compounds

To determine the effect of active ingredient on cell proliferation. PC-3 and Vero cells were seeded in 96 well plate at a density of 1×10^4 cell per well and allowed to adhere for 24 h. After that, the cells were treated with various concentrations of α-spinasterol (0–100 µM), ligballinol (0–500 µM), while the concentrations of; ethanol (EtOH; 1%), was used as the vehicle control and incubated for 72 h. The MTT dye (5 mg/ mL) was added in each well and further incubated for 4 h. The medium was discarded. Then, the formazan products were dissolved in 100 µl of DMSO. The

absorbance of each well was determined at wavelength 570 nm by using a multimode microplate reader (Synergy; BioTek Instruments, Inc.).

3.3.3 Part II: Study the effect of crude extracts from aril part of *M. cochinchinensis* on prostate cancer cell metastasis

3.3.3.1 Preparation of aril crude extracts

3.3.3.1.1 Sonicated water extracts

Aril parts were separated from mature fruits and kept at -80 °C until used in the experiment. The extraction processing was modified from Wimalasiri D, et al (2020) [87]. The aril sample (4 g) was placed in a bottle, protected from light, and mixed with 100 mL of distilled water. The mixture was sonicated at 50 Hz for 30 min, filtered through Whatman no.1 paper to discard any solid material/marc, and evaporated using a rotary evaporator (Büchi, Labortechnik AG, Thailand). The sample was lyophilized at -110 °C for 72 h using a lyophilizer machine (Scanvac, SPC RT CO., Thailand). Then, the lyophilized sample was stored at -20 °C as a working material. The lyophilized sample was weighed, dissolved to appropriate working concentrations (30 mg/mL) using Milli-Q water and further incubated in a water-bath sonicator (GT sonic, GT Ultrasonic Co., China) for 10 min. The extract was filter-sterilized using 0.45 µm filters before use.

3.3.3.1.2 Boil water extracts

The aril sample (4 g) was mixed with 100 mL of distilled water, as mentioned above. The mixture was boiled for 20 min and filtered through Whatman no.1 paper. Then, distilled water was evaporated to obtain a crude extract, dissolved with Milli Q water and sonicated by a water-bath sonicator for 10 min. The extract was filtered through a 0.45 µm filter before use.

3.3.3.1.3 Ethanol extracts

The sample (4 g) was mixed and soaked with 80% EtOH for 24 h and filtered through Whatman no.1 paper. Then, a solvent extract was evaporated to obtain to crude extract, which was dissolved with DMSO and sonicated by water-bath sonicator for 10 min before use.

3.3.3.1.4 Hexane: acetone: ethanol extracts

The sample (4 g) was placed in a bottle, protected from light and mixed with 100 mL of hexane:acetone:ethanol 2:1:1 extraction solvent (H:A:E) as previously described [87]. The dried carotenoid extract was weighed. All carotenoids are water insoluble, 0.5% DMSO was used as vehicles. The extract was filtered through 0.45 μm filters before use.

3.3.3.2 Cell lines and culturing condition

The PC-3 and LNCaP clone FGC (human androgen-sensitive prostate adenocarcinoma cancer (ATCC® CRL-4740™)) cell lines were purchased from ATCC. The PC-3 cells were cultured in DMEM containing 10% fetal bovine serum (FBS), 100 units/mL penicillin and 0.1 mg/mL streptomycin. The LNCaP cells were cultured in Roswell park memorial institute (RPMI) 1640 medium containing 10% FBS, 1 mM sodium pyruvate, 10 mM HEPES (4-(2-hydroxyethyl)-1-piperazineethane- sulfonic acid), 100 units/mL penicillin and 0.1 mg/mL streptomycin and incubated at 37 °C in an atmosphere of 5% CO_2.

The Vero (normal African green monkey kidney cell line (ATCC® CCL-81™)) cell line, a representative normal cell line, was purchased from ATCC. The cells were maintained in Eagle's minimum essential medium (EMEM) containing 10% FBS, 100 units/mL penicillin, and 0.1 mg/mL streptomycin and incubated at 37 °C in an atmosphere of 5% CO_2.

3.3.3.2.1 Cytotoxicity of aril crude extracts on PC-3 prostate cancer cell

Cytotoxicity of aril crude extracts against prostate cancer cells, PC-3 and LNCaP, and normal cells as Vero cells were harvested with 0.25% trypsin containing 1 mM EDTA, plated in a 96-well plate at a density of 1×10^4 cells per well containing 10% FBS medium and allowed to adhere for 24 h. Then, the cells were treated with various concentrations of each crude extract including sonicated water, boil water, 80% EtOH, and H:A:E (0 - 5 mg/mL). After incubation, the MTT dye (0.5 mg/mL; final concentration) was added to each well and further incubated for 4 h. Then, the medium was discarded and the formazan products were dissolved in 100 μl of DMSO.

The optical wavelength at 570 nm was determined in each well using a multimode microplate reader (Synergy; BioTek Instruments, Inc.).

3.3.3.2.2 Determination of cell damage using LDH assay

To confirm cell damage effect of sonicated water extract on PC-3 cells was determined using an LDH assay kit. Briefly, PC-3 cells (1×10^4) were treated with different concentrations of sonicated water extract (0-10 mg/ mL) for 24 h. After incubation, the supernatants were transferred to a new plate, and then reaction buffer was added into each well, further incubated for 20 min at 37 °C. The plate was read using a microplate reader (Synergy; BioTek Instruments, Inc.) at 490 nm. The amount of LDH release correlated proportion to the number of damage cells.

3.3.3.2.3 Determination of cell death using cell cycle assay

The effect of sonicated water extract on cell cycle was investigated by using PI stain. PC-3 cells were plated in 6-well plates at a density of 3×10^5 cells per well and allowed to adhere overnight. Then, cells were treated with different concentrations: 2, 4, 6, and 8 mg/ mL, respectively. After 24 h of treatment, the cells were harvested and fixed in 70% chill-EtOH for overnight at 4 °C. Then, the cells were centrifuged at 1,800 rpm for 5 min to remove EtOH out, washed PBS for twice times. Cells were stained with PI for 30 min and analyzed, respectively. The percentage of DNA content in each phase was determined by using a Guava EasyCyte^{TM} flow cytometry and GuavaSoft^{TM} software (Merck Millipore Crop., Merck KGaA).

3.3.3.2.4 Determination of cell migration using wound healing assay

This assay was done using the method described by Liang, et al [88]. The effect of the sonicated water extract on PC-3 cell migration was determined by a monolayer wound healing assay. PC-3 (6×10^5 cells per well) in serum-free medium, and allowed to adhere overnight. After 90% confluent, the cells were scratched with a 200-µl sterile pipette tip from one side to the other in each well. Subsequently, the floating cells were removed with PBS washing and replaced with a new fresh DMEM medium containing 0, 2, 4, and 6 mg/mL of sonicated water extracts. Cell migration was recorded by a Olympus light microscope (Olympus CKX41; Corporation) using a magnification of 10X at 0, and 24 h. The wound area was measured in wound sites per

group and compared with that in the control group at 0 h. The wound distances were quantified using ImageJ software [Java 1.8.0_112 (64_bit); National Institutes of Health].

3.3.3.2.5 Determination of cell migration using transwell migration assay

The effect of aril crude extract on the ability of PC-3 cell migration was assessed using a transwell migration assay. To perform the experiment, each well of a 24-well plate was firstly inserted with a transwell containing polycarbonate membranes with 8-µm pores (Corning). Then, 4×10^4 cells of PC-3 were resuspended in a 200 µl serum-free medium with or without 2, 4 and 6 mg/mL sonicated water extracts. The cells were then plated into the upper chambers of Transwell inserts. In the lower chamber, a 600 µl medium containing 10% FBS was used as a chemoattractant to stimulate cell migration from the upper chamber. The plate was then incubated at 37 °C for 24 h. After that, the transwell insert was separated, washed twice with cold PBS. Each sample was fixed with 100% ice-cold methanol for 20 min and followed by stained with 0.5% crystal violet for 15 min and washed with PBS several times until all the excess dye had been removed. The cells that did not migrate from the upper chamber were removed using cotton swabs. The cells that migrated through the pores of the insert into the lower chamber were photographed under a Olympus light microcope at a magnification of ×10. Finally, the optical density of the membrane with the migrated cells was measured at wavelength 570 nm [89].

3.3.3.2.6 Investigation of migration process mediators using Western blotting assay

PC-3 cells were seeded in a 6-well plate at a density of 5×10^5 cells per well. The cells were treated with 0, 2, 4, and 6 mg/mL of sonicated water extracts, and incubated for 24 h. Then, the cells were lysed and prepared as protein lysates. The protein extracts (50 µg) were separated by 8%-10% SDS-polyacrylamide gel electrophoresis (SDS-PAGE) and transferred to PVDF membranes. The membranes were blocked with 5% skim milk in TBS-T buffer (5% w/v skim milk, 1X Tris-buffered saline solution and 0.1% Tween-20) at room temperature for 1 h and then incubated with primary antibodies against MMP-2 (no. 87809), MMP-9 (no. 13667), TIMP-1 (no. 8946), TIMP-2 (no. 5738), and GAPDH (no. 2118S) at 4 °C overnight. After washing three times,

the membranes were incubated with horseradish peroxidase-conjugated anti-rabbit IgG antibodies (no. 7074P2) for 1 h. The membranes were visualized by enhanced chemiluminescence using ECL plus™ western blotting detection reagents (Bio-Rad Laboratories). The intensities of the protein bands were quantified by ImageJ software [Java 1.8.0_112 (64_bit)].

4. Statistics

All results were presented with mean ± standard error (SEM, of each group = 3). Statistical analysis was performed using Graph Pad Prism version 5.03 (GraphPad Software, Inc.). Comparisons of more than two groups were made by a one-way analysis of variance followed by Dunnett's test. P<0.05 was considered to indicate a statistically significant difference.
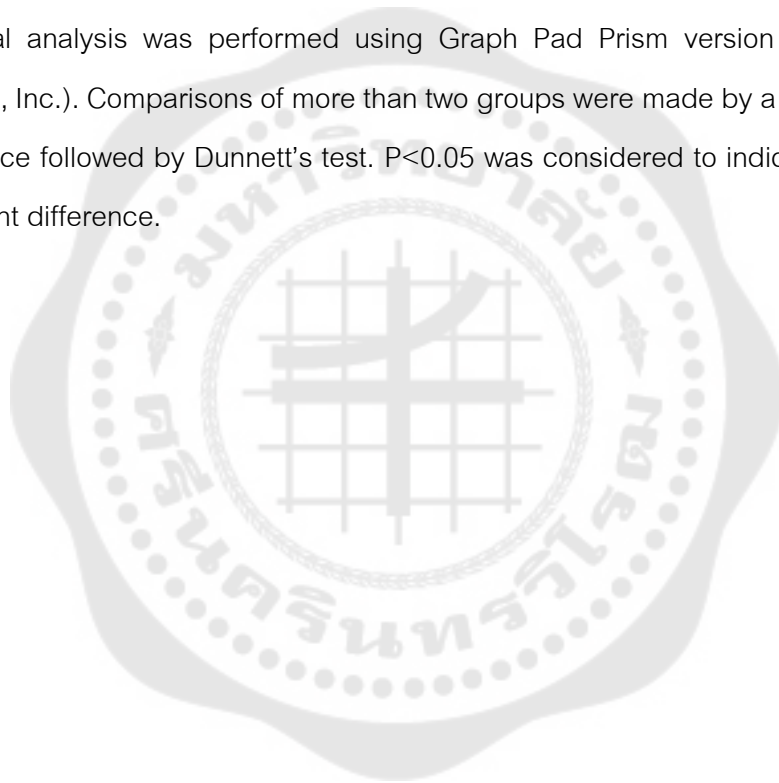
CHAPTER 4

RESULTS

4.1 Part: 1

Result have already been published in Molecules [90].

4.1.1 The extract from different parts (leaves, seeds, stems, and roots) of *M. cochinchinensis* (MC) demonstrated a cytotoxic effect against cancer cells but less in normal cells

The MC crude extracts from different parts (leaves, seeds, stems, and roots) were extracted with methanol following standard procedures. The antiproliferative activity of each soluble fraction against cancer cells was defined using an MTT assay. Several cancer cell models were selected for screening, including A549, HeLa, MDA-MB-231, and PC-3 cells. The cells were treated with or without MC extracts at 0–5 mg/mL for 24 h, while 0.5% DMSO was used as the vehicle control. The results were demonstrated as shown in Table 2. All extracts exhibited antiproliferative effects in all cancer cells tested but at different levels. Among these crude extracts, the stem extract showed the highest efficiency in all four types of cancer cells. The IC_{50} values for A549, HeLa, MDA-MB-231, and PC-3 cells were 0.44, 0.42, 0.62, and 0.62 mg/mL, respectively. These data showed that the stem extract is interesting to study the anticancer activity further. To confirm the potential of stem extract, PC-3 cell was selected as a model for study, and the cytotoxicity was compared with the representative of normal cells (Vero). As illustrated in Figure 13, the IC_{50} values of the PC-3 and Vero cells were 0.62 and 2 mg/mL, respectively. This data indicated the selectivity effect of stem extract against prostate cancer cells. Thus, the mechanism of cancer cell death induction by the stem extract was evaluated along with a characterization of its chemical composition.

Table 2 The antiproliferative effect of MC extracts were determined by MTT assays. All cells were treated with or without the different parts (leaves, seeds, stems, and roots) of extracts (0–5 mg/mL) for 24 h. Control cells were exposed to vehicle or 0.5% DMSO. The data are offered as the mean of triplicate values ± SEM.

Cell Lines	IC_{50} Values (mg/mL)			
	Leaves	Seeds	Stems	Roots
A549	1.98 ± 0.74	1.30 ± 0.96	0.44 ± 0.87	0.74 ± 3.14
HeLa	0.53 ± 0.37	2.09 ± 1.41	0.42 ± 1.07	0.48 ± 0.38
MDA-MB-231	2.10 ± 0.79	2.26 ± 1.18	0.62 ± 0.74	0.77 ± 3.72
PC-3	4.25 ± 0.66	4.65 ± 0.36	0.62 ± 0.74	0.73 ± 2.27

Figure 13 Dose-dependent inhibitory effects of an MC stem extract on the viability of (A) Vero and (B) PC-3 cells. Cells were treated with various concentrations (0–5 mg/mL) for 24 h. Data are presented as the mean of triplicate values ± SEM. *** indicates $p < 0.001$.

4.1.2 Stem extract induced apoptosis in PC-3 cells

To confirm the effect of stem extract on the apoptosis process, morphological changes, such as chromatin condensation, apoptotic bodies, membrane blebbing, and cell shrinkage, were evaluated. PC-3 cells were treated with or without stem extract at 0, 0.3, 0.6, 0.9, and 1.2 mg/mL for 24 h, followed by Hoechst 33342 staining, and the cells were imaged under a fluorescence microscope. Most treated cells exhibited chromatin condensation, and some cells demonstrated nuclear fragmentation in a concentration-dependent manner, whereas the vehicle control group exhibited an intact nuclear structure (Figure 14). Therefore, this specific characteristic of apoptotic cells was confirmed using sub-G1 peak analysis. As shown in Figure 15, treatment with stem extract at 0, 0.6, 0.9, and 1.2 mg/mL resulted a higher number of sub-G1 populations while increasing the concentration of stem extract: 0.86%, 5.9%, 25%, and 37%, respectively. These results support our hypothesis that stem extract has the ability to induce apoptosis in PC-3 prostate cancer cells.
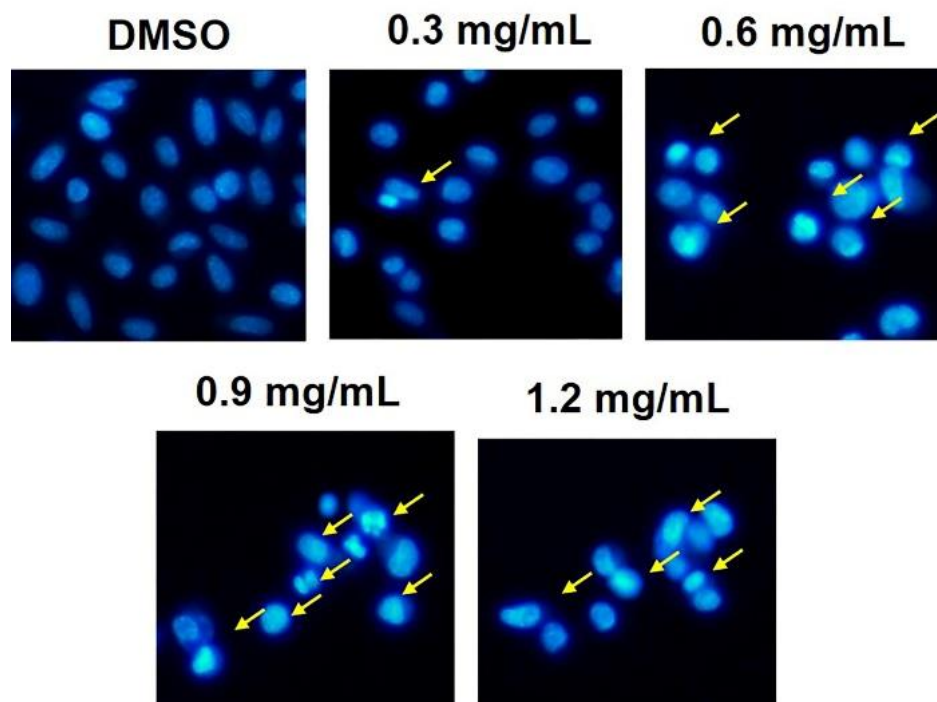
Figure 14 Fragmentation and nuclear condensation were observed by Hoechst 33342 staining. PC-3 cells were treated with stem extract (0, 0.3, 0.6, 0.9, and 1.2 mg/mL) for 24 h. Treated cells exhibited morphological changes in the nuclei typical of apoptosis. Photographs were taken under a fluorescence microscope (20×). Arrows represent apoptotic cells.

In addition, the apoptosis process usually causes mitochondrial damage, so we explored whether this effect would also be induced by stem extract. The experiment was conducted by using JC-1 dye staining. As shown in our results, the stem-extract-treated cells demonstrated a decrease in the red/green ratio in a concentration-dependent manner (Figure 16). The percentage of cells with JC-1 green fluorescence was not significantly altered in the control group (3.20%), while in the treated groups, the green fluorescence significantly increased by 8.19%, 8.90%, 22.34%, and 47.24% at 0.3, 0.6, 0.9, and 1.2 mg/mL of stem extract, respectively.

Overall, the present findings suggested that stem extract could trigger apoptosis in PC-3 cells by inducing morphological changes, increasing the sub-G1 population, and reducing the mitochondrial membrane potential.
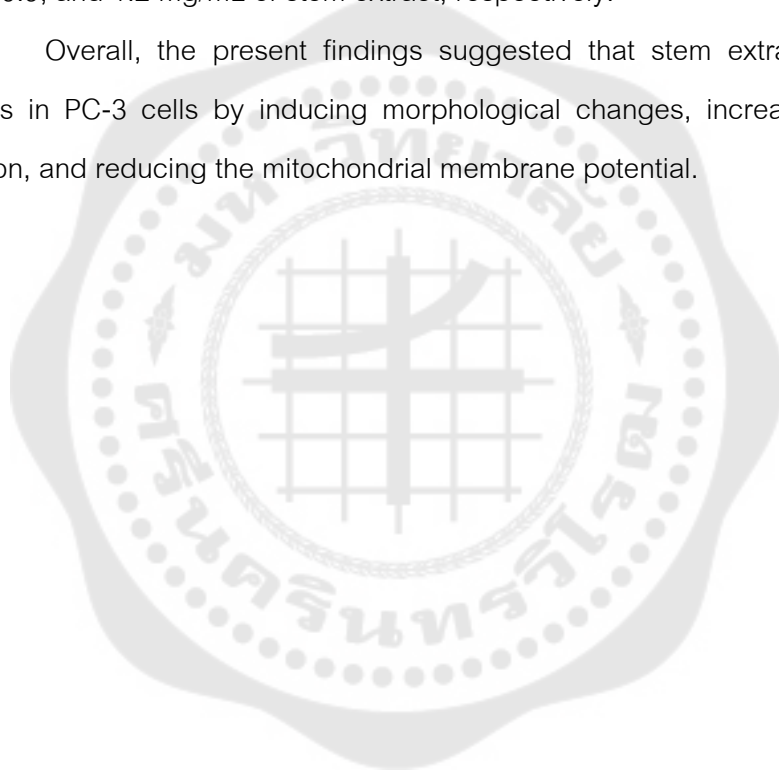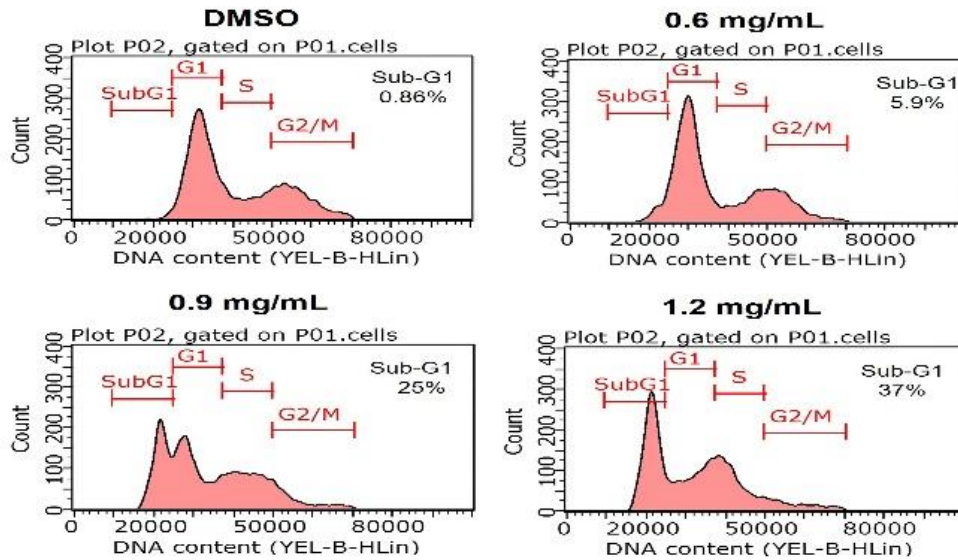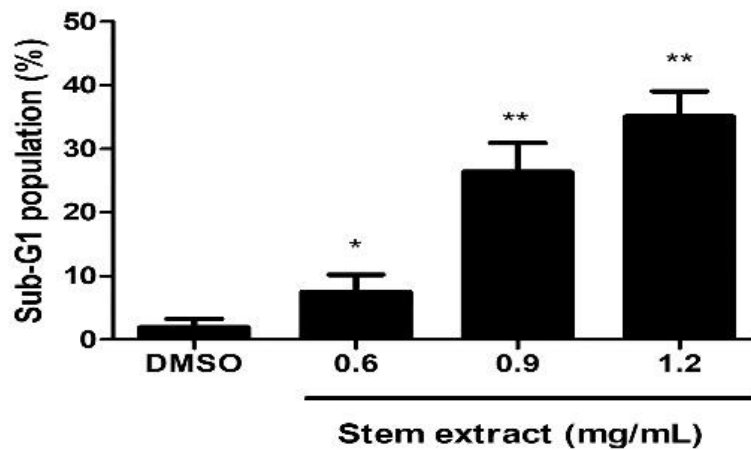
Figure 15 Sub-G1 peak analysis of PC-3 cells treated with stem extract. The flow cytometry analyzed PC-3 cells that were treated with stem extract at 0, 0.6, 0.9, and 1.2 mg/mL for 24 h. (A) Histograms demonstrate the number of cells (y-axis) vs. the DNA content (x-axis). The data shown are representative of three experiments with similar findings. (B) The quantitative values of the sub-G1 population. The significant differences of the treated cells from the untreated control group are indicated by * $p <$ 0.05 and ** $p <$ 0.01.
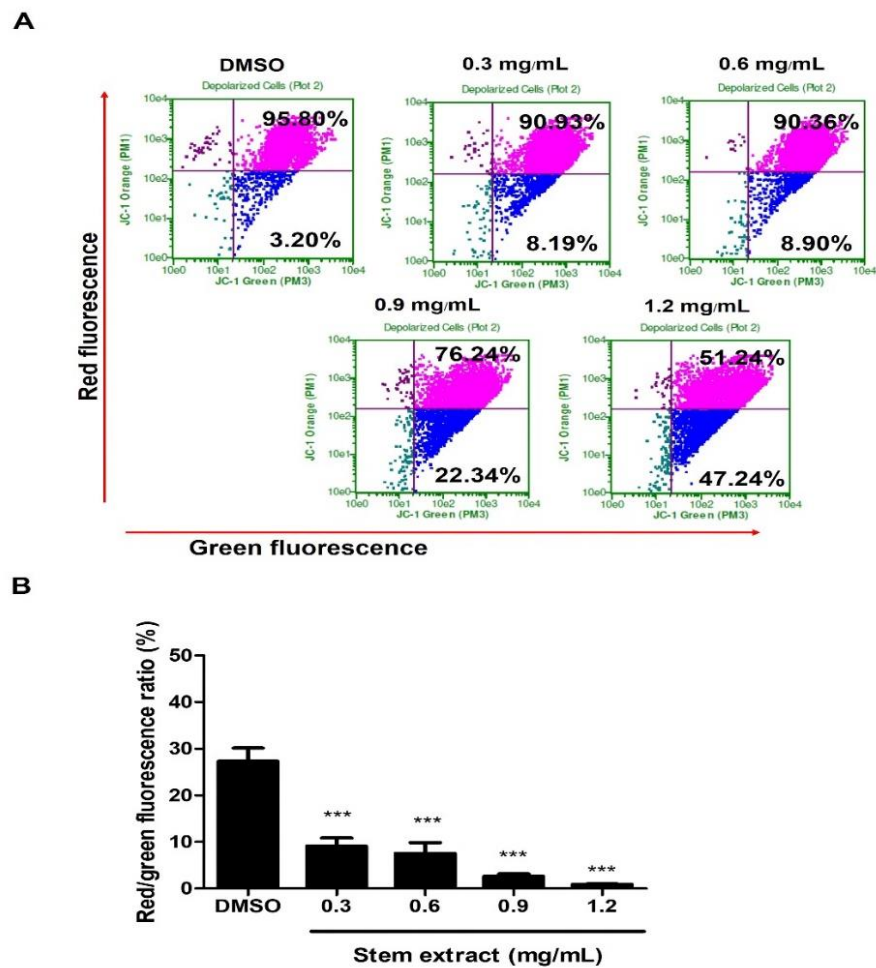
Figure 16 Effects of stem extract on the mitochondrial membrane potential ($\Delta\Psi$m) in PC-3 cells. (A) Cells were treated with stem extract at 0, 0.3, 0.6, 0.9, and 1.2 mg/mL for 24 h. Next, all samples were stained with JC-1 and analyzed by flow cytometry. The upper right quadrant indicates polarized mitochondria (red fluorescence), while the lower right quadrant illustrates membrane depolarization (green fluorescence). (B) Quantification of the red/green fluorescence ratio indicates low membrane potential following increasing concentrations of the stem extract. *** indicates $p < 0.0001$ compared to the control.

4.1.3 Stem extract affected the expression of apoptosis-related proteins in PC-3 cells

To deeply investigate the effect of the stem extract on the protein machinery involved in the apoptosis mechanism, several mediators were selected to determine by Western blotting. The representatives of pro-apoptotic mediators were caspase-3 and Noxa. Caspase-3 has been well-known as the main executioner caspase for apoptosis signaling. While Noxa is a member of a Bcl-2 family protein and belongs to a sub-class of the BH-3 only group. For the anti-apoptotic mediators, Mcl-1 and Bcl-xL are selected, due to both proteins are members of the Bcl-2 family protein that prevents apoptosis. Besides, the relationship between Mcl-1 and Noxa involving the chemotherapeutic resistance in prostate cancer is also another reason to support this selection. As shown in Figure 17, PC-3 cells treated with stem extract at 0, 0.3, 0.6, 0.9, and 1.2 mg/mL demonstrated a reduction in procaspase-3, Bcl-xL, and Mcl-1 protein expression. The results for these three proteins exhibited the same trend, in which their expression started decreasing from 0.6 mg/mL. Meanwhile, the level of Noxa increased significantly from 0.3–0.9 mg/mL and dropped at 1.2 mg/mL. Therefore, the stem extract decreased anti-apoptotic proteins and increased pro-apoptotic proteins.
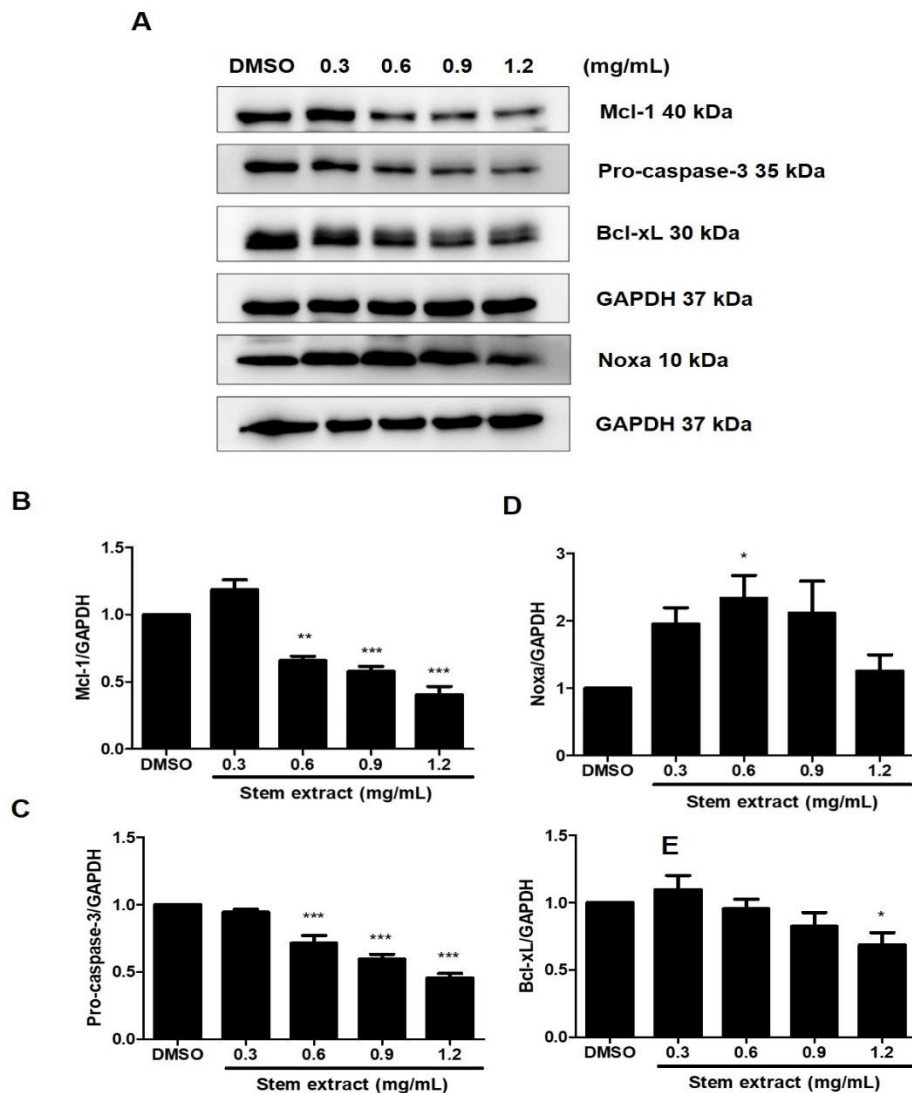
Figure 17 Effects of the stem extract on the expression of apoptosis-related proteins in PC-3 cells. Cells were treated with stem extract at 0, 0.3, 0.6, 0.9, and 1.2 mg/mL, and then Western blot analysis was performed with all samples. (A) Representative protein expression of McL-1, pro-caspase-3 Bcl-xL, and Noxa revealed by Western blot analysis. (B–E) The expression levels of each protein were quantified and normalized to GAPDH. The results are expressed as means ± SEM. * indicates $p < 0.05$, ** indicates $p < 0.01$, and *** indicates $p < 0.001$: a significant difference versus the control.

4.1.4 Chemical compositions of stem extract and the active compounds

Since anticancer activity and apoptosis induction of the stem extract was demonstrated in PC-3 cells, the active compound that is responsible for this function was further determined. Bioassay-guided fractionation of the stem extract was then carried out and yielded two fractions, EtOAc (IC_{50} 1.25 mg/mL) and *n*-BuOH (IC_{50} 1.46 mg/mL). Subsequently, chromatographic phytochemical investigations of the more active EtOAc soluble part produced a pale-yellow oil at 0.16% (*w/w*) from fraction E1 as the most abundant fraction, which was quantified for fatty acid content using GC-FID. The percentage of the identified fatty acid composition is presented in Table 3, and the GC-FID chromatogram is shown in Figure 18. The unsaturated fatty acids (USFAs) were characterized as palmitoleic acid (1.34%), oleic acid (7.30%), linoleic acid (11.85%), and α-linolenic acid (27.0%), while those of the saturated fatty acids (SFAs) were lauric acid (0.18%), myristic acid (1.54%), palmitic acid (35.07%), stearic acid (14.09%), and arachidic acid (1.63%). Both palmitic acid and α-linolenic acid were obviously the main fatty acid constituents obtained from the stem part.

Fraction E2-5 and E6.5.4 were collected and proved to be α-spinasterol (**1**) and (−) ligballinol (**2**), respectively, by spectroscopic examination, mainly ^{1}H, ^{13}C NMR, and MS data, as well as X-ray crystallography (Figures 19-26). A comparison of their physicochemical and spectral data with published values was also performed. Compound **2** exhibited a negative specific rotation $[\alpha]_D^{25.5}$ −11.5 (c = 0.20, MeOH), and its X-ray crystal structure supported the stereochemical assignment, as shown (Fig 20). Therefore, compound **2** was deduced to be (−) 4,4′-((1*R*,3a*S*,4*R*,6a*S*)-tetrahydro-1*H*,3*H*-furo[3,4-c] furan-1,4-diyl)diphenol or (−) ligballinol. This compound has also been reported from the MC seed [91] [92].

Compound **1** was obtained as a white amorphous powder, mp. 168–169 °C (lit [93]169 °C). ^{1}H-NMR (300 MHz, CDCl$_3$) δ_H: 5.16 (m, 2H, H-7 and H-22), 5.03 (dd, *J* = 15.1, 8.6 Hz, 1H, H-23), 3.59 (m, 1H, H-3), 2.00–0.95 (m, for methine and methylene protons), 1.03 (d, *J* = 6.6 Hz, CH$_3$-21), 0.84 (d, *J* = 6.6 Hz, 3H, CH$_3$-26), 0.80 (s, 3H, CH$_3$-19), 0.79 (d, *J* = 5.5 Hz, 3H, CH$_3$-27), 0.55 (s, 3H, CH$_3$-18); ^{13}C-NMR (75 MHz,

CDCl$_3$) δ_C: 139.5 (C-8), 138.1 (C-22), 129.5 (C-23), 117.4 (C-7), 71.0 (C-3), 55.9 (C-17), 55.1 (C-14), 51.2 (C-24), 49.4 (C-9), 43.3 (C-13), 40.7 (C-20), 40.2 (C-5), 39.4 (C-12), 38.0 (C-4), 37.1 (C-25), 34.2 (C-10), 31.8 (C-1), 31.5 (C-2), 29.6 (C-6), 28.3 (C-16), 25.3 (C-28), 23.0 (C-15), 21.5 (C-11), 21.3 (C-26), 20.9 (C-21), 18.9 (C-27), 25.3 (C-28), 23.0 (C-29); HR-TOFMS (APCI$^+$) m/z 395.3674 [M $-$ H$_2$O + H]$^+$ (calc. for C$_{29}$H$_{47}$, 395.3672).

Compound **2** was obtained as a colorless needle, mp 263–264 °C (lit [94] 264–266 °C); [α]$_D^{25.5}$ $-$11.5 (c = 0.20, MeOH) (lit [95] [α]$_D^{25}$ $-$24 (c = 0.1, MeOH), [94] [α]$_D$ $-$7.1 (c = 1.61, MeOH)). ^{1}H-NMR (300 MHz, CDCl$_3$ + DMSO-d_6) δ_H: 8.56 (br s, 2H, OH), 7.03 (d, J = 8.4 Hz, 4H, H-2, 2$'$, 6 and 6$'$), 6.69 (dd, J = 8.4, 1.8 Hz, 4H, H-3, 3$'$, 5 and 5$'$), 4.58 (d, J = 4.4 Hz, 2H, H-7 and 7$'$), 4.07 (br t, J = 6.9 Hz, 2H, H-9 and 9$'$), 3.69 (dd, J = 6.3, 1.5 Hz, 2H, H-9 and 9$'$), 2.98 (br s, 2H, H-8 and 8$'$); ^{13}C-NMR (75 MHz, CDCl$_3$ + DMSO-d_6) δ_C: 156.5 (C-4 and 4$'$), 131.3 (C-1 and 1$'$), 127.1 (C-2, 2$'$, 6 and 6$'$), 115.2 (C-3, 3$'$, 5 and 5$'$), 85.5 (C-7 and 7$'$), 71.2 (C-9 and 9$'$), 53.7(C-8 and 8$'$); HR-TOFMS (ESI$^-$) m/z 297.1121 [M $-$ H]$^-$ (calc. for C$_{18}$H$_{17}$O$_4$, 297.1132). X-ray crystallographic data for Compound **2**: C$_{18}$H$_{17}$O$_4$, M = 297.32, Monoclinic, Space Group $P21/c$, a = 5.8554(7) Å, b = 7.3656(9) Å, c = 16.959(2) Å, α = γ = 90°, β = 91.421(4)°, V = 731.20(15) Å3, Z = 2, Dcalcd = 1.350 Mg/m^3, crystal size 0.32 × 0.11 × 0.07 mm^3, F(000) = 314, 25268 reflection collected, 1817 independent reflections (R_{int} = 0.0359), R_1 = 0.0549 [$I > 2\sigma(I)$], wR_2 = 0.1521 [$I > 2\sigma(I)$], R_1 = 0.0617 (all data), wR_2 = 0.1574 (all data), goodness of fit = 1.153.

A single crystal of **C2** was pasted on MiTeGen micromounts using paratone oil. X-ray scattering data were collected using a BRUKER D8 QUEST CMOS PHOTON II operating at T = 296(2) K. The collection of data used ω and φ scans and Mo-Kα radiation (λ = 0.71073 Å). The program APEX3 calculates, runs, and images the total number, and unit cell indexing was refined using SAINT [96]. Data reduction was performed using SAINT, and SADABS was used for absorption correction. The ShelXT structure solution program was used and combined dual-space recycling methods [97] and Patterson were used to solve the structure. The structure was refined by least

squares using ShelXL ⁽⁹⁸⁾ and the OLEX2 interface ⁽⁹⁹⁾. In the final refinement cycles, all nonhydrogen atoms were cultured anisotropically. All hydrogen atoms were settled in different Fourier maps but were refined using a rigid model (C—H = 0.93–0.98 Å and O—H = 0.82 Å). CCDC-2102982, containing supplementary crystallographic data, can be used free of charge from the Cambridge Crystallographic Data Centre via www.ccdc.cam.ac.uk/data_request/cif.
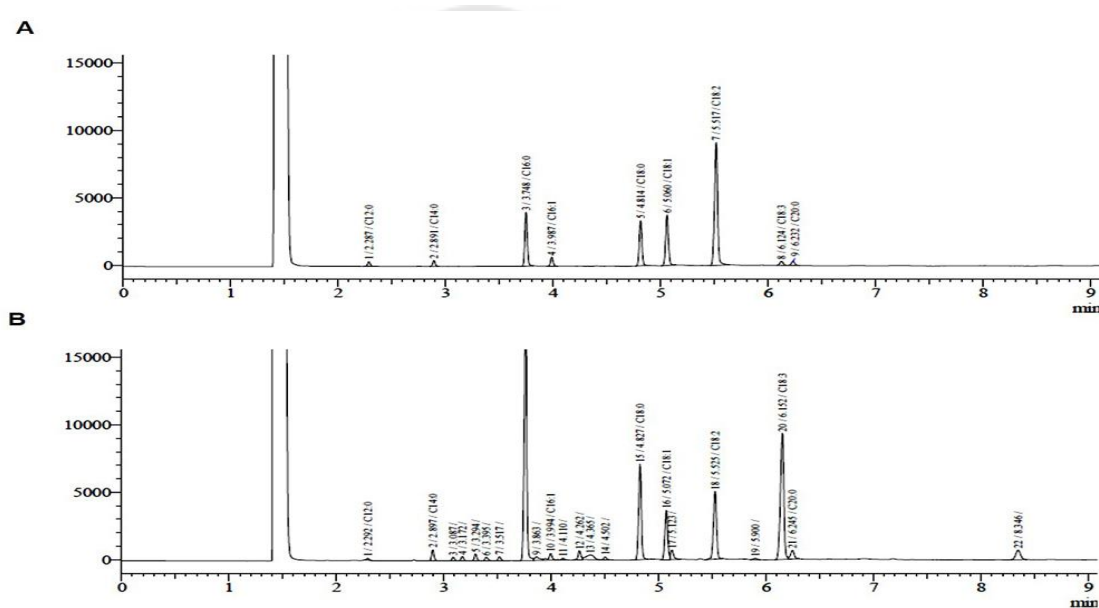
Figure 18 Chromatograms of the fatty acid content of the oil fraction obtained by the GC-FID analysis. (A) Standard chromatogram of 9 fatty acids that are known as lauric acid (C12:0), myristic acid (C14:0), palmitic acid (C16:0), palmitoleic acid (C16:1), stearic acid (C18:0), oleic acid (C18:1), linoleic acid (C18:2), α-linolenic acid (C18:3), and arachidic acid (C20:0). (B) Identification chromatogram of fatty acids from the sample.

Table 3 The fatty acids identified from the MC stem extracts by GC/FID analysis.

Peak	RT	Fatty acid names	Mean ± SEM
1	2.292	Lauric acid (C12:0)	0.18 ± 0.01
3	2.897	Myristic acid (C14:0)	1.54 ± 0.02
8	3.761	Palmitic acid (C16:0)	35.07 ± 0.19
10	3.994	Palmitoleic acid (C16:1)	1.34 ± 0.02
15	4.827	Stearic acid (C18:0)	14.09 ± 0.05
16	5.072	Oleic acid (C18:1)	7.30 ± 0.02
18	5.525	Linoleic acid (C18:2)	11.85 ± 0.07
20	6.125	α-Linolenic acid (C18:3)	27.0 ± 0.09
21	6.245	Arachidic acid (C20:0)	1.63 ± 0.16
		Total	100 ± 0.07
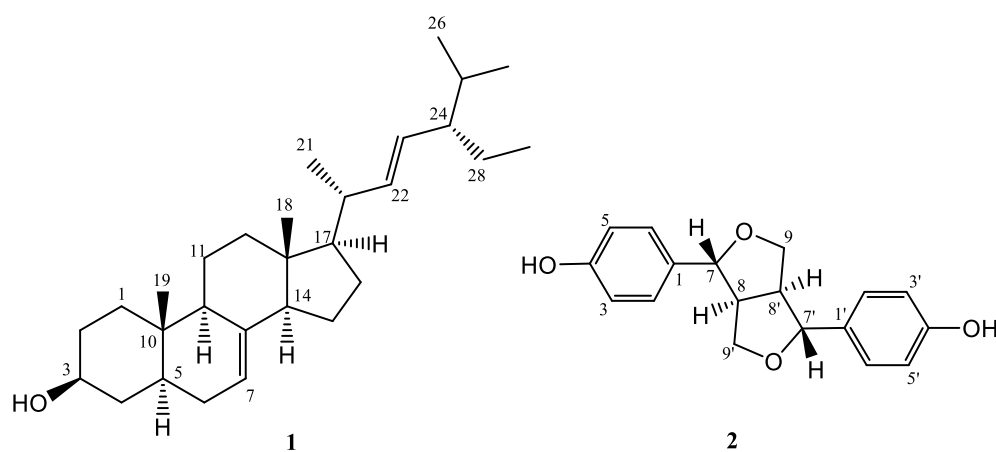
Figure 19 Chemical structures of *α*-spinasterol (1) and ligballinol (2).
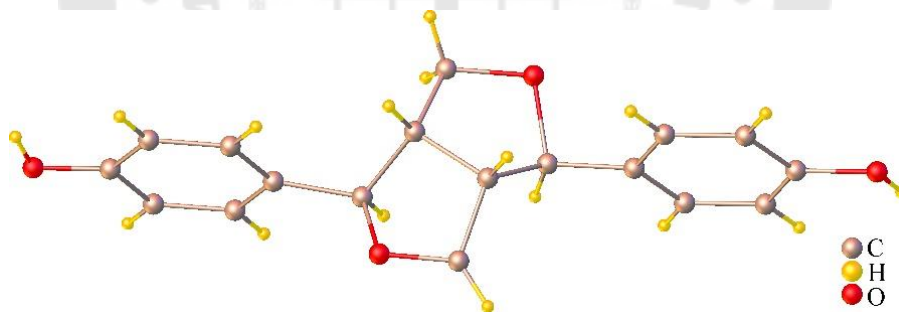
Figure 20 ORTEP plot of the X-ray crystal structure for ligballinol.
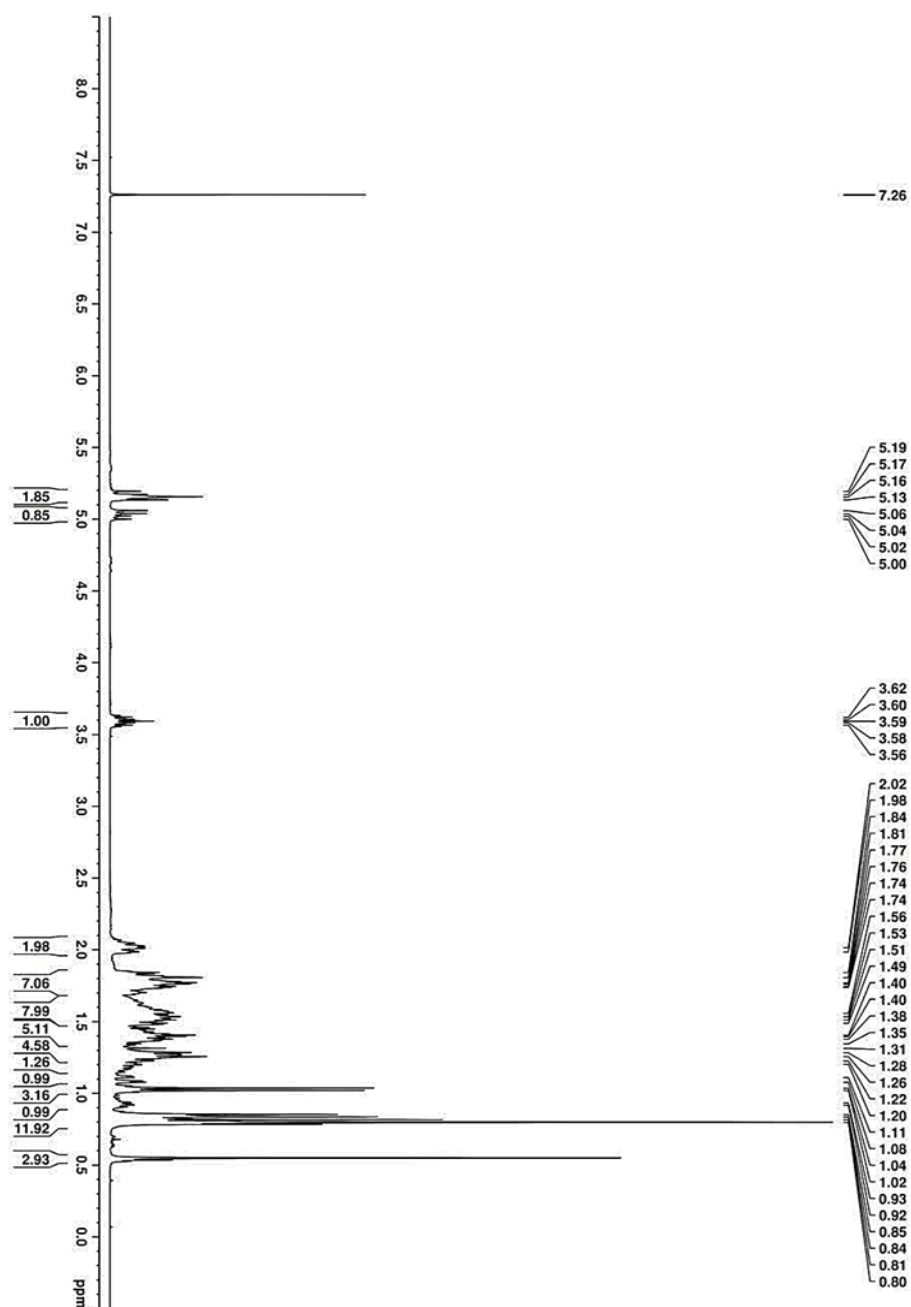
Figure 21 ^{1}H-NMR spectrum of Alpha-spinasterol in CDCl$_3$.
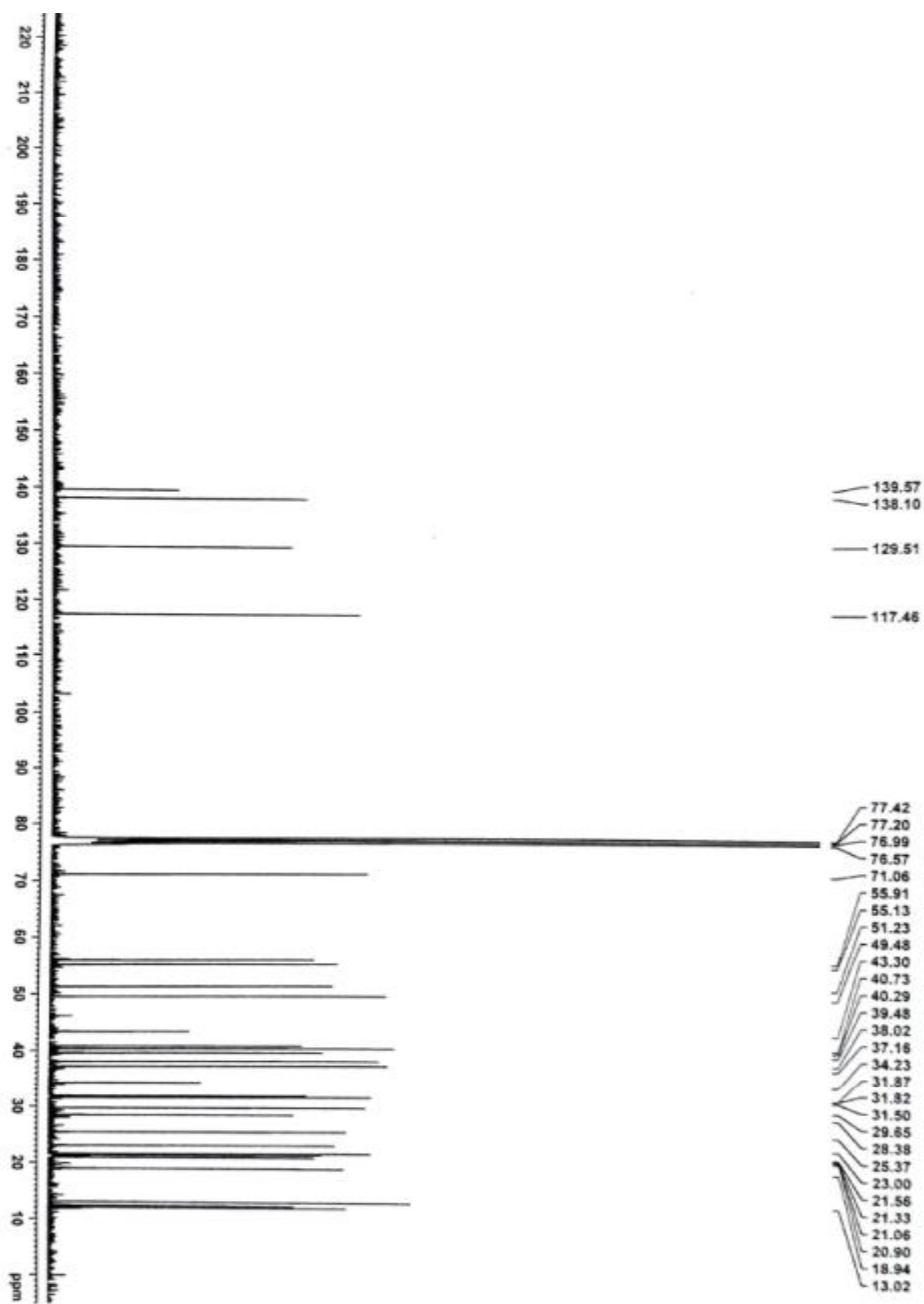
Figure 22 ^{13}C-NMR spectrum of Alpha-spinasterol in CDCl$_3$.
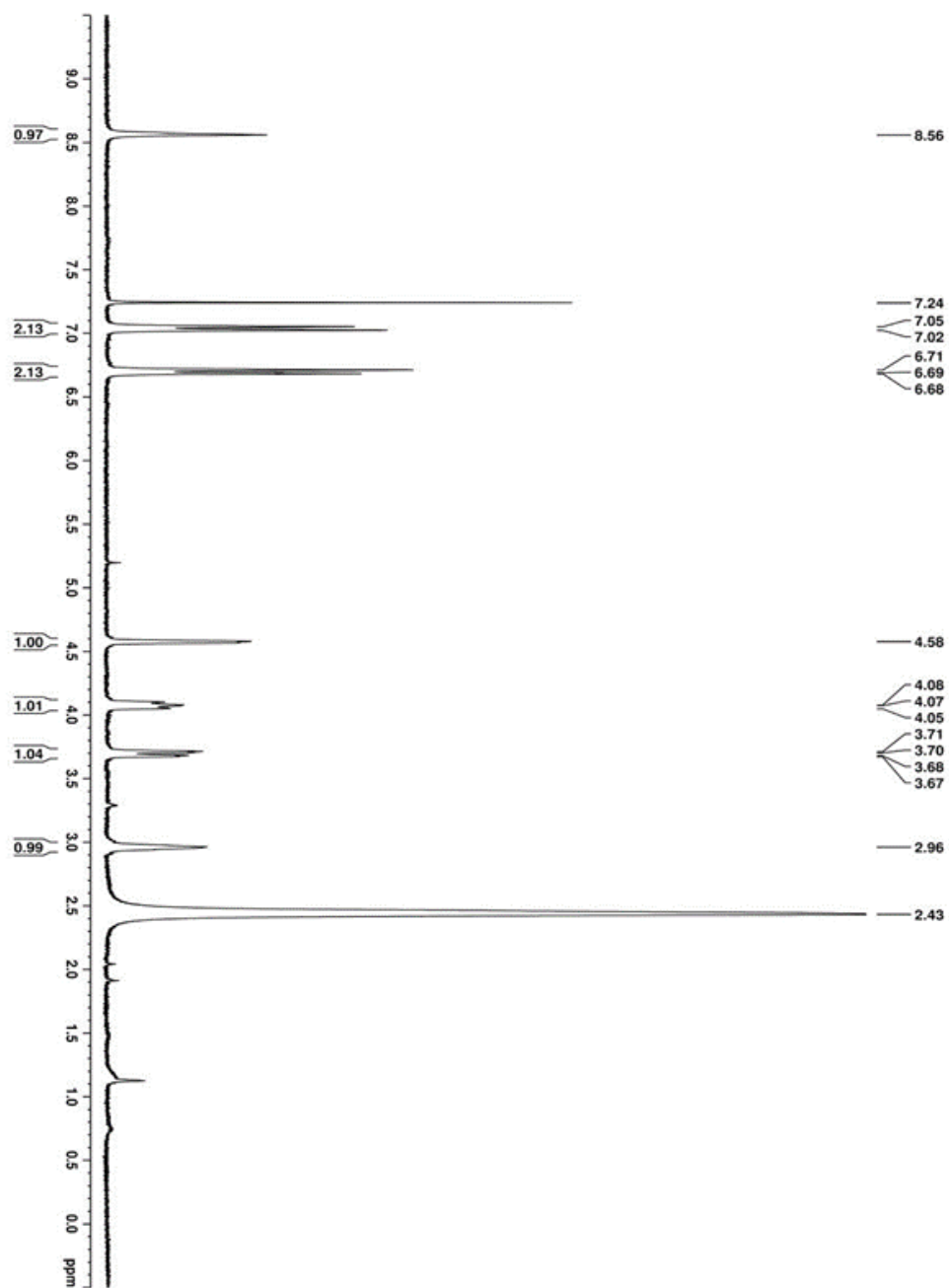
Figure 23 ^{1}H-NMR spectrum of ligballinol in CDCl$_3$ + DMSO-d_6.
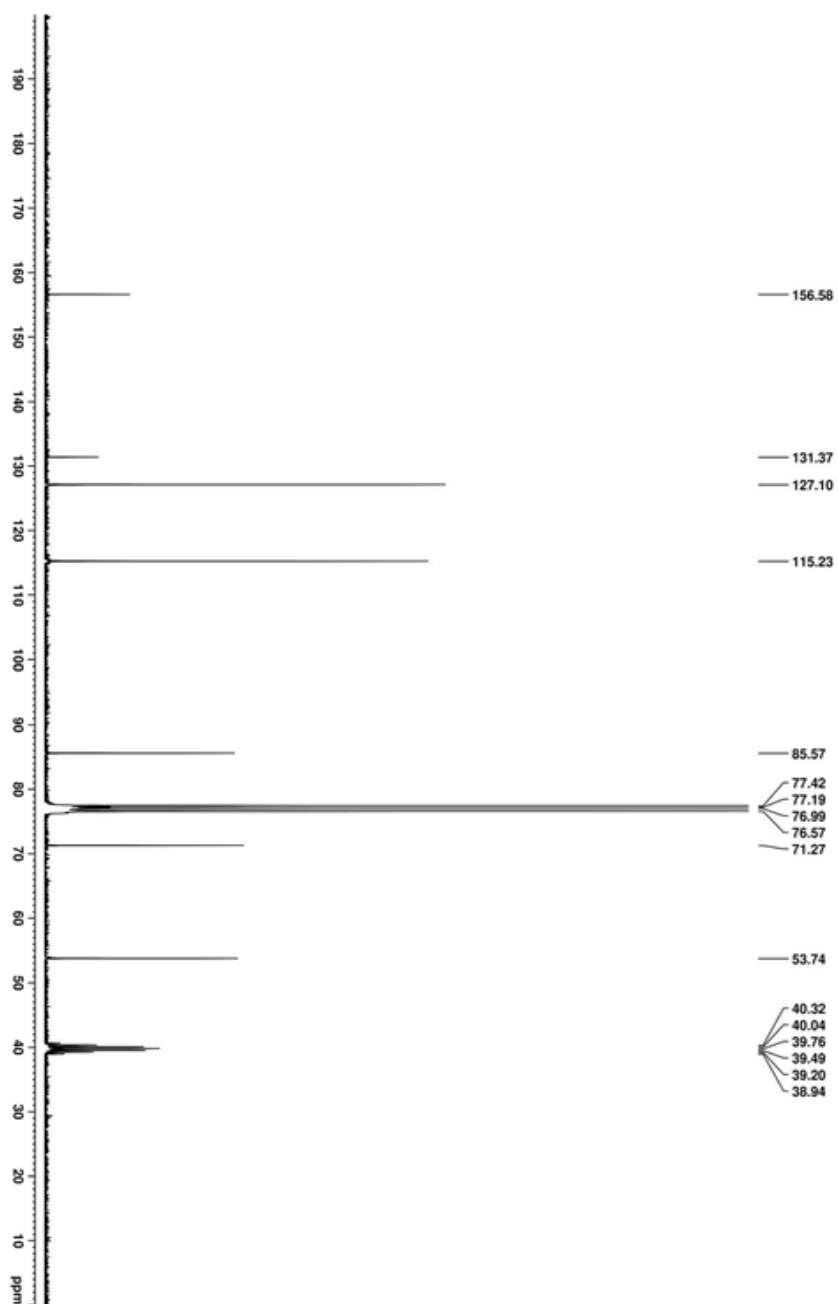
Figure 24 ^{13}C-NMR spectrum of ligballinol in CDCl$_3$ + DMSO-d_6.
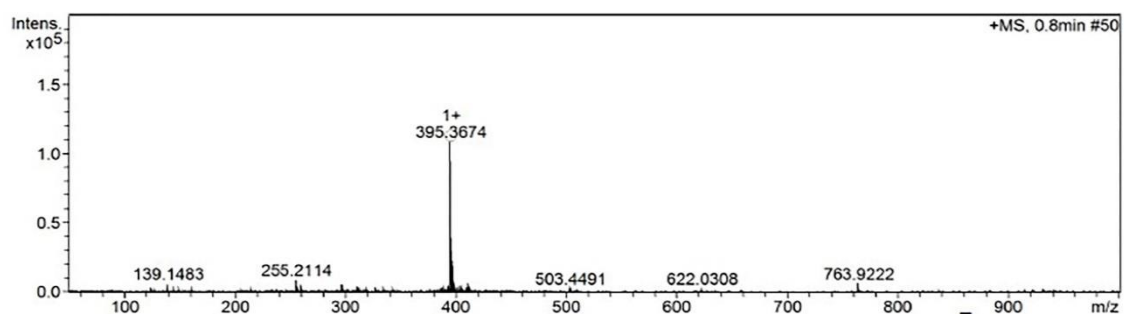
Figure 25 HR-TOFMS spectrum of *α*-spinasterol.
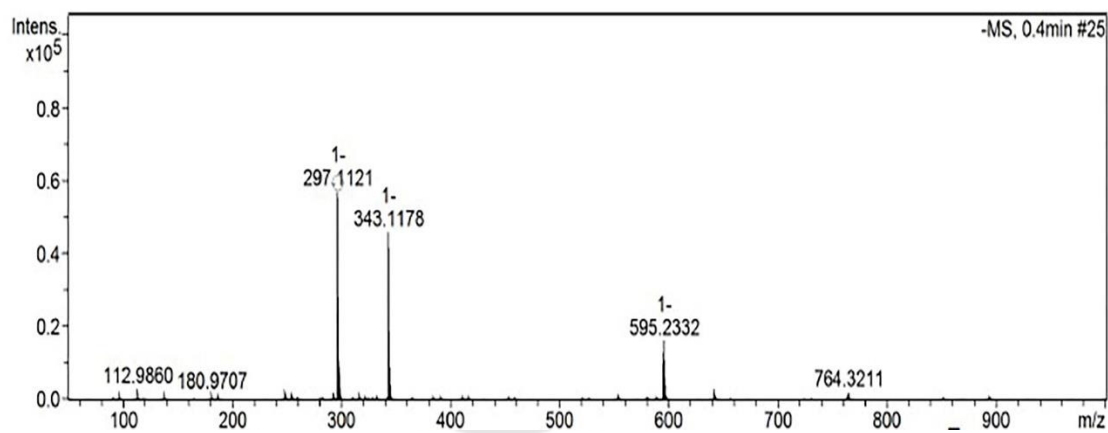
Figure 26 HR-TOFMS spectrum of ligballinol.

4.1.5 The effect of isolated compounds on PC-3 Cell viability

The activities of the pure compounds after isolation and identification were investigated for their antiproliferative effects on PC-3 cells compared to Vero cells. The MTT assay was performed using α-spinasterol at 0–100 µM and ligballinol at 0–500 µM for 72 h, while the vehicle control was treated with 1% EtOH. As illustrated in Figure 27, an inhibitory effect was clearly seen for ligballinol. The antiproliferative activity was demonstrated in PC-3 cells with an IC_{50} of 230 µM, but not in normal Vero cells. These results suggest that ligballinol may be an active compound responsible for the anticancer activity of the stem extract.
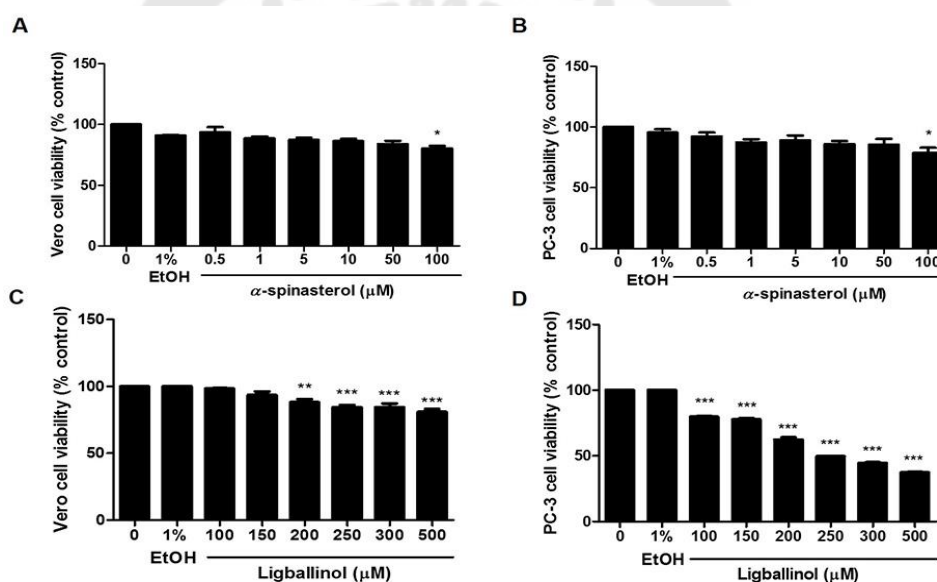
Figure 27 The antiproliferative effect of α-spinasterol and ligballinol on PC-3 and Vero cells. Cells were treated with various concentrations of α-spinasterol and ligballinol, and MTT assays were conducted. The results are expressed as means ± SEM. * indicates $p < 0.05$, ** indicates $p < 0.01$, and *** indicates $p < 0.001$: a significant difference versus control.

4.2 Part: 2 Study the effect of crude extracts from the aril part of *M. cochinchinensis* on prostate cancer cell metastasis.

4.2.1 Cytotoxicity screening of aril extract on PC-3, LNCaP, Vero cells

To continue to observe the effect of MC extract on the inhibition of prostate cancer cell migration, the potential stem extract (from Part I) was preliminarily screened in PC-3 cell migration using a wound healing assay. The results showed that stem extract had no effect on the migration of PC-3 cells (data not shown). Thus, the other part of MC was selected to test this aim. Aril part which has been reported of having several biological activities but has never been studied for migration inhibition in prostate cancer was chosen. The preparation of crude extracts from aril with different methods was first performed including boiling, sonication in water, 80% EtOH, and Hexane: acetone: ethyl acetate (H:A:E) extraction. The obtaining crude extracts further investigated the cytotoxic activity using an MTT assay. Two prostate cancer cell lines, PC-3 (high-aggressive), and LNCaP (low-aggressive) were used as models and compared the level of cytotoxicity with normal Vero cells (African green monkey kidney). The maximum final concentration of DMSO (0.5%) was used as the vehicle control. All cells were treated with 0-5 mg/mL of each aril extract as a boil water, sonicated water, 80% EtOH, and HAE for 24, 48, and 72 h. The results are demonstrated as shown in Figure 28. The effect of the sonicated water extract was better than other extracts, especially on PC-3 cells. The IC_{50} values were 2.01 ± 0.02 and 0.59 ± 0.02 mg/mL at 48 and 72 h, respectively (Figure 28B). While an IC_{50} of LNCaP at 24 h was found at 0.56 ± 0.03 mg/mL, as shown in Figure 28F. Interestingly, all crude extracts had a less toxic effect on Vero cells (Figure 29). Thus, aril extract prepared with sonication has the highest efficiency and be selected to further study.
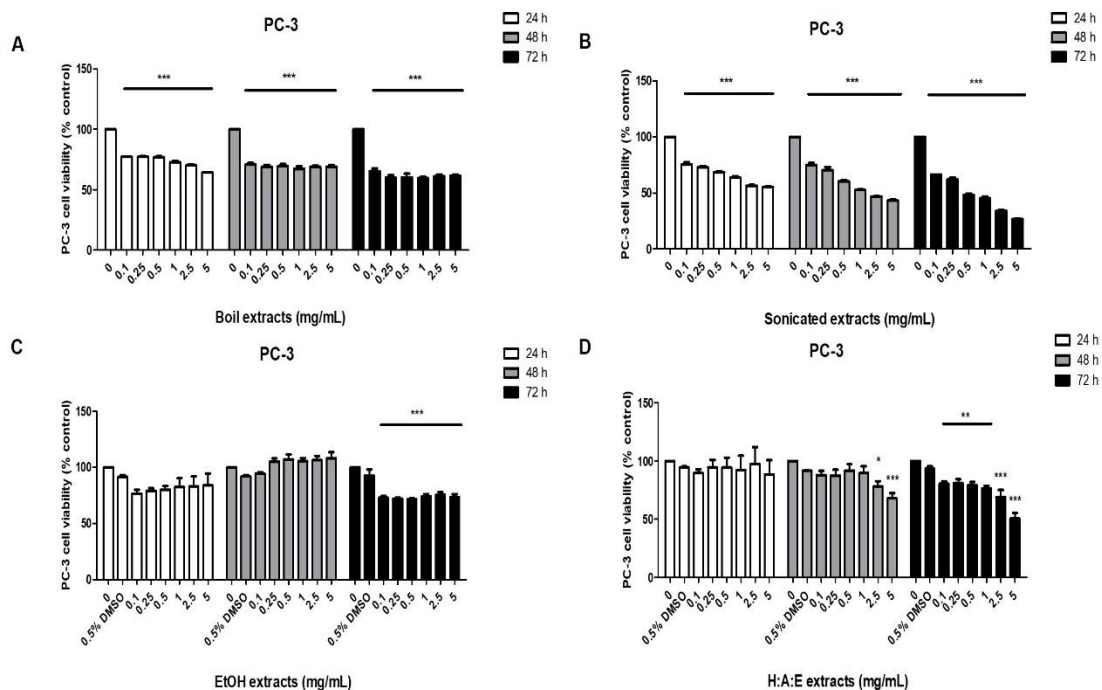
Figure 28The cytotoxicity of various crude extracts from aril part in PC-3, LNCaP cells. (A-H) Cells were cultured in 96 well plates and treated with various concentrations of different crude extracts (0-5 mg/mL) and incubated for 24 h, 48, and 72 h, respectively. Cell viability of each extract was determined by MTT assay. Data are presented as mean ± SEM (n=3) (* $p < 0.05$, ** $p < 0.01$, *** $p < 0.001$ was considered significant compared to control) of three independent experiments.
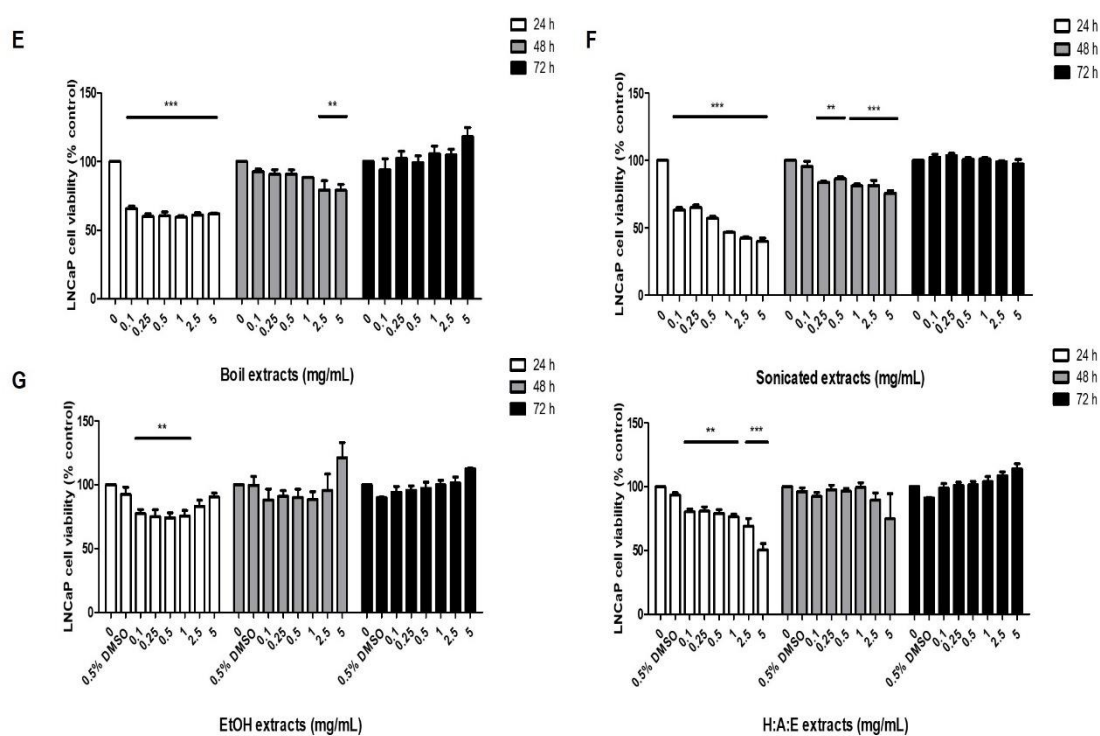
Figure 29 The cytotoxicity of various crude extracts from aril part in LNCaP cells. (E-H) Cells were cultured in 96 well plates and treated with various concentrations of different crude extracts (0-5 mg/mL) and incubated for 24 h, 48, and 72 h, respectively. Cell viability of each extract was determined by MTT assay. Data are presented as mean ± SEM (n=3) (* $p < 0.05$, ** $p < 0.01$, *** $p < 0.001$ was considered significant compared to control) of three independent experiments.
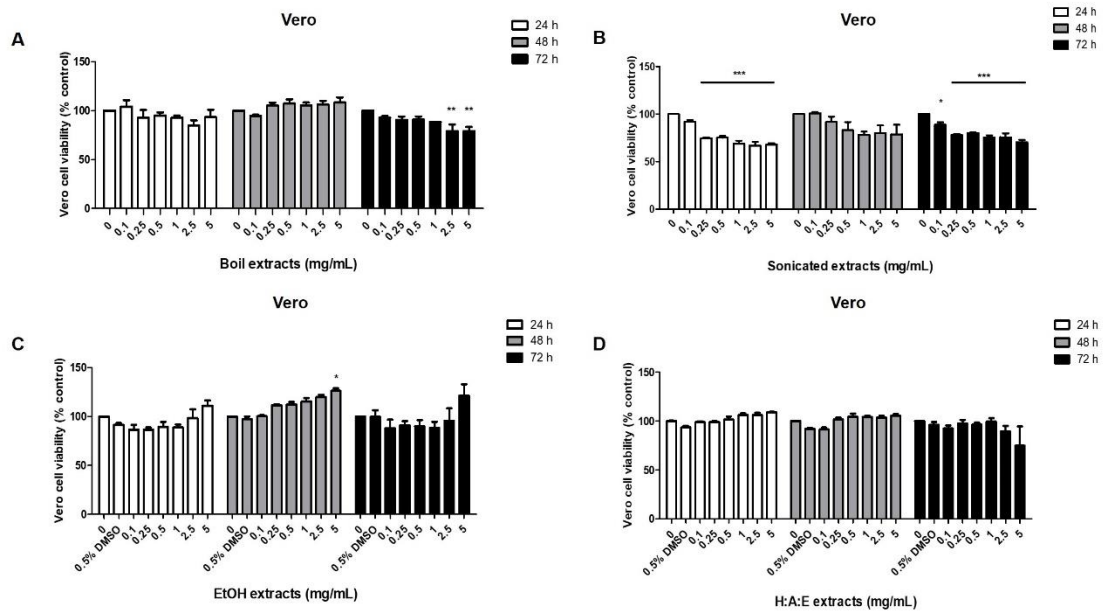
Figure 30 The cytotoxicity of various crude extracts from aril part in Vero cells. A-D) Vero cells were cultured in 96 well plates and treated with various concentrations of different crude extracts (0-5 mg/mL) and incubated for 24 h, 48, and 72 h, respectively. Cell viability of each extract was determined by MTT assay. Data are presented as mean ± SEM (*n*=3). (* *p* < 0.05, ** *p* < 0.01, *** *p* < 0.001 was considered significant compared to control) of three independent experiments.

4.2.2 The effect of the sonicated water extract on PC-3 did not induce cell damage or cell death

In a thorough observation of the result of Figure 28B, the cell characteristics indicated an intact membrane, and the number of dead cells was not observed. So, it is postulated that the effect of sonicated water extract may affect the process of cell proliferation but not the induction of cell damage or death. Thus, an LDH assay was used to test whether sonicated water extract causes damage to PC-3 cells. LDH is a cytosolic enzyme that is usually used as an indicator of cell death or cytotoxic. It is rapidly released into the cell culture medium when cells are damaged. As shown in Figure 30, the range of concentrations of sonicated water extract from 1-10 mg/mL were not induced PC-3 cells damage. The LDH levels are in the same amount as a negative untreated control sample. H_2O_2 was used as a positive control which clearly showed a high value of LDH release. These results suggested that sonicated water extract probably affects only the proliferation process. To confirm this possibility, a cell cycle analysis was further performed. Propidium iodide was used for DNA staining and the amount of DNA content in each cell cycle was determined by a flow cytometer. As shown in Figure 31A-B, the sonicated water extract at 0, 2, 4, 6, and 8 mg/mL could not induce cancer cell death. The sub-G1 or apoptotic populations did not detect in all treated samples. The number of populations of the G1 and G2/M phases was also similar. However, it is noteworthy that the population of the S phase was significantly reduced. The values are 11.82%, 11.80%, 10.08%, and 10.09%, at 2, 4, 6, and 8 mg/mL, respectively. These results indicated that sonicated water extract did not cause cell death but may interfere with the cancer cell cycle at the S phase.

A

Control | 150 µM H₂O₂ | 1 mg/mL | 2 mg/mL

4 mg/mL | 6 mg/mL | 8 mg/mL | 10mg/mL

B
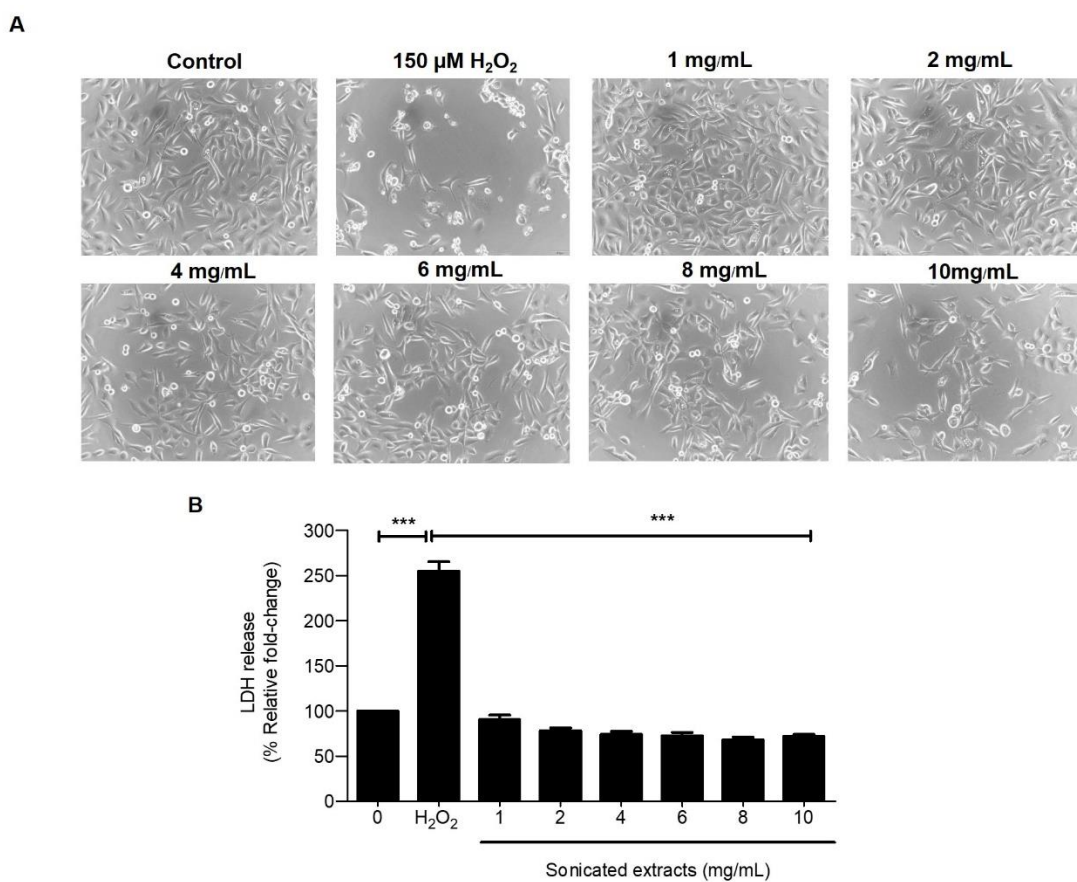
Figure 31 shows the cell damage effect of sonicated water extract on PC-3 cells. A) PC-3 cells were treated with sonicated water extracts and incubated for 24 h, which LDH released into media was determined at 490 nm using a microplate reader. B) Histogram presents the LDH release in medium collected from sample groups. Data are presented as mean ± SEM (n=3). (*** $p < 0.001$ was considered significant compared between negative control and treated group / positive and negative control) of three independent experiments.

A

Sonicated extracts (mg/mL)
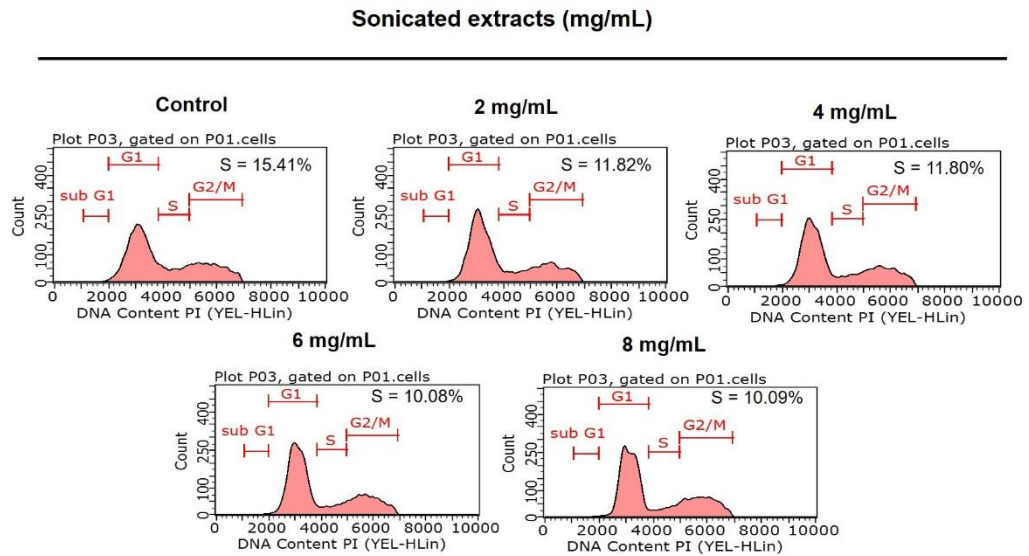
B
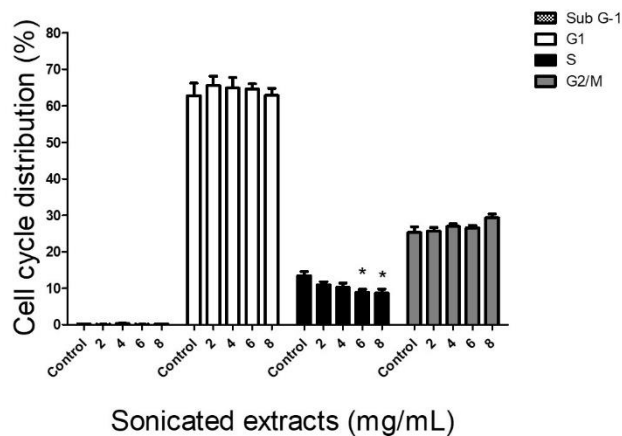
Figure 32 Cell Cycle analysis in sonicated-treated prostate cancer cells. A) PC-3 cells were treated with sonicated water extract for 24 hours and cell cycle analysis was analyzed by flow cytometry using Propidium Iodide (PI). B) Percentage of cells in sub-G1, G1, S, and G2/M phases is indicated in the histogram. Data are presented as mean ± SEM (n=3). * $p < 0.05$ compared with the control group by one way ANOVA (Dunnett's)

4.2.3 Sonicated water extract inhibits prostate cancer (PC-3) cells migration

Cell migration is critical step implicated in the progression of cancer metastasis. To determine the effect of the sonicated water extract on prostate cancer cell metastasis, the process of cancer cell migration was chosen as a target for investigation. A wound healing assay was performed by treating PC-3 cells with the sonicated water extracts at 0, 2, 4, and 6 mg/mL for 0, and 24 h. As shown in Figure 32A and B, relative wound recovery of 100% was clearly shown in the untreated control sample and at 2 mg/ml sonicated water extract treated sample. Meanwhile, at 4 and 6 mg/mL of sonicated water extracts, the percentage of wound recovery significantly reduced to less than 50% compared to the untreated control. The results revealed that sonicated water extract significantly inhibited cell migration at 24 h. The ability of sonicated water extract suppresses the migration of PC-3 prostate cancer cells was further confirmed using a transwell migration assay. Results are illustrated in Figure 32C-D, showing that PC-3 cells that migrated through the lower chamber significantly reduced after being treated with sonicated water extracts in a dose-dependent manner.
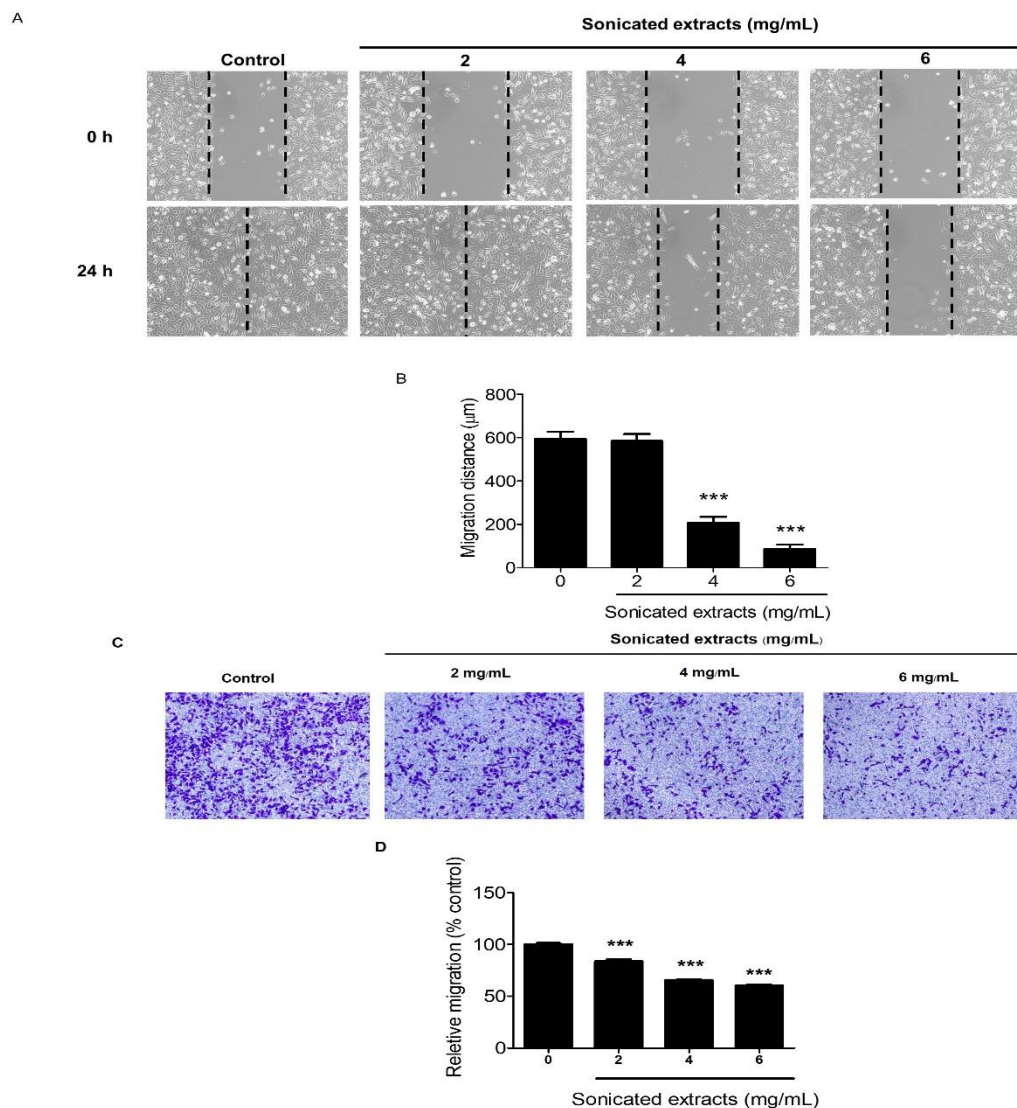
Figure 33 Shows effect of sonicated water extract inhibits migration in PC-3 cells. PC-3 cells were treated with sonicated water extract at 2, 4, and 6 mg/mL and incubated for 24 h. A) The migration of PC-3 cells was measured using wound healing assay. After 0 and 24 h migration, the scratches were photographed (left). B) The relative of wound recovery was calculated (right). (C) The migration of PC-3 cells were measured using Transwell insert migration assay. D) The relative migration of PC-3 cells were determined by using MTT assay. All experiments were repeated three times. Data are presented as means ± SEM (n=3), ** p <0.01, *** p <0.01 versus control group.

4.2.4 The sonicated water extract affects the expression of protein regulators related to cancer cell migration

In order to understand how sonicated water extract suppresses prostate cancer cell migration, the expression of protein regulators was detected using western blotting. Matrix metalloproteinase-9 (MMP-9) is selected as it is one important enzyme used in prostate cancer cell migration and invasion. Tissue inhibitor of metalloproteinase-1 (TIMP-1) and Tissue inhibitor of metalloproteinase-2 (TIMP-2), inhibitors of MMP, have also been selected. PC-3 cells were treated with 0, 2, 4, and 6 mg/mL of sonicated water extract for 24 h. Western blot analysis showed that sonicated water extract significantly decreased MMP-9 expression compared with the untreated control (Figure 33). The expression level of TIMP-1 was increased in the sonicated water extract-treated groups, while TIMP-2 was not changed in all treated samples. These results indicated that sonicated water extract suppresses the process of prostate cancer cell migration through downregulation of MMP-9 and upregulation of TIMP-1.
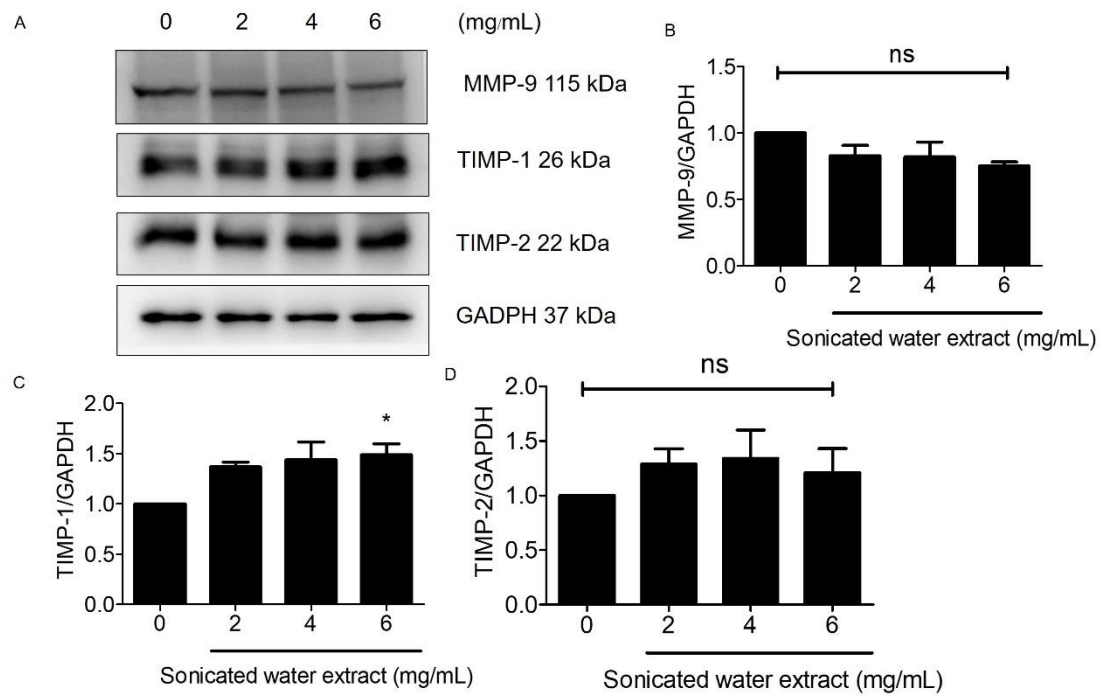
Figure 34 The effect of the sonicated water extract on the expression of protein regulators in cancer cell migration. PC-3 cells were treated with the sonicated water extracts at 0, 2, 4, and 6 mg/mL for 24 h. The protein expressions of MMP-9, TIMP-1, and TIMP-2 were evaluated using a Western blot assay. A) the expression of MMP-9, TIMP-1, TIMP-2 and GAPDH was used as a loading control. B) Shows the relative band intensity quantified by Image software. Data are presented as mean ± SEM (n=3). * $p <$ 0.05 compared with the control group by one way ANOVA (Dunnett's)

CHAPTER 5

SUMMARY DISSCUSSION AND SUGGESTION

5.1 Discussion

Prostate cancer is grown by an abnormal cell in the prostate gland area. The incidence and mortality rates are related to age, with the highest incidence in older men (> 65 years of age). Prostate cancer is often a successfully treated cancer identified in the early stage, especially in developed countries with a good cancer screening system. Lack of early detection is usually linked to metastatic diagnosis, which is difficult to treat. It is estimated that prostate cancer mortality worldwide will be 379,005 deaths from 2018 to 2040 [100]. Although advanced cancer research and new therapeutics are discovered; however, more novel anticancer agents, especially natural resources, are still required. With this aim, the present work selected *Momordica cochinchinensis* (MC) or Gac fruit that has the potential of biological activities to evaluate the anticancer function in prostate cancer cells. Various biological functions of MC are including anti-oxidant [101], anti-cancer [87], anti-inflammatory [102], anti-bacterial [103], anti-angiogenesis [104], anti-obesity [105], anti-melanogenesis [106], gastroprotective [107, 108], and duodenal ulcer protective [109] activities. These activities are mainly from the part of seeds and arils, while leaves, stems, and roots have not been studied yet. Also, a deep mechanism of anticancer activity in prostate cancer has not been elucidated.

Therefore, several parts of MC, including leaves, stems, roots, and seeds, were collected and prepared as crude extracts. The cytotoxic activity of these extracts was performed in a prostate cancer cell line (PC-3) compared with other cancer types and the representative of normal cells, Vero. As shown in Figure 13 and Table 2, the effect of crude extracts demonstrated a cytotoxic effect in all cancer cells tested but to a lesser extent in normal cells. The IC_{50} of A549 cells, HeLa cells, MDA-MB-231 cells, PC-3 cells, and Vero cells were at 0.44, 0.42, 0.62, 0.62, and 2 mg/mL, respectively. These results are consistent with other studies. The antiproliferative activities against cancer cells of a water extract from aril parts were in the range of 0.49–0.73 mg/mL [87]. Of these

extracts, the part of stem extract demonstrated the highest activity in prostate cancer cells. Therefore, stem extract was selected to further evaluate the mechanism of cell death in the prostate cancer cell line. As apoptosis is well-known and recognized as a target mechanism for an anticancer agent, so apoptotic characteristics were investigated. As depicted in Figure 14, morphology changes such as membrane blebbing, apoptotic bodies, cell shrinkage, and chromatin condensation were detected in PC-3 cells after being treated with stem extract. Liu, et al (2012) also reported that Momordica spp. extracts could induce the condensation and the fragmentation of nuclei in human gastric cancer cells, SGC7901 and MKN-28 cells [4]. Subsequently, propidium iodide (PI), a DNA intercalating agent, was used to evaluate apoptotic cell death in the sub-G1 peak that had diminished DNA content [110]. As shown in Figure 15, the treatment with stem extract increased the sub-G1 population or apoptotic members, suggesting that the stem extract could induce cellular apoptosis, correlated well with the effect of Momordica spp. on apoptosis induction in HCT-116 colorectal carcinoma cells, and CL1-0 lung adenocarcinoma cells, via increase sub-G1 population [111]. In addition, the stem extract induced damage to mitochondria. As indicated in Figure 16, the ratio of red/green was decreased in a dose-dependent manner compared with vehicle control. Similarly, Ehigie, et al (2021) reported that ethyl acetate extract of *M. charentia* L. decreased mitochondrial membrane potential, contribute to apoptosis induction in MDA-MB-436 and A549 cancer cells [112]. These data demonstrated that stem extract could trigger apoptosis in PC-3 cells by inducing morphological changes, increasing the Sub-G1 population, and reducing the mitochondrial membrane potential.

Further investigation through the expression of apoptotic signaling was also performed which demonstrated that the stem extract affects both pro-apoptotic and anti-apoptotic mediators. A pro-caspase-3 reduced significantly in a dose-dependently after being treated with stem extract (Figure 17). Normally, all caspases are present in normal cells as inactive zymogens (pro-form) and they undergo activation into a cleaved form when the apoptosis mechanism is induced. In this case, a reduction in a pro-form could therefore indicate the activation of the apoptosis pathway. Nachshon-Kedmi et al. 2004

reported that the level of pro-caspase-3 decreased following treatment in PC-3 cells, resulting to undergo apoptosis, which corresponds to our work [113]. Caspase-3 is a cysteine–aspartic protease that cleaves cellular targets and executes cell death in almost cancer cell types. Detection of cleaved caspase-3 is considered a reliable marker for cells that are died by apoptosis [114]. Besides, several members of the Bcl-2 family proteins found changes in their expression. Noxa, a pro-apoptotic BH-3-only member, increased the amount of protein expression. While Bcl-xL and Mcl-1, function as anti-apoptotic proteins decreased their expression is dose-dependent. Bcl-2 family members are key regulators of apoptotic signaling. It is divided into three subgroups based on their primary functions; pro-apoptotic pore formers (Bax, Bak, Box); pro-apoptotic BH-3 only proteins (Bad, Bid, Bim, Bmf, Noxa, Puma etc.), and anti-apoptotic proteins (Bcl-2, Bcl-xL, Bcl-W etc.) [115]. The first sub-group induces apoptosis by oligomerization and forms pores on the mitochondrial outer membrane, resulting in the release of cytochrome c. Then cytochrome c binds to APAF-1 and caspase-9 to form apoptosome, contributing to activates of caspase -9, and then leading to activate the effector caspase-3. For BH-3-only proteins, different models have been proposed. First, they could directly bind to pro-apoptotic members such as Bax and Bak and promote pore formation at the outer mitochondrial membrane. Second, BH3-only proteins can selectively bind a defined range of anti-apoptotic proteins and promote apoptosis. For example, Bad and Bmf bind to Bcl-2, Bcl-xL; Bik binds to Bcl-xL, Bcl-W; Noxa only binds to Mcl-1 and A1 [116]. Meanwhile, the last sub-group functions as anti-apoptotic by sequestering pro-apoptotic members at the outer mitochondrial membrane which causes the blockage of pore formation. As shown in this work, stem extract could reduce pro-caspase-3, Bcl-xL and Mcl-1, while increasing Noxa expression. Therefore, stem extract can promote apoptotic cell death, a crucial target for cancer treatment.

Furthermore, previous studies reported that overexpression of Bcl-xL and McL-1 are found in prostate cancer cells and contribute to chemo-resistance and uncontrolled cell growth [117, 118]. Noxa has also been indicated to react specifically with Mcl-1 and promote Mcl-1 degradation [119, 120]. According to the results of this study, a reduction in Mcl-1 may result from an increase in Noxa that causes Mcl-1 degradation. Therefore, the downregulation of pro-caspase 3, Bcl-xL, McL-1 and an increase in the amount of Noxa in PC-3 cells upon stem extract treatment may have caused a disruption in the integrity of the outer mitochondria membrane by increasing its permeability, resulting in induced apoptosis, which correlated with Ai, et al (2021) suggested that ethanol extract of *M. cochinchinensis* seed induced Chronic Myeloid Leukemia cells (KBM5 and KBM5-T315I) apoptosis through activating caspase-3,8,9 and down regulating Mcl-1 [121]. These data indicate another possible role of the stem extract that could reverse the chemoresistance property of prostate cancer cells. However, it is noticeable that the amount of stem extract at 1.2 mg/mL or higher may have a strong toxic effect on the cells, as the amount of Noxa was decreased. Hence, the effective concentration of stem extract should be in the range of 0.6–0.9 mg/mL.

Due to a promising effect of stem extract of MC, a further investigation of the possible active compounds was chemically characterized. As a result, α-spinasterol and ligballinol were successfully isolated from stem extract with a phytosterol and furanoid lignan structure. The cytotoxicity of these two compounds in PC-3 cells has been determined. As demonstrated in Figure 27, only ligballinol inhibited PC-3 cell proliferation with an IC_{50} of 230 µM, while it did not work in Vero cells. Ligballinol has also been reported for antiproliferative effect in human colorectal cancer cells (HT-29) with an IC_{50} value of 45.5 µM [122]. Additionally, Sedky, et al (2018) reported that α-spinasterol could induce DNA fragmentation and upregulate p53 in breast cancer cells (MCF-7), ovarian cancer cells (SKOV-3) [123], which correlated with Ravikumar, et al (2010) [124] reported that α-spinasterol induced apoptosis in colorectal cancer cells (CACO-2). For α-spinasterol, Meneses-Sagrero, et al (2017) reported that it did not cause cytotoxicity in PC-3 cells, which correlated with this work [125]. These results

suggest that ligballinol may be an active compound responsible for the anticancer activity of the stem extract.

The present work also demonstrated another role of MC. Aril part was prepared as crude extracts (boil water, sonicated water, 80% EtOH, and H:A:E extracts) and screened for the cytotoxicity in PC-3, LNCaP, and Vero cells. Figure 28-29 shows that only sonicated and H:A:E crude extracts have the cytotoxic to both prostate cancer cells (PC-3 and LNCaP). However, the sonicated water extract is more potential and selectively cytotoxic in PC-3 cells. This result correlated well with Wimalasiri, et al. (2020) reported that H:A:E extract from the aril part of MC exhibited low cytotoxicity [87]. To confirm the cytotoxicity and damaging effect of the sonicated water extract, the LDH assay was used. As revealed in Fig. 30, 1–10 mg/mL of the sonicated water extract could not induce PC-3 cells damage when compared with H_2O_2, a positive control. This effect was confirmed by an undetectable sub-G1 peak or apoptotic populations (Figure 31). However, the reduction of S-phase populations implies that the sonicated water extract may interfere with the process of DNA synthesis or replication [126]. These results demonstrate that the sonicated water extract from the aril part could inhibit cell proliferation but not cause cell damage or death.

To explore other possible functions of the sonicated water extract, the inhibition of prostate cancer cell migration was performed as it is a mainly problem for cancer treatment. Metastasis comprises several processes including cell migration, cell invasion, cell adhesion, and angiogenesis, in which the migration of cancer cells is the first step. So, the present work selected cancer cell migration as a target for evaluation. Wound healing and transwell migration assay were then selected to perform. As depicted in Figure 32 A-B, the concentration of sonicated water extract at 4-6 mg/mL significantly reduced the migratory ability of PC-3 cells, in accordance with the result of the transwell migration assay (Figure 32 D-C). Yang, et al (2015) reported that ECMS suppress the proliferation and metastasis of human lung cancer cells, increase the level of E-cadherin and decrease of the level of STAT-3 and MMP-2, and resulted in the

inhibition of migration and invasion [3]. The present data demonstrated that sonicated water extract from the aril part could inhibit prostate cancer cell migration.

To further examine the signaling involved in cancer cell migration, MMP-9, TIMP-1, and TIMP-2 are determined. MMPs are proteolytic enzymes that are considered key mediators for cancer progression. They degrade the extracellular matrix (ECM) and basement membrane which facilitate the migration and invasion of cancer cells [127]. Increased expression of MMPs has been associated with poor prognosis in aggressive prostate cancer stages, especially MMP-2 and MMP-9 [128]. MMP-2 and MMP-9 belong to gelatinase, which is one of five groups of the MMP family. MMP-2 is released by cancer cells in the form of a zymogen and can specifically degrade collagen type IV. While MMP-9 enhances metastasis of cancer cells by degrading collagen proteins of the ECM. TIMP-1 and TIMP-2, are tissue inhibitors of metalloproteinases (TIMPs), which are endogenous inhibitors of metalloproteinases. TIMP-1 binds with high affinity to MMP-9, while TIMP-2 binds with MMP-2 [129]. Indeed, Brehmer, et al (2003) reported that the imbalance between MMPs and TIMPs results in progression and metastases in prostate cancer [130, 131]. So, it is postulated that the sonicated water extract may affect the expression of these molecules resulting in the suppression of prostate cancer cell migration. As shown in Figure 33, PC-3 cells treated with the sonicated water extract at 2, 4, and 6 mg/mL for 24 h demonstrated a reduction of MMP-9 expression in a dose-dependent manner, which correlated well with an increase of TIMP-1, but not TIMP-2. Zheng, et al (2014) reported that ESMC has the potential to suppress the migration and invasion of ZR-75-30 breast cancer cells, through down regulation of MMP-2 and MMP-9 [132] Our results indicated that the sonicated water extract suppresses prostate cancer cell migration via the regulation of MMP-9 and TIMP-1. These findings suggested that the sonicated water extract from the aril part has the potential to act as an anti-metastatic agent, which is a novel biological activity in this plant.

5.2 Conclusion

In summary, the present work confirms at the cellular level that stem extract from *M. cochinchinensis* could inhibit the proliferation of prostate cancer cells and induce cell

death by apoptosis. The effect of stem extract is via caspase-3 and Noxa, pro-apoptotic mediators. In addition, stem extract may reverse chemo-resistance's property by reducing Mcl-1. The possible active compound was ligballinol which has antiproliferative ability on PC-3 prostate cancer cells. Additionally, the present study demonstrated the effect of the sonicated water extract from the aril part of *M. cochinchinensis* to act as an anti-proliferative and anti-metastatic agent in prostate cancer cells. The inhibition of cancer cell migration was via MMP-9 and TIMP-1 regulations. These results support the value of *M. cochinchinensis* as a resource for anticancer agent development.

REFERENCES

1.	Siegel RL, Miller KD, Jemal A. Cancer statistics, 2020. CA Cancer J Clin. 2020;70(1):7-30.

2.	Yu JS RH, Lee S, Jung K, Baek KH, Kim KH. Antiproliferative effect of *Momordica cochinchinensis* seeds on human lung cancer cells and isolation of the major constituents. Rev Bras Farmacogn. 2017;27(3):329-33.

3.	Shen Y, Meng L, Sun H, Zhu Y, Liu H. Cochinchina momordica seed suppresses proliferation and metastasis in human lung cancer cells by regulating multiple molecular targets. Am J Chin Med. 2015;43(1):149-66.

4.	Liu HR, Meng LY, Lin ZY, Shen Y, Yu YQ, Zhu YZ. Cochinchina momordica seed extract induces apoptosis and cell cycle arrest in human gastric cancer cells via PARP and p53 signal pathways. Nutr Cancer. 2012;64(7):1070-7.

5.	Meng LY LH, Shen Y, Yu YQ, Tao X. Cochinchina momordica seed extract induces G2/M arrest and apoptosis in human breast cancer MDA-MB-231 cells by modulating the PI3K/Akt pathway. Asian Pac J Cancer Prev. 2011;12(12):3483-8.

6.	Tien PG, Kayama F, Konishi F, Tamemoto H, Kasono K, Hung NT, et al. Inhibition of tumor growth and angiogenesis by water extract of Gac fruit (*Momordica cochinchinensis* Spreng). Int J Oncol. 2005;26(4):881-9.

7.	Chuethong J, Oda K, Sakurai H, Saiki I, Leelamanit W. Cochinin B, a novel ribosome-inactivating protein from the seeds of *Momordica cochinchinensis*. Biol Pharm Bull. 2007;30(3):428-32.

8.	Brandywine Urology Consultants [Internet]. New Castle: Helen F. Graham Cancer Center; 2014 [cited 2014 April 19]. Available from: Aviable from: https://www.brandywineuc.com/about-us/.

9.	Hospital based cancer registry 2020. Bangkok: National Cancer Institute; 2022 [cited 2022 Fabruary 14]. Available from: https://www.nci.go.th/e_book/hosbased_2563/index.html.

10.   Thomas TH. What to know about prostate cancer: MedicalNewsToday; 2018 [updated 2021 November 18; cited 2018 February 12]. Available from: https://www.medicalnewstoday.com/articles/150086#outlook.

11.   Prostate cancer: Urology Care Foundation; 2018 [updated 2018 January 31; cited 2018 February 12]. Available from: https://www.urologyhealth.org/urologic-conditions/prostate-cancer.

12.   Borno HT, Small EJ. Apalutamide and its use in the treatment of prostate cancer. Future Oncol. 2019;15(6):591-9.

13.   Linder S, van der Poel HG, Bergman AM, Zwart W, Prekovic S. Enzalutamide therapy for advanced prostate cancer: efficacy, resistance and beyond. Endocr Relat Cancer. 2018;26(1):R31-R52.

14.   Paller CJ, Carducci MA, Philips GK. Management of bone metastases in refractory prostate cancer--role of denosumab. Clin Interv Aging. 2012;7:363-72.

15.   Nevedomskaya E, Baumgart SJ, Haendler B. Recent Advances in Prostate Cancer Treatment and Drug Discovery. Int J Mol Sci. 2018;19(5).

16.   Macherey S, Monsef I, Jahn F, Jordan K, Yuen KK, Heidenreich A, et al. Bisphosphonates for advanced prostate cancer. Cochrane Database Syst Rev. 2017;12:CD006250.

17.   Mulders PF, De Santis M, Powles T, Fizazi K. Targeted treatment of metastatic castration-resistant prostate cancer with sipuleucel-T immunotherapy. Cancer Immunol Immunother. 2015;64(6):655-63.

18.   Wyllie AH, Kerr JFR, Currie AR. Cell death: the significance of apoptosis. International Review of Cytology 1980;68:251-306.

19.   Makin G, Dive C. Apoptosis and cancer therapy. Trends Cell Biol. 2001;11:22-6.

20.   Andre N, Breguer D, Brasseur G, Goncalves A, Lemesle-Meunier D, Guise S. Paclitaxel induces release of cytochrome c from mitochondria isolated from human neuroblastoma. Cancer Res Treat. 2000;60:5349-53.

21.   Bush JA, Cheung KJ, Jr., Li G. Curcumin induces apoptosis in human melanoma cells through a Fas receptor/caspase-8 pathway independent of p53. Exp Cell Res. 2001;271(2):305-14.

22.   Srinivasula SM, Ahmad M, Fernandes-Alnemri T, Alnemri ES. Autoactivation of procaspase-9 by Apaf-1-mediated oligomerization. Mol Cell. 1998;1(7):949-57.

23.   Lavrik IN, Golks A, Krammer PH. Caspases: pharmacological manipulation of cell death. J Clin Invest. 2005;115(10):2665-72.

24.   Walters J, Pop C, Scott FL, Drag M, Swartz P, Mattos C, et al. A constitutively active and uninhibitable caspase-3 zymogen efficiently induces apoptosis. Biochem J. 2009;424(3):335-45.

25.   Porter AG, Janicke RU. Emerging roles of caspase-3 in apoptosis. Cell Death Differ. 1999;6(2):99-104.

26.   Yilmaz SG, Yencilek F, Yildirim A, Yencilek E, Isbir T. Effects of Caspase 9 Gene Polymorphism in Patients with Prostate Cancer. In Vivo. 2017;31(2):205-8.

27.   Bratton SB, Salvesen GS. Regulation of the Apaf-1-caspase-9 apoptosome. J Cell Sci. 2010;123(Pt 19):3209-14.

28.   Theodoropoulos GE, Michalopoulos NV, Pantou MP, Kontogianni P, Gazouli M, Karantanos T, et al. Caspase 9 promoter polymorphisms confer increased susceptibility to breast cancer. Cancer Genet. 2012;205(10):508-12.

29.   Beug ST, Cheung HH, LaCasse EC, Korneluk RG. Modulation of immune signalling by inhibitors of apoptosis. Trends Immunol. 2012;33(11):535-45.

30.   Hunter AM, LaCasse EC, Korneluk RG. The inhibitors of apoptosis (IAPs) as cancer targets. Apoptosis. 2007;12(9):1543-68.

31.   Ribe EM, Serrano-Saiz E, Akpan N, Troy CM. Mechanisms of neuronal death in disease: defining the models and the players. Biochem J. 2008;415(2):165-82.

32.   Kulig E, Jin L, Qian X, Horvath E, Kovacs K, Stefaneanu L, et al. Apoptosis in nontumorous and neoplastic human pituitaries: expression of the Bcl-2 family of proteins. Am J Pathol. 1999;154(3):767-74.

33.   Strasser A, Cory S, Adams JM. Deciphering the rules of programmed cell death to improve therapy of cancer and other diseases. EMBO J. 2011;30(18):3667-83.

34.   Youle RJ, Strasser A. The BCL-2 protein family: opposing activities that mediate cell death. Nat Rev Mol Cell Biol. 2008;9(1):47-59.

35.   Kelekar A, Thompson CB. Bcl-2-family proteins: the role of the BH3 domain in apoptosis. Trends Cell Biol. 1998;8(8):324-30.

36.   Cory S, Huang DC, Adams JM. The Bcl-2 family: roles in cell survival and oncogenesis. Oncogene. 2003;22(53):8590-607.

37.   Lomonosova E, Chinnadurai G. BH3-only proteins in apoptosis and beyond: an overview. Oncogene. 2008;27 Suppl 1:S2-19.

38.   Ow YP, Green DR, Hao Z, Mak TW. Cytochrome c: functions beyond respiration. Nat Rev Mol Cell Biol. 2008;9(7):532-42.

39.   Orrenius S, Zhivotovsky B. Cardiolipin oxidation sets cytochrome c free. Nat Chem Biol. 2005;1(4):188-9.

40.   Shi Y. A structural view of mitochondria-mediated apoptosis. Nat Struct Biol. 2001;8(5):394-401.

41.   Anguiano-Hernandez YM, Chartier A, Huerta S. Smac/DIABLO and colon cancer. Anticancer Agents Med Chem. 2007;7(4):467-73.

42.   Bajt ML, Cover C, Lemasters JJ, Jaeschke H. Nuclear translocation of endonuclease G and apoptosis-inducing factor during acetaminophen-induced liver cell injury. Toxicol Sci. 2006;94(1):217-25.

43.   Jang DS, Penthala NR, Apostolov EO, Wang X, Crooks PA, Basnakian AG. Novel cytoprotective inhibitors for apoptotic endonuclease G. DNA Cell Biol. 2015;34(2):92-100.

44.   Diener T, Neuhaus M, Koziel R, Micutkova L, Jansen-Durr P. Role of endonuclease G in senescence-associated cell death of human endothelial cells. Exp Gerontol. 2010;45(7-8):638-44.

45.   Ashkenazi A, Dixit VM. Death receptors: signaling and modulation. Science. 1998;281(5381):1305-8.

46. Fulda S, Debatin KM. Extrinsic versus intrinsic apoptosis pathways in anticancer chemotherapy. Oncogene. 2006;25(34):4798-811.

47. Elmore S. Apoptosis: a review of programmed cell death. Toxicol Pathol. 2007;35(4):495-516.

48. Rager JE. The Role of Apoptosis-Associated Pathways as Responders to Contaminants and in Disease Progression. . Systems Biology in Toxicology and Environmental Health. 2015:187-205.

49. Tamm I, Schriever F, Dorken B. Apoptosis: implications of basic research for clinical oncology. Lancet Oncol. 2001;2(1):33-42.

50. Kang MH, Reynolds CP. Bcl-2 inhibitors: targeting mitochondrial apoptotic pathways in cancer therapy. Clin Cancer Res. 2009;15(4):1126-32.

51. Cuda CM, Pope RM, Perlman H. The inflammatory role of phagocyte apoptotic pathways in rheumatic diseases. Nat Rev Rheumatol. 2016;12(9):543-58.

52. Wirtz D, Konstantopoulos K, Searson P. The physics of cancer: the role of physical interactions and mechanical forces in metastasis. Nat Rev Cancer. 2011;11:512-22.

53. Bauvois B. New facets of matrix metalloproteinases MMP-2 and MMP-9 as cell surface transducers: outside-in signaling and relationship to tumor progression. Biochim Biophys Acta. 2012;1825(1):29-36.

54. Snoek-van Beurden PA, Von den Hoff JW. Zymographic techniques for the analysis of matrix metalloproteinases and their inhibitors. Biotechniques. 2005;38(1):73-83.

55. Cathcart J, Pulkoski-Gross A, Cao J. Targeting Matrix Metalloproteinases in Cancer: Bringing New Life to Old Ideas. Genes Dis. 2015;2(`1):26-34.

56. Sliwowska I, Kopczyński Z. [Zymography-method for quantitation of activity on gelatinase A (pro-MMP-2, 72 kDa) and gelatinase B (pro-MMP-9, 92 kDa) in serum of patients with breast cancer]. Wiad Lek. 2007;60(5-6):241-7.

57. Friedl P, Wolf K. Tumour-cell invasion and migration: diversity and escape mechanisms. Nat Rev Cancer. 2003;3(5):362-74.

58.   Mendes O, Kim HT, Stoica G. Expression of MMP2, MMP9 and MMP3 in breast cancer brain metastasis in a rat model. Clin Exp Metastasis. 2005;22(3):237-46.

59.   Murphy G. Tissue inhibitors of metalloproteinases. . Genome Biolo. 2011;12(11):233.

60.   Roderfeld M, Graf J, Giese B, Salguero-Palacios R, Tschuschner A, Muller-Newen G, et al. Latent MMP-9 is bound to TIMP-1 before secretion. Biol Chem. 2007;388(11):1227-34.

61.   Li G, Fridman R, Kim HR. Tissue inhibitor of metalloproteinase-1 inhibits apoptosis of human breast epithelial cells. Cancer Res. 1999;59(24):6267-75.

62.   Liu XW, Taube ME, Jung KK, Dong Z, Lee YJ, Roshy S, et al. Tissue inhibitor of metalloproteinase-1 protects human breast epithelial cells from extrinsic cell death: a potential oncogenic activity of tissue inhibitor of metalloproteinase-1. Cancer Res. 2005;65(3):898-906.

63.   Sang QX. Complex role of matrix metalloproteinases in angiogenesis. Cell Res. 1998;8(3):171-7.

64.   Zhang Y, Qian H, Lin C, Lang J, Xiang Y, Fu M, et al. Adenovirus carrying TIMP-3: a potential tool for cervical cancer treatment. Gynecol Oncol. 2008;108(1):234-40.

65.   Lizarraga F, Espinosa M, Ceballos-Cancino G, Vazquez-Santillan K, Bahena-Ocampo I, Schwarz-Cruz YCA, et al. Tissue inhibitor of metalloproteinases-4 (TIMP-4) regulates stemness in cervical cancer cells. Mol Carcinog. 2016;55(12):1952-61.

66.   Lizarraga F, Ceballos-Cancino G, Espinosa M, Vazquez-Santillan K, Maldonado V, Melendez-Zajgla J. Tissue Inhibitor of Metalloproteinase-4 Triggers Apoptosis in Cervical Cancer Cells. PLoS One. 2015;10(8):e0135929.

67.   Koskivirta I, Rahkonen O, Mayranpaa M, Pakkanen S, Husheem M, Sainio A, et al. Tissue inhibitor of metalloproteinases 4 (TIMP4) is involved in inflammatory processes of human cardiovascular pathology. Histochem Cell Biol. 2006;126(3):335-42.

68.   Wang M, Liu Y, Greene J, Sheng S, Fuchs A, Rosen E, et al. Inhibition of tumor growth and metastasis of human breast cancer cells transfected with tissue inhibitor of metalloproteinase 4. Oncogene. 1997:2767-.

69.   Vuong le T, Dueker SR, Murphy SP. Plasma beta-carotene and retinol concentrations of children increase after a 30-d supplementation with the fruit *Momordica cochinchinensis* (gac). Am J Clin Nutr. 2002;75(5):872-9.

70.   Aoki H, Kieu NT, Kuze N, Tomisaka K, Van Chuyen N. Carotenoid pigments in GAC fruit (*Momordica cochinchinensis* SPRENG). Biosci Biotechnol Biochem. 2002;66(11):2479-82.

71.   Muller-Maatsch J, Sprenger J, Hempel J, Kreiser F, Carle R, Schweiggert RM. Carotenoids from gac fruit aril (*Momordica cochinchinensis* [Lour.] Spreng.) are more bioaccessible than those from carrot root and tomato fruit. Food Res Int. 2017;99(Pt 2):928-35.

72.   Jan-on G, Kukongviriyapan U, Pakdeechote P, Kukongviriyapan V, Kongsaktrakoon B, O B. Alleviation of Hypertension and Oxidative Stress by *Momordica cochinchinensis* Aril Extract in Rats with Nitric Oxide Deficiency. . Srinagarind Med J. 2015;30(3):229-35.

73.   Sampannang A AS, Burawat J, Sukhorum W , S I. Non-toxic Effect of *Momordica cochinchinensis* Spreng Aril Extract on Reproductive System of Male Mice Srinagarind Med J 2017;32(1):52-7.

74.   Bowen P, Chen L, Stacewicz-Sapuntzakis M, Duncan C, Sharifi R, Ghosh L, et al. Tomato sauce supplementation and prostate cancer: lycopene accumulation and modulation of biomarkers of carcinogenesis. Exp Biol Med (Maywood). 2002;227(10):886-93.

75.   Clinton SK, Emenhiser C, Schwartz SJ, Bostwick DG, Williams AW, Moore BJ, et al. cis-trans lycopene isomers, carotenoids, and retinol in the human prostate. Cancer Epidemiol Biomarkers Prev. 1996;5(10):823-33.

76.   Unlu NZ, Bohn T, Francis DM, Nagaraja HN, Clinton SK, Schwartz SJ. Lycopene from heat-induced cis-isomer-rich tomato sauce is more bioavailable than from all-trans-rich tomato sauce in human subjects. Br J Nutr. 2007;98(1):140-6.

77.   Ishida BK, Turner C, Chapman MH, McKeon TA. Fatty acid and carotenoid composition of gac (*Momordica cochinchinensis* Spreng) fruit. J Agric Food Chem. 2004;52(2):274-9.

78.   Vuong LT, Franke AA, Custer LJ, Murphy SP. *Momordica cochinchinensis* Spreng. (gac) fruit carotenoids reevaluated. J Food Compost Anal. 2006;19:664-68.

79.   Le AV, Huynh TT, Parks SE, Nguyen MH, Roach PD. Bioactive Composition, Antioxidant Activity, and Anticancer Potential of Freeze-Dried Extracts from Defatted Gac (*Momordica cochinchinensis* Spreng) Seeds. Medicines (Basel). 2018;5(3).

80.   Jung K, Chin YW, Yoon K, Chae HS, Kim CY, Yoo H, et al. Anti-inflammatory properties of a triterpenoidal glycoside from *Momordica cochinchinensis* in LPS-stimulated macrophages. Immunopharmacol Immunotoxicol. 2013;35(1):8-14.

81.   Jung K, Lee D, Yu JS, Namgung H, Kang KS, Kim KH. Protective effect and mechanism of action of saponins isolated from the seeds of gac (*Momordica cochinchinensis* Spreng.) against cisplatin-induced damage in LLC-PK1 kidney cells. Bioorg Med Chem Lett. 2016;26(5):1466-70.

82.   Klungsupya P, Saenkhum J, Muangman T, Rerk-Am U, Laovitthayanggoon S, W L. Non-Cytotoxic Property and DNA Protective Activity against H2O2 and UVC of Thai GAC Fruit Extracts in Human TK6 Cells. J Applied Pharma Sci. 2012;2(4):4-8.

83.   Zheng L, Zhang Y, Liu Y, Yang XO, Zhan Y. *Momordica cochinchinensis* Spreng. seed extract suppresses breast cancer growth by inducing cell cycle arrest and apoptosis. Mol Med Rep. 2015;12(4):6300-10.

84.   Petchsak P, Sripanidkulchai B. *Momordica cochinchinensis* Aril Extract Induced Apoptosis in Human MCF-7 Breast Cancer Cells. Asian Pac J Cancer Prev. 2015;16(13):5507-13.

85.   Hacker G, Weber A. BH3-only proteins trigger cytochrome c release, but how? Arch Biochem Biophys. 2007;462(2):150-5.

86.   Sivandzade F, Bhalerao A, Cucullo L. Analysis of the Mitochondrial Membrane Potential Using the Cationic JC-1 Dye as a Sensitive Fluorescent Probe. Bio Protoc. 2019;9(1).

87.   Wimalasiri D, Dekiwadia C, Fong SY, Piva TJ, Huynh T. Anticancer activity of *Momordica cochinchinensis* (red gac) aril and the impact of varietal diversity. BMC Complement Med Ther. 2020;20(1):365.

88.   Liang CC, Park AY, Guan JL. In vitro scratch assay: a convenient and inexpensive method for analysis of cell migration in vitro. Nat Protoc. 2007;2(2):329-33.

89.   Zhang ZH, Xie DD, Xu S, Xia MZ, Zhang ZQ, Geng H, et al. Total glucosides of paeony inhibits lipopolysaccharide-induced proliferation, migration and invasion in androgen insensitive prostate cancer cells. PLoS One. 2017;12(8):e0182584.

90.   Chainumnim S, Saenkham A, Dolsophon K, Chainok K, Suksamrarn S, Tanechpongtamb W. Stem Extract from *Momordica cochinchinensis* Induces Apoptosis in Chemoresistant Human Prostate Cancer Cells (PC-3). Molecules. 2022;27(4).

91.   Kan LD, Hu Q, Chao ZM, Song X, Cao XL. [Chemical constituents of unsaponifiable matter from seed oil of *Momordica cochinchinensis*]. Zhongguo Zhong Yao Za Zhi. 2006;31(17):1441-4.

92.   Zhao LM, Sun GG, Han LN, Liu LH, Ren FZ, Li L, et al. P-Hydroxycinnamaldehyde Induces B16-F1 Melanoma Cell Differentiation via the RhoA-MAPK Signaling Pathway. Cell Physiol Biochem. 2016;38(6):2247-60.

93.   Herath HM, Athukoralage PS, Jamie JF. A new oleanane triterpenoid from Gordonia ceylanica. Nat Prod Lett. 2001;15(5):339-44.

94.   Rao M, Lavie D. The constituents of Ecballium elaterium L.—XXII, phenolics as minor components. Tetrahedron. 1974;30:3309–13.

95.   Minh CV, Nhiem NX, Yen HT, Kiem PV, Tai BH, Le Tuan Anh H, et al. Chemical constituents of *Trichosanthes kirilowii* and their cytotoxic activities. Arch Pharm Res. 2015;38(8):1443-8.

96.   Bruker. APEX3, SAINT, SADABS and XP. In: Inc BA, editor. Madison, WI, USA2016.

97.   Sheldrick GM. SHELXT - integrated space-group and crystal-structure determination. Acta Crystallogr A Found Adv. 2015;71(Pt 1):3-8.

98.   Sheldrick GM. Crystal structure refinement with SHELXL. Acta Crystallogr C Struct Chem. 2015;71(Pt 1):3-8.

99.   Dolomanov OV, Bourhis LJ, Gildea RJ, Howard JAK, Puschmann H. OLEX2: A complete structure solution, refinement and analysis program. J Appl Crystallogr. 2009;42:339-41.

100.   Rawla P. Epidemiology of Prostate Cancer. World J Oncol. 2019;10(2):63-89.

101.   Kubola J, Siriamornpun S. Phytochemicals and antioxidant activity of different fruit fractions (peel, pulp, aril and seed) of Thai gac (*Momordica cochinchinensis* Spreng). Food Chem. 2011;127(3):1138-45.

102.   Sukboon P, Tuntipopipat S, Praengam K. Ethanol Extract of Aril and Pulp from Momordica cochinchinensis Fruit Exhibits Anti-inflammatory Effect in LPS-induced Macrophage RAW264.7 Cells. Thai Journal of Toxicology. 2019;34:71-90.

103.   Chantarangsee M. Antioxidant and Antibacterial Activities of Ethanolic Extracts from Different Parts of Gac Fruit. KKU Sci J. 2015;43:490-502.

104.   Tien PG, Kayama F, Konishi F, Tamemoto H, Kasono K, Hung NT, et al. Inhibition of tumor growth and angiogenesis by water extract of Gac fruit (*Momordica cochinchinensis* Spreng). Int J Oncol. 2005;26(881-889).

105.   Huang HC, Chen CJ, Lai YH, Lin YC, Chiou WC, Lu HF, et al. *Momordica cochinchinensis* Aril Ameliorates Diet-Induced Metabolic Dysfunction and Non-Alcoholic Fatty Liver by Modulating Gut Microbiota. Int J Mol Sci. 2021;22(5).

106.   Kim J, Hong SC, Lee EH, Lee JW, Yang SH, Kim JC. Preventive Effect of *M. cochinchinensis* on Melanogenesis via Tyrosinase Activity Inhibition and p-PKC Signaling in Melan-A Cell. Nutrients. 2021;13(11).

107.   Kang JM, Kim N, Kim B, Kim JH, Lee BY, Park JH, et al. Enhancement of gastric ulcer healing and angiogenesis by cochinchina Momordica seed extract in rats. J Korean Med Sci. 2010;25(6):875-81.

108.   Lim JH, Kim JH, Kim N, Lee BH, Seo PJ, Kang JM, et al. Gastroprotective effect of Cochinchina momordica seed extract in nonsteroidal anti-inflammatory drug-induced acute gastric damage in a rat model. Gut Liver. 2014;8(1):49-57.

109. Choi KS, Kim EH, Hong H, Ock CY, Lee JS, Kim JH, et al. Attenuation of cysteamine-induced duodenal ulcer with Cochinchina momordica seed extract through inhibiting cytoplasmic phospholipase A2/5-lipoxygenase and activating gamma-glutamylcysteine synthetase. J Gastroenterol Hepatol. 2012;27 Suppl 3:13-22.

110. Darzynkiewicz Z, Halicka H, Zhao H. Analysis of cellular DNA content by flow and laser scanning cytometry. Adv Exp Med Biol. 2010;676:137-47.

111. Li CJ, Tsang SF, Tsai CH, Tsai HY, Chyuan JH, Hsu HY. *Momordica charantia* Extract Induces Apoptosis in Human Cancer Cells through Caspase- and Mitochondria-Dependent Pathways. Evid Based Complement Alternat Med. 2012;2012:261971.

112. Ehigie AF, Wei P, Wei T, Yan X, Olorunsogo OO, Ojeniyi FD, et al. *Momordica charantia* L. induces non-apoptotic cell death in human MDA-MB-436 breast and A549 lung cancer cells by disrupting energy metabolism and exacerbating reactive oxygen species' generation. J Ethnopharmacol. 2021;277:114036.

113. Nachshon-Kedmi M, Yannai S, Fares F. Induction of apoptosis in human prostate cancer cell line, PC3, by 3,3′-diindolylmethane through the mitochondrial pathway. Br J Cancer 2014;91:1358–63

114. Fulda S, Debatin K. Extrinsic versus intrinsic apoptosis pathways in anticancer chemotherapy. Oncogene. 2006;25:4798–811.

115. Kale J, Osterlund EJ, Andrews DW. BCL-2 family proteins: changing partners in the dance towards death. Cell Death Differ. 2018;25(1):65-80.

116. Shamas-Din A, Brahmbhatt H, Leber B, Andrews DW. BH3-only proteins: Orchestrators of apoptosis. Biochim Biophys Acta. 2011;1813(4):508-20.

117. Reiner T, de Las Pozas A, Parrondo R, Palenzuela D, Cayuso W, Rai P, et al. Mcl-1 protects prostate cancer cells from cell death mediated by chemotherapy-induced DNA damage. Oncoscience. 2015;2(8):703-15.

118. Greaves G, Milani M, Butterworth M, Carter RJ, Byrne DP, Eyers PA, et al. BH3-only proteins are dispensable for apoptosis induced by pharmacological inhibition of both MCL-1 and BCL-XL. Cell Death Differ. 2019;26(6):1037-47.

119. Chen L, Willis SN, Wei A, Smith BJ, Fletcher JI, Hinds MG, et al. Differential targeting of prosurvival Bcl-2 proteins by their BH3-only ligands allows complementary apoptotic function. Mol Cell. 2005;17(3):393-403.

120. Willis SN, Chen L, Dewson G, Wei A, Naik E, Fletcher JI, et al. Proapoptotic Bak is sequestered by Mcl-1 and Bcl-xL, but not Bcl-2, until displaced by BH3-only proteins. Genes Dev. 2005;19(11):1294-305.

121. Ai Z, Ma C, Wan R, Yin J, Li G, Li Y, et al. Anticancer Activity and Molecular Mechanism of *Momordica cochinchinensis* Seed Extract in Chronic Myeloid Leukemia Cells. Nutr Cancer. 2021:1-13.

122. Van Minh C, Nhiem NX, Yen HT, Van Kiem P, Tai BH, Anh HLT. Chemical constituents of *Trichosanthes kirilowii* and their cytotoxic activities. Arch Pharmacal Res. 2015;38:1443–8.

123. Sedky NK, El Gammal ZH, Wahba AE, Mosad E, Waly ZY, El-Fallal AA, et al. The molecular basis of cytotoxicity of alpha-spinasterol from Ganoderma resinaceum: Induction of apoptosis and overexpression of p53 in breast and ovarian cancer cell lines. J Cell Biochem. 2018;119(5):3892-902.

124. Ravikumar YS, Mahadevan KM, Manjunatha H, Satyanarayana ND. Antiproliferative, apoptotic and antimutagenic activity of isolated compounds from Polyalthia cerasoides seeds. Phytomedicine. 2010;17(7):513-8.

125. Meneses-Sagrero SE, Navarro-Navarro M, Ruiz-Bustos E, Del-Toro-Sanchez CL, Jimenez-Estrada M, Robles-Zepeda RE. Antiproliferative activity of spinasterol isolated of *Stegnosperma halimifolium* (Benth, 1844). Saudi Pharm J. 2017;25(8):1137-43.

126. Limas JC, Cook JG. Preparation for DNA replication: the key to a successful S phase. FEBS Lett. 2019;593(20):2853-67.

127. Xie T, Dong B, Yan Y, Hu G, Xu Y. Association between MMP-2 expression and prostate cancer: A meta-analysis. Biomed Rep. 2016;4(2):241-5.

128. Incorvaia L, Badalamenti G, Rini G, Arcara C, Fricano S, Sferrazza C, et al. MMP-2, MMP-9 and activin A blood levels in patients with breast cancer or prostate cancer metastatic to the bone. Anticancer Res. 2007;27(3B):1519-25.

129.   Bourboulia D, Stetler-Stevenson WG. Matrix metalloproteinases (MMPs) and tissue inhibitors of metalloproteinases (TIMPs): Positive and negative regulators in tumor cell adhesion. Semin Cancer Biol. 2010;20(3):161-8.

130.   Brehmer B, Biesterfeld S, Jakse G. Expression of matrix metalloproteinases (MMP-2 and -9) and their inhibitors (TIMP-1 and -2) in prostate cancer tissue. Prostate Cancer Prostatic Dis. 2003;6(3):217-22.

131.   Lambert E, Dasse E, Haye B, Petitfrere E. TIMPs as multifacial proteins. Crit Rev Oncol Hematol. 2004;49(3):187-98.

132.   Zheng L, Zhang YM, Zhan YZ, Liu CX. Momordica cochinchinensis seed extracts suppress migration and invasion of human breast cancer ZR-75-30 cells via down-regulating MMP-2 and MMP-9. Asian Pac J Cancer Prev. 2014;15(3):1105-10.

Appendix

molecules

MDPI

Stem Extract from *Momordica cochinchinensis* Induces Apoptosis in Chemoresistant Human Prostate Cancer Cells (PC-3)

Seksom Chainumnim [1], Audchara Saenkham [2], Kulvadee Dolsophon [2], Kittipong Chainok [3], Sunit Suksamrarn [2,*] and Wanlaya Tanechpongtamb [1,*]

[1] Department of Biochemistry, Faculty of Medicine, Srinakharinwirot University, Bangkok 10110, Thailand; seksom.chainumnim@g.swu.ac.th

[2] Department of Chemistry and Center of Excellence for Innovation in Chemistry, Faculty of Science, Srinakharinwirot University, Bangkok 10110, Thailand; audchara.sk@gmail.com (A.S.); kulvadee@g.swu.ac.th (K.D.)

[3] Thammasat University Research Unit in Multifunctional Crystalline Materials and Applications (TU-MCMA), Faculty of Science and Technology, Thammasat University, Khlong Luang, Pathum Thani 12121, Thailand; kc@tu.ac.th

* Correspondence: sunit@g.swu.ac.th (S.S.); wanlaya@g.swu.ac.th (W.T.); Tel.: +66-813446669 (W.T.)

Abstract: Natural compounds have been recognized as valuable sources for anticancer drug development. In this work, different parts from *Momordica cochinchinensis* Spreng were selected to perform cytotoxic screening against human prostate cancer (PC-3) cells. Chromatographic separation and purification were performed for the main constituents of the most effective extract. The content of the fatty acids was determined by Gas Chromatography-Flame Ionization Detector (GC–FID). Chemical structural elucidation was performed by spectroscopic means. For the mechanism of the apoptotic induction of the most effective extract, the characteristics were evaluated by Hoechst 33342 staining, sub-G1 peak analysis, JC-1 staining, and Western blotting. As a result, extracts from different parts of *M. cochinchinensis* significantly inhibited cancer cell viability. The most effective stem extract induced apoptosis in PC-3 cells by causing nuclear fragmentation, increasing the sub-G1 peak, and changing the mitochondrial membrane potential. Additionally, the stem extract increased the pro-apoptotic (caspase-3 and Noxa) mediators while decreasing the anti-apoptotic (Bcl-xL and Mcl-1) mediators. The main constituents of the stem extract are α-spinasterol and ligballinol, as well as some fatty acids. Our results demonstrated that the stem extract of *M. cochinchinensis* has cytotoxic and apoptotic effects in PC-3 cells. These results provide basic knowledge for developing antiproliferative agents for prostate cancer in the future.

Keywords: *Momordica cochinchinensis*; stem extract; apoptosis; chemoresistant; prostate cancer; Noxa

1. Introduction

Prostate cancer is the most frequently diagnosed cancer in men worldwide [1]. In 2020, 191,930 (21%) new cases and 33,330 (10%) prostate-cancer-related deaths were reported. The incidence of prostate cancer increases with age and it is more likely to develop at age 65 or older [1]. Additionally, its incidence tends to increase steadily in both developed and developing countries. Most prostate cancer patients usually progress to the metastatic and chemoresistance stages, which are obstacles to treatment. Thus, searching for alternative treatments or better chemotherapeutic drugs is significant for patient survival.

To date, several targets for anticancer drug development have been identified. One target mechanism that is often used during drug investigation is apoptosis or programmed cell death. This is a normal process that occurs under various physiological or pathological situations in our body. It is involved in normal development, function, and homeostasis, especially for controlling the number of cells [2]. The initiation of apoptosis can be triggered

by diverse extracellular and intracellular factors, such as harmful carcinogens or mutagenic agents, viral infections, ultraviolet radiation, growth factor withdrawal, and inflammation. The characteristics of apoptotic cells are highly specific, with DNA fragmentation, cell shrinkage, and membrane blebbing. To induce apoptosis, two major pathways, intrinsic and extrinsic, are well recognized. The extrinsic pathway is triggered by the interaction of cell death receptors with their ligands, while the intrinsic pathway is related to mitochondrial dysfunction. Many protein mediators are involved in these two pathways, which can be grouped as pro-apoptotic (Bax, Bak, Bad, Bid, Bim, Puma, Noxa, etc.) and anti-apoptotic (Bcl-2, Bcl-XL, Mcl-1, etc.) molecules [3]. The activation of the caspase cascade is the main mediator of both pathways and it is well accepted as a specific marker of apoptotic signaling.

Although most anticancer drugs that are currently used in the clinic have the ability to induce apoptosis in many cancers, there are some aggressive or resistant cancer types that cannot be successfully cured with either synthetic or natural agents. Hence, new anticancer drugs must be developed. *Momordica cochinchinensis* (Lour.) Spreng (MC) or "Gac" (belonging to the Cucurbitaceae family) is a type of perennial vine grown throughout northeastern Australia and southeastern Asian countries, including Thailand [4]. MC fruit has been commonly used, mainly as food and traditional medicine for various diseases such as cardiovascular disease and arthritis [5].

Different parts of MC were extracted to identify the various candidate compounds. MC arils have been found to contain a number of phytochemicals, such as fatty acids, phenolics, flavonoids, and carotenoids (mostly lycopenes and beta-carotenes). The quantities of both lycopene and beta-carotene in MC fruit are reported to be much higher than those in other plants [6]. Additionally, numerous studies have shown that these phytochemicals possess interesting biological effects, including cardio- and testicular protective effects [7,8], anticancer effects [9–12], and antioxidant and anti-inflammatory effects [13]. Meanwhile, MC seeds contain saponins, saponin glycosides, and macrocyclic peptides (e.g., momordins I-III, momordins Ia-c, and momordins IIa-d), which also exhibit noticeable activities, such as anticancer [14–17], antioxidant [18], anti-inflammatory [19,20], and reno-protective activities [21]. However, the chemical composition and biological activity of other parts of MC, including its leaves, seeds, stems, and roots, have not yet been elucidated. Therefore, the present work aimed to explore the anticancer activity of these parts of MC and investigate the possibility of the active extract having apoptosis-inducing activity. In addition, the main constituents of this active extract were chemically characterized.

2. Results and Discussion

2.1. The Stem Extract Demonstrated Antiproliferative Effects against Cancer Cells but Not against Normal Cells

To study the antiproliferative activity of the MC extract against cancer cells, several types of cancer cell models were selected for screening, including A549, HeLa, MDA-MB-231, and PC-3 cells. To prepare the MC crude extracts, different parts of MC (leaves, seeds, stems, and roots) were extracted with methanol following standard procedures. The antiproliferative activity of each soluble fraction against cancer cells was defined using an MTT assay. The cells were treated with or without several concentrations of MC extracts at 0–5 mg/mL for 24 h, while 0.5% DMSO was used as the vehicle control. The results were demonstrated as shown in Table 1. All extracts exhibited antiproliferative effects in all cancer cells tested, but at different levels. Among these crude extracts, the stem extract showed the highest efficiency in all four types of cancer cells. The IC_{50} values for A549, HeLa, MDA-MB-231, and PC-3 cells were 0.44, 0.42, 0.62, and 0.62 mg/mL, respectively. These results are consistent with other studies. The antiproliferative activity against cancer cells of a water extract from aril parts was in the range of 0.49–0.73 mg/mL [10]. Thus, the stem extract was selected for the following experiments. One important characteristic of an ideal anticancer agent is that it is less toxic to normal cells, so Vero was used as a representative of normal cells. For a model of cancer cells, PC-3 was selected for investigation due

to its chemoresistance and high metastasis potential. As illustrated in Figure 1, the IC_{50} values of the PC-3 and Vero cells were 0.62 and 2 mg/mL, respectively. These data revealed that the stem extract exhibited more specific inhibitory activity against cancer cells. Thus, the mechanism of cancer cell death induction by the stem extract was evaluated along with a characterization of its chemical composition.

Table 1. The antiproliferative effect of MC extracts were determined by MTT assays. All cells were treated with or without the different parts (leaves, seeds, stems, and roots) of extracts (0–5 mg/mL) for 24 h. Control cells were exposed to vehicle or 0.5% DMSO. The data are offered as the mean of triplicate values $\pm$ SEM.

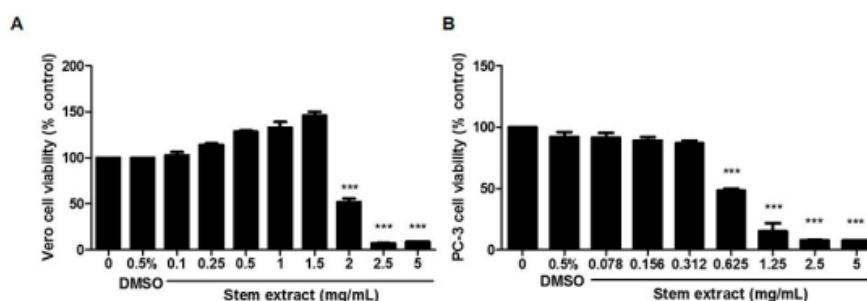| Cell Lines	IC_{50} Values (mg/mL)			
	Leaves	Seeds	Stems	Roots
A549	1.98 ± 0.74	1.30 ± 0.96	0.44 ± 0.87	0.74 ± 3.14
HeLa	0.53 ± 0.37	2.09 ± 1.41	0.42 ± 1.07	0.48 ± 0.38
MDA-MB-231	2.10 ± 0.79	2.26 ± 1.18	0.62 ± 0.74	0.77 ± 3.72
PC-3	4.25 ± 0.66	4.65 ± 0.36	0.62 ± 0.74	0.73 ± 2.27

Figure 1. Dose-dependent inhibitory effects of an MC stem extract on the viability of (**A**) Vero and (**B**) PC-3 cells. Cells were treated with various concentrations (0–5 mg/mL) for 24 h. Data are presented as the mean of triplicate values $\pm$ SEM. *** indicates $p < 0.001$.

2.2. Stem-Extract-Induced Apoptosis in PC-3 Cells

As shown in the cytotoxic screening, the stem extract affected all of the cancer cells tested, so we investigated the potential mechanism by which the stem extract induces cancer cell death. Apoptosis was selected as a target because it is the main pathway triggered by most anticancer agents [2,22]. To confirm this process, morphological changes, such as chromatin condensation, apoptotic bodies, membrane blebbing, and cell shrinkage, were evaluated. PC-3 cells were treated with or without stem extract at 0, 0.3, 0.6, 0.9, and 1.2 mg/mL for 24 h, followed by Hoechst 33342 staining and the cells were imaged under a fluorescence microscope. Most treated cells exhibited chromatin condensation, and some cells demonstrated nuclear fragmentation (Figure 2). This specific characteristic of apoptotic cells was confirmed by using sub-G1 peak analysis. The method used propidium iodide, a DNA intercalating agent, to stain the population of apoptotic cells that had diminished DNA content [23]. As shown in Figure 3, PC-3 cells were treated with various concentrations of stem extract (0, 0.6, 0.9, and 1.2 mg/mL) exhibited a higher number of sub-G1 populations while increasing the concentration of stem extract: 0.86%, 5.9%, 25%, and 37%, respectively. These results support our hypothesis that stem extract has the ability to induce apoptosis in PC-3 cells.
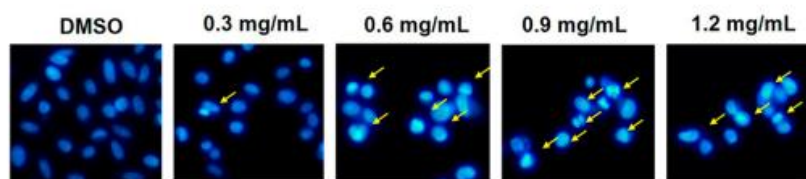
Figure 2. Fragmentation and nuclear condensation were observed by Hoechst 33342 staining. PC-3 cells were treated with stem extract (0, 0.3, 0.6, 0.9, and 1.2 mg/mL) for 24 h. Treated cells exhibited morphological changes in the nuclei typical of apoptosis. Photographs were taken under a fluorescence microscope (20×). Arrows represent apoptotic cells.
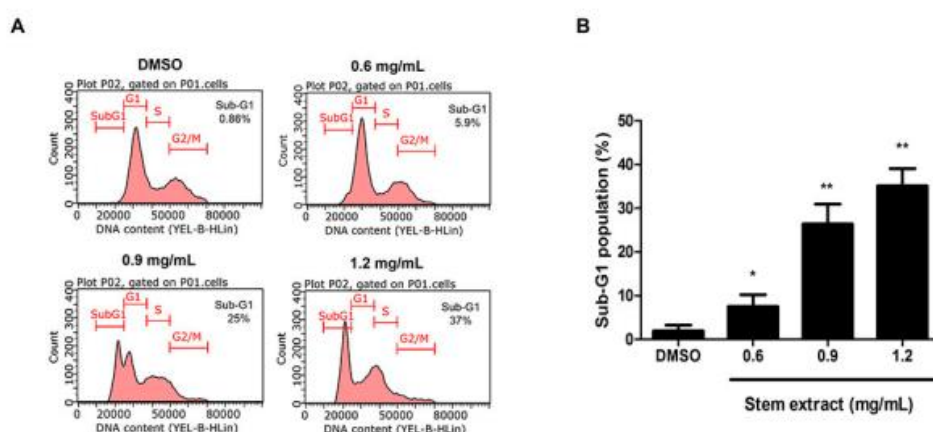

Figure 3. Sub-G1 peak analysis of PC-3 cells treated with stem extract. The flow cytometry analyzed PC-3 cells that were treated with stem extract at 0, 0.6, 0.9, and 1.2 mg/mL for 24 h. (**A**) Histograms demonstrate the number of cells (y-axis) vs. the DNA content (x-axis). The data shown are representative of three experiments with similar findings. (**B**) The quantitative values of the sub-G1 population. The significant differences of the treated cells from the untreated control group are indicated by * $p < 0.05$ and ** $p < 0.01$.

In addition, the apoptosis process usually causes mitochondrial damage, so we explored whether this effect would also be induced by stem extract. The experiment was conducted by using JC-1 dye staining. It is a fluorescent lipophilic cationic dye that is sensitive to the mitochondrial membrane potential. In normal cells, a high level of mitochondrial membrane potential causes JC-1 to accumulate in mitochondria and it exists in the J-aggregate form, which is shown in the red spectrum. In contrast, JC-1 is present as a monomer in cells with lower potential or mitochondrial damage and yields green fluorescence [24,25]. Therefore, the changes in the red to green ratio could indicate the status between healthy and apoptotic cells. As shown in our results, the stem-extract-treated cells demonstrated a decrease in the red/green ratio in a dose-dependent manner (Figure 4). The percentage of cells with JC-1 green fluorescence was not significantly altered in the control group (3.20%), while in the treated samples, the green fluorescence significantly increased by 8.19%, 8.90%, 22.34%, and 47.24% at 0.3, 0.6, 0.9, and 1.2 mg/mL of stem extract, respectively. The present findings suggested that stem extract could trigger apoptosis in PC-3 cells by inducing morphological changes, increasing the sub-G1 population, and reducing the mitochondrial membrane potential.
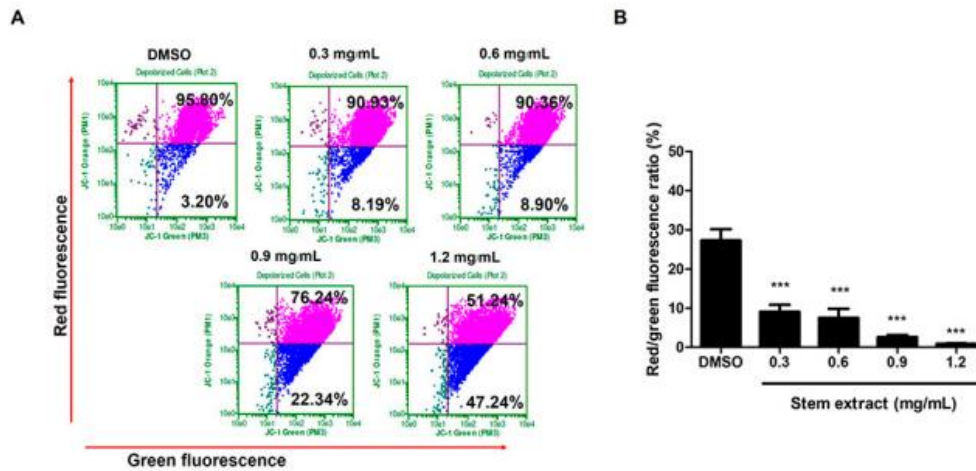
Figure 4. Effects of stem extract on the mitochondrial membrane potential ($\Delta\Psi$m) in PC-3 cells (**A**) Cells were treated with stem extract at 0, 0.3, 0.6, 0.9, and 1.2 mg/mL for 24 h. Next, all samples were stained with JC-1 and analyzed by flow cytometry. The upper right quadrant indicates polarized mitochondria (red fluorescence), while the lower right quadrant illustrates membrane depolarization (green fluorescence). (**B**) Quantification of the red/green fluorescence ratio indicates low membrane potential following increasing concentrations of the stem extract. *** indicates $p < 0.0001$ compared to the control.

2.3. The Stem Extract Affected the Expression of Apoptosis-Related Proteins in PC-3 Cells

To deeply investigate the effect of the stem extract on the protein machinery involved in the apoptosis mechanism, several mediators were determined by Western blotting, including procaspase-3, Mcl-1, Noxa, and Bcl-xL. As shown in Figure 5, PC-3 cells treated with stem extract at 0, 0.3, 0.6, 0.9, and 1.2 mg/mL demonstrated a reduction in procaspase-3, Bcl-xL, and Mcl-1 protein expression. The results for these three proteins exhibited the same trend, in which their expression started decreasing from 0.6 mg/mL. Meanwhile, the level of Noxa increased significantly from 0.3–0.9 mg/mL and dropped at 1.2 mg/mL. Caspase-3 is the main executioner caspase in the apoptosis mechanism. Normally, all caspases are present in normal cells as inactive zymogens (pro-form) and they undergo activation into a cleaved form when the apoptosis mechanism is induced. In this case, a reduction in a pro-form could therefore indicate the activation of the apoptosis pathway. Both Bcl-xL and Mcl-1 are members of the Bcl-2 family of proteins that play important roles in apoptosis inhibition. They prevent the release of cytochrome c into the cytoplasm by sequestering Bak and Bax at the mitochondrial membrane [26,27]. Therefore, the stem extract not only decreased anti-apoptotic proteins, but also increased pro-apoptotic proteins. Notably, both Bcl-xL and Mcl-1 are highly expressed in PC-3 cells and are related to the chemotherapeutic resistance of prostate cancer cells. The stem extract is therefore a possible therapeutic agent for prostate cancer treatment. For Noxa, a BH-3-only protein that normally functions as a pro-apoptotic molecule, we found an increase after treatment with the stem extract. Noxa has been indicated to react specifically with Mcl-1 and promote Mcl-1 degradation [28–30]. In the present study, a reduction in Mcl-1 may result from an increase in Noxa, which causes Mcl-1 degradation. Thus, the data indicate another possible role of the stem extract that could reverse the chemoresistance property of prostate cancer cells. However, it is noticeable that the amount of stem extract at 1.2 mg/mL or higher may have a strong toxic effect on the cells, as the amount of Noxa was decreased. Hence, the effective concentration of stem extract should be in the range of 0.6–0.9 mg/mL.
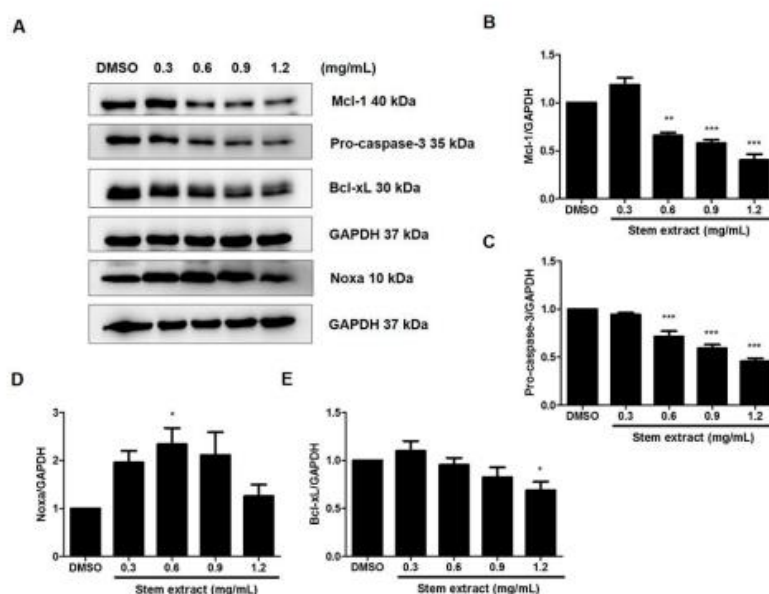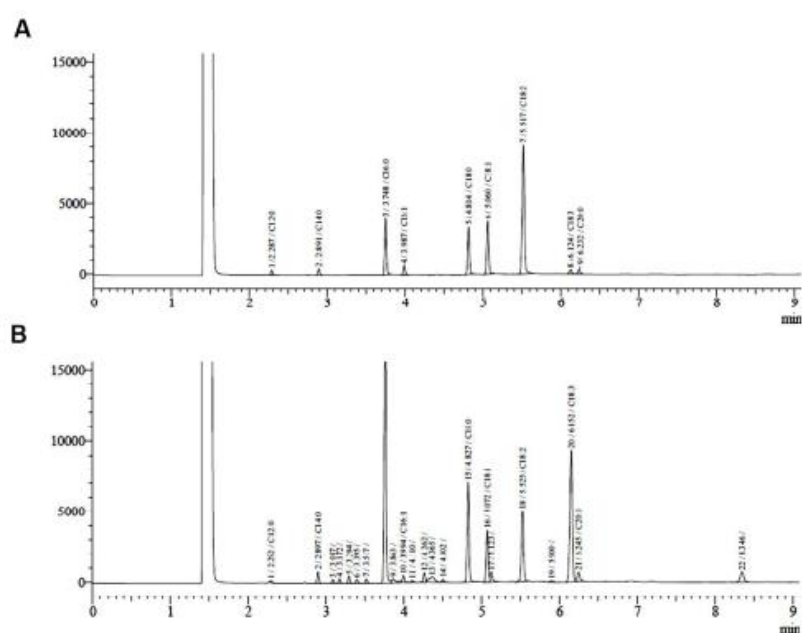
Figure 5. Effects of the stem extract on the expression of apoptosis-related proteins in PC-3 cells. Cells were treated with stem extract at 0, 0.3, 0.6, 0.9, and 1.2 mg/mL, and then Western blot analysis was performed with all samples. (**A**) Representative protein expression of McL-1, pro-caspase-3 Bcl-xL, and Noxa revealed by Western blot analysis. (**B–E**) The expression levels of each protein were quantified and normalized to GAPDH. The results are expressed as means ± SEM. * indicates $p < 0.05$, ** indicates $p < 0.01$, and *** indicates $p < 0.001$: a significant difference versus the control.

2.4. Chemical Compositions of the Stem Extract and Its Active Compounds

Since an anticancer activity of the stem extract was clearly demonstrated in PC-3 cells, we asked what active compound could be responsible for this function. Bioassay-guided fractionation of this MC stem extract was then carried out and it yielded two fractions, EtOAc (IC$_{50}$ 1.25 mg/mL) and n-BuOH (IC$_{50}$ 1.46 mg/mL). Subsequently, chromatographic phytochemical investigations of the more active EtOAc soluble part produced a pale-yellow oil at 0.16% (w/w) from fraction E1 as the most abundant fraction, which was quantified for fatty acid content using GC-FID. The percentage of the identified fatty acid composition is presented in Table 2, and the GC-FID chromatogram is shown in Figure 6. The unsaturated fatty acids (USFAs) were characterized as palmitoleic acid (1.34%), oleic acid (7.30%), linoleic acid (11.85%), and α-linolenic acid (27.0%), while those of the saturated fatty acids (SFAs) were lauric acid (0.18%), myristic acid (1.54%), palmitic acid (35.07%), stearic acid (14.09%), and arachidic acid (1.63%). Both palmitic acid and α-linolenic acid were obviously the main fatty acid constituents obtained from the stem part. Fraction E2-5 and E6.5.4 were collected and proved to be α-spinasterol (**1**) and (−) ligballinol (**2**), respectively, by spectroscopic examination, mainly ^{1}H, ^{13}C NMR, and MS data, as well as X-ray crystallography (Figures 7 and 8) (Supplementary Materials Figures S1–S6). A comparison of their physicochemical and spectral data with published values was also performed. Compound **2** exhibited a negative specific rotation $[\alpha]_D^{25.5}$ −11.5 (c = 0.20, MeOH), and its X-ray crystal structure supported the stereochemical assignment, as shown (Figure 8). Therefore, Compound **2** was deduced to be (−) 4,4′-((1R,3aS,4R,6aS)-tetrahydro-1H,3H-furo[3,4-c] furan-1,4-diyl)diphenol or (−) ligballinol. This compound has also been reported from the MC seed [31,32].

Table 2. The fatty acids identified from the MC stem extracts by GC/FID analysis.

Peak	RT	Fatty Acid Names	Mean ± SEM
1	2.292	Lauric acid (C12:0)	0.18 ± 0.01
3	2.897	Myristic acid (C14:0)	1.54 ± 0.02
8	3.761	Palmitic acid (C16:0)	35.07 ± 0.19
10	3.994	Palmitoleic acid (C16:1)	1.34 ± 0.02
15	4.827	Stearic acid (C18:0)	14.09 ± 0.05
16	5.072	Oleic acid (C18:1)	7.30 ± 0.02
18	5.525	Linoleic acid (C18:2)	11.85 ± 0.07
20	6.125	α-Linolenic acid (C18:3)	27.0 ± 0.09
21	6.245	Arachidic acid (C20:0)	1.63 ± 0.16

Figure 6. Chromatograms of the fatty acid content of the oil fraction obtained by the GC-FID analysis. (**A**) Standard chromatogram of 9 fatty acids that are known as lauric acid (C12:0), myristic acid (C14:0), palmitic acid (C16:0), palmitoleic acid (C16:1), stearic acid (C18:0), oleic acid (C18:1), linoleic acid (C18:2), α-linolenic acid (C18:3), and arachidic acid (C20:0). (**B**) Identification chromatogram of fatty acids from the sample.
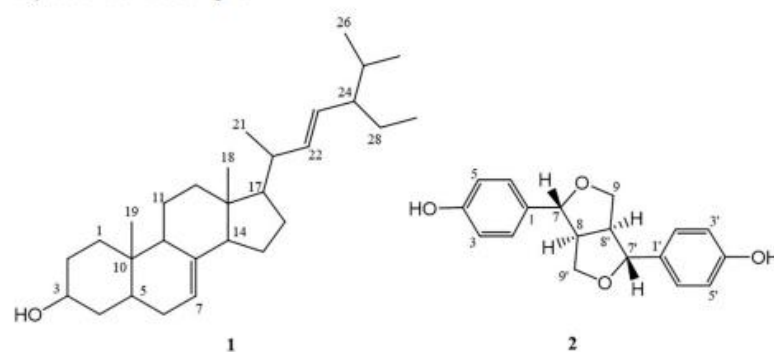
Figure 7. Chemical structures of α-spinasterol (**1**) and ligballinol (**2**).
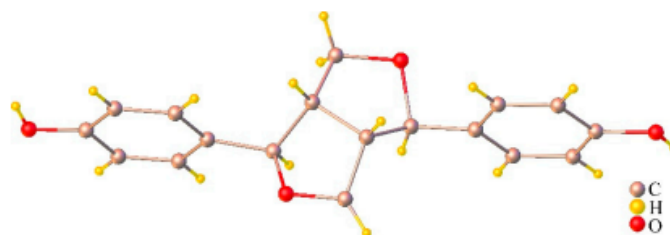
Figure 8. ORTEP plot of the X-ray crystal structure for ligballinol.

Compound **1** was obtained as a white amorphous powder, mp. 168–169 °C (lit [33] 169 °C). ^{1}H-NMR (300 MHz, CDCl$_3$) δ$_H$: 5.16 (m, 2H, H-7 and H-22), 5.03 (dd, J = 15.1, 8.6 Hz, 1H, H-23), 3.59 (m, 1H, H-3), 2.00–0.95 (m, for methine and methylene protons), 1.03 (d, J = 6.6 Hz, CH$_3$-21), 0.84 (d, J = 6.6 Hz, 3H, CH$_3$-26), 0.80 (s, 3H, CH$_3$-19), 0.79 (d, J = 5.5 Hz, 3H, CH$_3$-27), 0.55 (s, 3H, CH$_3$-18); ^{13}C-NMR (75 MHz, CDCl$_3$) δ$_C$: 139.5 (C-8), 138.1 (C-22), 129.5 (C-23), 117.4 (C-7), 71.0 (C-3), 55.9 (C-17), 55.1 (C-14), 51.2 (C-24), 49.4 (C-9), 43.3 (C-13), 40.7 (C-20), 40.2 (C-5), 39.4 (C-12), 38.0 (C-4), 37.1 (C-25), 34.2 (C-10), 31.8 (C-1), 31.5 (C-2), 29.6 (C-6), 28.3 (C-16), 25.3 (C-28), 23.0 (C-15), 21.5 (C-11), 21.3 (C-26), 20.9 (C-21), 18.9 (C-27), 25.3 (C-28), 23.0 (C-29); HR-TOFMS (APCI$^+$) m/z 395.3674 [M − H$_2$O + H]$^+$ (calc. for C$_{29}$H$_{47}$, 395.3672).

Compound **2** was obtained as a colorless needle, mp 263–264 °C (lit [34] 264–266 °C); $[\alpha]_D^{25.5}$ −11.5 (c = 0.20, MeOH) (lit [35] $[\alpha]_D^{25}$ −24 (c = 0.1, MeOH), [34] $[\alpha]_D$ −7.1 (c = 1.61, MeOH)). ^{1}H-NMR (300 MHz, CDCl$_3$ + DMSO-d_6) δ$_H$: 8.56 (br s, 2H, OH), 7.03 (d, J = 8.4 Hz, 4H, H-2, 2′, 6 and 6′), 6.69 (dd, J = 8.4, 1.8 Hz, 4H, H-3, 3′, 5 and 5′), 4.58 (d, J = 4.4 Hz, 2H, H-7 and 7′), 4.07 (br t, J = 6.9 Hz, 2H, H-9 and 9′), 3.69 (dd, J = 6.3, 1.5 Hz, 2H, H-9 and 9′), 2.98 (br s, 2H, H-8 and 8′); ^{13}C-NMR (75 MHz, CDCl$_3$ + DMSO-d_6) δ$_C$: 156.5 (C-4 and 4′), 131.3 (C-1 and 1′), 127.1 (C-2, 2′, 6 and 6′), 115.2 (C-3, 3′, 5 and 5′), 85.5 (C-7 and 7′), 71.2 (C-9 and 9′), 53.7 (C-8 and 8′); HR-TOFMS (ESI$^−$) m/z 297.1121 [M − H]$^−$ (calc. for C$_{18}$H$_{17}$O$_4$, 297.1132). X-ray crystallographic data for Compound **2**: C$_{18}$H$_{17}$O$_4$, M = 297.32, Monoclinic, Space Group P21/c, a = 5.8554(7) Å, b = 7.3656(9) Å, c = 16.959(2) Å, α = γ = 90°, β = 91.421(4)°, V = 731.20(15) Å3, Z = 2, Dcalcd = 1.350 Mg/m^3, crystal size 0.32 × 0.11 × 0.07 mm^3, F(000) = 314, 25268 reflection collected, 1817 independent reflections (R$_{int}$ = 0.0359), R$_1$ = 0.0549 [I > 2σ(I)], wR$_2$ = 0.1521 [I > 2σ(I)], R$_1$ = 0.0617 (all data), wR$_2$ = 0.1574 (all data), goodness of fit = 1.153.

A single crystal of **2** was pasted on MiTeGen micromounts using paratone oil. X-ray scattering data were collected using a BRUKER D8 QUEST CMOS PHOTON II (Bruker Switzerland AG, Fallanden, Switzerland) operating at T = 296(2) K. The collection of data used ω and φ scans and Mo-Kα radiation (λ = 0.71073 Å). The program APEX3 calculates, runs, and images the total number, and unit cell indexing was refined using SAINT [36]. Data reduction was performed using SAINT, and SADABS was used for absorption correction. The ShelXT structure solution program was used and combined dual-space recycling methods [37] and Patterson were used to solve the structure. The structure was refined by least squares using ShelXL [38] and the OLEX2 interface [39]. In the final refinement cycles, all nonhydrogen atoms were cultured anisotropically. All hydrogen atoms were settled in different Fourier maps but were refined using a rigid model (C−H = 0.93–0.98 Å and O−H = 0.82 Å). CCDC-2102982, containing supplementary crystallographic data, can be used free of charge from the Cambridge Crystallographic Data Centre via www.ccdc.cam.ac.uk/data_request/cif (accessed on 13 August 2021).

2.5. The Effect of Isolated Compounds on PC-3 Cell Viability

The activities of the pure compounds after isolation and identification were investigated for their antiproliferative effects on PC-3 cells compared to Vero cells. The MTT assay was performed using α-spinasterol at 0–100 μM and ligballinol at 0–500 μM for 72 h,

while the vehicle control was treated with both 0.5% DMSO and 1% EtOH. As illustrated in Figure 9, an inhibitory effect was clearly seen for ligballinol. The antiproliferative activity was demonstrated in PC-3 cells with an IC_{50} of 230 μM, but not in normal Vero cells. These results suggest that ligballinol may be an active compound responsible for the anticancer activity of the stem extract. Ligballinol has a furanoid lignan structure and has demonstrated cytotoxic activities against human colorectal cancer cells (HT-29) with an IC_{50} value of 45.5 μM [35]. α-Spinasterol could induce DNA fragmentation and upregulate p53 in breast cancer cells (MCF-7) and ovarian cancer cells (SKOV-3) [40,41]. However, α-spinasterol did not cause cytotoxicity in PC-3 cells, which correlated with our work [42].
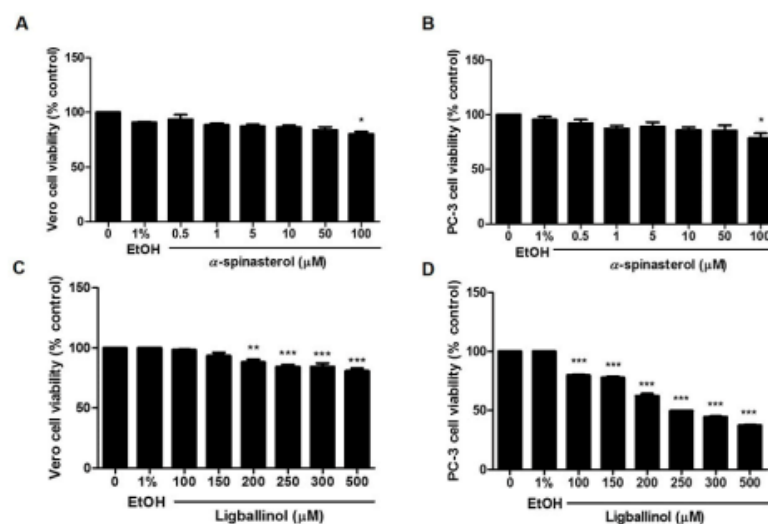

Figure 9. The antiproliferative effect of α-spinasterol and ligballinol on PC-3 and Vero cells. Cells were treated with various concentrations of (**A,B**) α-spinasterol and (**C,D**) ligballinol, and MTT assays were conducted. The results are expressed as means ± SEM. * indicates $p < 0.05$, ** indicates $p < 0.01$, and *** indicates $p < 0.001$: a significant difference versus control.

3. Materials and Methods

3.1. General Procedures

^{1}H- and ^{13}C-NMR spectra were recorded on a Bruker Avance 300 FT-NMR spectrometer (Bruker Switzerland AG, Fallanden, Switzerland) operating at 300 MHz (^{1}H) and 75 MHz (^{13}C) using $CDCl_3$ as the solvent. Specific optical rotations were measured using a Jasco-1020 polarimeter (Jasco Corporation, Tokyo, Japan). Column chromatography and TLC were carried out using Merck silica gel 60 (>230 mesh) and precoated silica gel 60 F_{254} plates, respectively. Spots on the TLC were visualized under UV light (245 or 365 nm) and by spraying with anisaldehyde–H_2SO_4 reagent followed by heating at 80 °C until maximum color formation occurred. Only analytical grade chemicals were used: JC-1 reagent (Biotium, Biotium, Inc., Fremont, CA, USA), Hoechst 33342 (Invitrogen, Thermo Fisher Scientific, Inc., Waltham, MA, USA), MTT or 3-(4,5-dimethylthiazol-2-yl)-2,5-diphenyltetrazolium bromide (Sigma-Aldrich, St. Louis, MO, USA), fetal bovine serum (FBS), and DMEM (Gibco, Thermo Fisher Scientific, Inc., Waltham, MA, USA). DMSO and PI (propidium iodide) reagents were purchased from Merck KGaA, St. Louis, MO, USA.

3.2. Plant Materials

MC plants were locally cultivated in a community in Nakhon Pathom Province, Thailand. Leaves, seeds, stems, and roots of the adult plant were collected in September 2016. A voucher has been deposited under number SC001 at the Laboratory of Natural

Product Research Unit, Department of Chemistry, Faculty of Science, Srinakharinwirot University, Thailand.

3.2.1. Preparation of MC Extracts

Each plant part was thoroughly washed with tap water, cut into small pieces, and sun dried. The leaves, seeds, stems, and roots of the MC (each 100 g) were individually macerated in MeOH (500 mL) 3 times for two weeks each at room temperature. After that, the methanol extract was filtered (Whatman no. 1 paper), combined, and evaporated to dryness using a rotary evaporator at 40 °C. The obtained dried MeOH extracts (leaves 3.15 g, seeds 6.25 g, stems 0.77 g, and roots 0.8 g) were stored at −20 °C prior to cytotoxic screening. All parts were dissolved in dimethyl sulfoxide (DMSO) by using a water-bath sonicator until completely dissolved.

3.2.2. Phytochemical Isolation of the Stem Extract

For further phytochemical isolation of the stem extract that exhibited the highest cytotoxicity screening, dried stems (16 kg) were collected and then extracted with MeOH at room temperature to yield a brownish residue (320 g). Next, the dried MeOH stem extract was suspended in water and successively partitioned with ethyl acetate (EtOAc) and *n*-butanol (*n*-BuOH), and the combined solution of each extract was evaporated under reduced pressure to yield the EtOAc (greenish sticky mass, 61 g) and *n*-BuOH (brownish sticky mass, 17 g) extracts. Based on the yield of the two fractions, the EtOAc soluble fraction was considered as the main fraction and was subjected to further isolation. The EtOAc fraction (56 g) was subjected to column chromatography (CC) using a gradient system of hexane–EtOAc (98:2 to 0:100) as the eluent to produce 6 main fractions (E1–E6) based on the thin-layer chromatography (TLC) investigations. An oily fraction E1 (26.4 g, 0.16% *w/w* based on the dry plant weight) was then evaluated for its fatty acid content. Subfractions E2–E5 displayed similar TLC results, and a colorless solid of α-spinasterol (**1**, 979 mg) was precipitated from fraction E2 (4.3 g). Fraction E6 (12.5 g) was subjected to repeated CC eluting with a gradient of EtOAc–CH_2Cl_2 (98:2 to 0:100) to obtain 10 subfractions (E.6.1–E.6.10). Subfraction E.6.5 (4.5 g) was further purified by CC using the same eluent to provide 8 subfractions (E6.5.1–E6.5.8). Ligballinol (**2**, colorless needle, 27 mg) was successfully obtained from subfraction E.6.5.4 (2.8 g).

3.2.3. Analysis of Fatty Acid Composition
Preparation of Fatty Acid Methyl Esters

A solution of methanolic sodium hydroxide (9:1, 5 mL) was added to an oil sample (30 mg) and the mixture was heated under reflux for 90 min. After cooling, deionized water (10 mL) was added and the mixture was shaken for a few seconds. Unsaponified fatty acids were discarded by extraction with hexane (3 × 5 mL). The layer below was collected and adjusted to pH 3 (by 6 N HCl), followed by extraction with hexane (3 × 5 mL). The organic layer was removed under reduced pressure. The obtained fatty acid was further mixed with a solution of 2% H_2SO_4 in methanol, and the mixture was heated under reflux at 80 °C for 90 min. After cooling to ambient temperature, water (0.5 mL) was added, followed by extraction with hexane (3 × 5 mL). The methyl ester was evaporated to dryness, weighed and solubilized in hexane (1 mL) before injection into the gas chromatograph.

GC FID-analysis. Gas chromatography was performed with a Shimadzu version 3, model GC-17A, equipped with a flame ionization detector (FID). FAME analyses were achieved on a Phenomenex BPX70 capillary column (30 m, 0.25 mm i.d.). The initial oven temperature for the analysis of the injection port and FID detector was programmed at 60 °C for 0.5 s and heated to 200 °C for 4 min. The injector and detector temperatures were 250 °C. Helium was used as the carrier gas at a flow rate of 1.25 mL/min, and the split-less time was 1 min for both instruments. The experiment was analyzed by Shimadzu GC solution software V. 2.10, and the results were compared with known standards of fatty acids.

3.3. Cell Lines and Cell Culture

The human androgen-independent prostate adenocarcinoma grade IV (PC-3) cell line (ATCC® CRL-1435™), human non-small-cell lung cancer (NSCLC) (A549) cell line (ATCC® CCL-185™), human breast adenocarcinoma (MDA-MB-231) cell line (ATCC® HTB-26™), and normal African green monkey kidney (Vero) cell line (ATCC® CCL-81™) were purchased from ATCC (American Type Culture Collection). All cancer cell lines were grown in high glucose Dulbecco's modified Eagle's medium (DMEM) supplemented with 10% fetal bovine serum (FBS), 0.1 mg/mL streptomycin, and 100 units/mL penicillin. The Vero cell line, a representative normal cell line, was maintained in Eagle's minimum essential medium (EMEM) containing 10% FBS and 1% penicillin/streptomycin at 37 °C in an atmosphere of 5% CO_2.

3.4. Cell Viability Assay

The assay was performed using the standard MTT method. Cells were seeded in a 96-well plate at a density of 1×10^4 cells/well and incubated for 24 h. Next, the cells were treated with various concentrations of the compound tested, including MC crude extracts (0–5 mg/mL), α-spinasterol (0–100 µM), or ligballinol (0–500 µM), while the concentrations of both dimethyl sulfoxide (DMSO; 0.5%) and ethanol (EtOH; 1%) were used as the vehicle control. After treatment, the medium was removed, and MTT solution (0.5 mg/mL) was added to each well. The culture plate was incubated for 4 h at 37 °C in the dark. Next, the supernatant was discarded and DMSO was added to each well to dissolve the formazan precipitate. The optical density (OD) at a wavelength of 570 nm was measured with a multimode microplate reader (Synergy; BioTek Instruments, Inc., Santa Clara, CA, USA) The inhibitory concentration at 50% (IC_{50}) was calculated with GraphPad Prism 5.03 software (GraphPad Software, Inc., San Diego, CA, USA).

3.5. Nuclei Staining

Apoptotic nuclei were investigated by using Hoechst 33342 staining. Briefly, the cells were seeded in a 6-well plate at a density of 5×10^5 cells/well and incubated for 24 h. The next day, when the cells reached >80% confluence, the media was replaced with 2 mL of fresh complete medium containing 0, 0.3, 0.6, 0.9, and 1.2 mg/mL stem extract for 24 h. Next, the cells were stained with Hoechst 33342 (10 µM) for 30 min at 37 °C in the dark. The characteristics of the cells with fragmented and condensed nuclei were recorded under a fluorescence microscope (IX73; Olympus, Tokyo, Japan) using a magnification of ×20 for 24 h.

3.6. Sub-G1 Apoptosis Assay

Sub-G1 peak analysis was performed using a flow cytometer. Cells were seeded in a 6-well plate at a density of 5×10^5 cells per well and incubated for 24 h at 37 °C in a 5% CO_2 atmosphere. Next, the cells were treated with various concentrations (0, 0.6, 0.9, and 1.2 mg/mL) of stem extract. After incubation for 24 h, the cells were harvested and fixed with 70% ice-cold ethanol at 4 °C for at least 1 h. Subsequently, the cells were washed with ice-cold PBS, followed by incubation in 20 µg/mL RNase A (Sigma, St. Louis, MO, USA) and 50 µg/mL PI (Merck KGaA, St. Louis, MO, USA) with 1.5% Triton X-100 for 30 min at 37 °C in the dark. The cells were analyzed with a flow cytometer (Guava EasyCyte and GuavaSoft software version 3.3 (Merck KGaA, St. Louis, MO, USA)). The data are depicted as a histogram and the percentage of sub-G1 peaks display the apoptotic populations.

3.7. Measurement of Mitochondrial Membrane Potential (MMP)

The MMP was measured using JC-1 fluorescent staining. To perform the experiment, the cells were treated with various concentrations (0, 0.6, 0.9, and 1.2 mg/mL) of stem extract, and 0.5% DMSO was used for the control group. Next, the cells were collected by trypsinization and centrifuged at $500 \times g$ for 5 min at 4 °C, followed by PBS washing. After that, the cells were incubated with JC-1 dye for 15 min, centrifuged at $500 \times g$ for

5 min, resuspended in PBS, and analyzed with flow cytometry (Guava EasyCyte and Guava Mitopoteintial software (Merck KGaA)).

3.8. Western Blot Analysis

Cells were seeded in 6-well plates at a density of 5×10^5 cells per well in DMEM containing 10% FBS and cultured for 24 h. Next, the cells were treated with various concentrations (0, 0.3, 0.6, 0.9, and 1.2 mg/mL) of stem extract. After incubation, the cells were lysed with RIPA buffer (1 M Tris-HCl pH 7.4, 5 M NaCl, 20% NP-40, 10% sodium deoxycholate, 20% SDS, and a protease inhibitor cocktail) on ice for 30 min and centrifuged at 14,000 rpm at 4 °C for 20 min. The concentration of protein was analyzed using a Bradford protein assay. Following protein quantification, 12% SDS-polyacrylamide gel electrophoresis (SDS–PAGE) separated 20–30 μg of the total protein extracts and was then transferred to PVDF membranes and blocked with 5% skim milk in TBS-T buffer (5% w/v skim milk, 0.1% Tween-20 and $1\times$ Tris-buffered saline solution) for 1 h at room temperature, then incubated with primary antibodies against caspase-3 (1:1000; product no. 9662), Mcl-1 (1:1000; product no. 5453T), Bcl-xl (1:1000; product no. 2764T), GAPDH (1:1000; product no. 2118S; all from Cell Signaling Technology, Inc., Danvers, MA, USA), and Noxa (1:1000; product no. 14766S) at 4 °C overnight. The membranes were washed 3 times and then incubated with anti-rabbit IgG antibodies (1:5000; product no. 7074P2) or horseradish peroxidase-conjugated anti-mouse antibodies ((1:5000; product no. 7076P2); both from Cell Signaling Technology, Inc.) for 1 h. The membranes were visualized by enhanced chemiluminescence using ECL plus™ Western blotting detection reagents (Bio-Rad Laboratories). The intensities of the protein bands were quantified by ImageJ software [Java 1.8.0_112 (64_bit)].

3.9. Statistics

All results are presented as the mean $\pm$ standard error (SEM, of each group = 3). Statistical analysis was performed using GraphPad Prism version 5.03 (GraphPad Software, Inc.). Statistical comparisons with paired observations were made by a one-way analysis of variance followed by Dunnett's test. $p < 0.05$ was considered to indicate a statistically significant difference.

4. Conclusions

In the present study, the MC extract from leaves, seeds, stems, and roots demonstrated cytotoxic effects in several types of cancer cells, including lung, cervical, breast, and prostate cancer cells. However, the most effective extract was from the stem part, which not only exhibited a strong effect on cancer cells but also showed less toxicity on normal cells. In addition, the stem extract clearly indicated apoptosis induction in prostate cancer cells. Additionally, the stem extract showed an interesting ability to reduce the expression of anti-apoptotic proteins (Bcl-xL and Mcl-1) and increase the expression of pro-apoptotic proteins (caspase-3 and Noxa) in prostate cancer cells. The isolated compound ligballinol may be responsible for this function; however, additional investigations are necessary.

VITA

NAME   Seksom Chainumnim

DATE OF BIRTH   06 March 1991

PLACE OF BIRTH   Phichit

INSTITUTIONS ATTENDED   2014-present Doctor of Philosophy (Ph.D) in Biomedical

                         Sciences, Srinakharinwirot University, Bangkok, Thailand

                         2009-2013 Bachelor of Science (Biology), Phayao

                         University, Phayao, Thailand

                         2006-2008 High school, Phichitpittayakom school, Phichit,

                         Thailand

HOME ADDRESS   33/1 Village No. 8, Phai Khwang Sub-district, Muang District,

                         Phichit Province, Thailand

PUBLICATION   1. Chainumnim S, Saenkham A, Dolsophon K, Chainok K,

                         Suksamrarn S, Tanechpongtamb W. Stem Extract from

                         Momordica cochinchinensis Induces Apoptosis in

                         Chemoresistant Human Prostate Cancer Cells (PC-3).

                         Molecules. 2022; 27(4):1313.